Acquisition, degradation, and cycling of organic matter within sea-ice brines by bacteria and their viruses

Gordon Maxwell Showalter

A dissertation

submitted in partial fulfillment of the

requirements for the degree of

Doctor of Philosophy

University of Washington

2020

Reading Committee:

Jody W. Deming, Chair

John A. Baross

Jodi N. Young

Program Authorized to Offer Degree:

School of Oceanography

University of Washington

Abstract

Acquisition, degradation, and cycling of organic matter within sea-ice brines by bacteria and their viruses

Gordon Maxwell Showalter

Chair of the Supervisory Committee:
Prof. Jody W. Deming
School of Oceanography

Marine dissolved organic carbon (DOC) is a major component of the global carbon pool, and thus can have significant effects on global carbon cycling. Within the oceans, DOC is largely regulated by microbial communities, which can serve as both a source and sink of organic carbon. Microbial controls on DOC cycling within sea ice are especially relevant to global processes, as sea ice can act as an inhibitor of exchange between the ocean and the atmosphere while also affecting carbon export to the deep sea. However, how sea-ice communities influence DOC cycling, especially in very cold conditions of winter sea ice, is poorly understood.

This dissertation explores how bacterial communities, which dominate winter sea ice, may influence DOC cycling. Chapter 1 presents an introduction of sea-ice microbial communities in the low-temperature, high salinity conditions which characterize sea-ice brines. How bacteria within brines swim in response to temperature, salinity, and chemical gradients in sea ice is presented in Chapter 2, which demonstrates a low-temperature record for directed bacterial swimming and suggests explanations for how bacteria position themselves within brines to access DOC. However, most DOC within the marine environment is too large for bacterial uptake, necessitating degradation by enzymes. Chapter 3 demonstrates bacterial extracellular enzyme activity both in a laboratory setting and *in situ*, showing growth-dependent enzyme activity down

to –8˚C and up to 142 ppt salts and across a freeze-thaw cycle within sea ice and sea-surface microlayer samples. Finally, Chapter 4 presents a model of bacterially and virally mediated DOC cycling. This model uses simple differential equations, explained further in Appendix 1, to probe the potential existence of a viral shunt within sea-ice brines by demonstrating the role of bacteriophage in population dynamics of a theoretical brine, suggesting low viral production, high host-specificity, and virally-driven DOC cycling may be common within this environment. The results of this dissertation have implications for the understanding of DOC within polar seas and demonstrate the potential for active DOC cycling mediated by bacteria and their viruses within winter sea ice, which serves as an analog for very cold ice elsewhere.

TABLE OF CONTENTS

LIST OF FIGURES

LIST OF TABLES

ACKNOWLEDGEMENTS

I've had the opportunity to work with a great number of people over the last six years who have had significant impact on the development of my dissertation and my growth as a scientist and person. Primarily, I'm incredibly grateful to Jody Deming for her mentorship and the many opportunities to do field work, attend workshops, and explore connections between science and society which have shaped my trajectory. My committee members, John Baross, Jodi Young, Rebecca Woodgate, Nadine Fabbi, Cecilia Bitz, and Chris Anderson, comprise what must be one of the largest committees in Oceanography, and I thank them all for their input and conversations. I'm especially thankful to Rebecca, for her keen leadership and humor (and riddles) on land and at sea, and to Nadine, for guiding me during the transition into science policy and introducing me to the human element of sea ice. I'm also thankful to John, for his thought-provoking feedback, and to Jodi, for her positive encouragement and attentive feedback.

My work was made lighter by the current and former members of the Deming Lab: Zac Cooper, Frida the Gecko, Josephine Rapp, Anders Torstensson, Erin Firth, and most of all Shelly Carpenter, without whose expertise and encouragement I'd have given up on virus-counting long ago – or more likely, would have never gotten there in the first place. The extended Jody-Jodi lab has been like an extended scientific family: thank you Hannah, Susan, Katrin, and Meng for bringing the eukaryotes to the fore.

I've had the extreme luck to go through graduate school flanked by an ideal cohort and community of graduate students and friends. Angie, Justin, Susanna, Robin, Paige - thanks for the

support, coffee dates, and dissertation pastries, and Theresa – for taking on the extra duty of being a roommate and best friend (and excelling, as with all things). Thank you Anna, Sasha, Amy, and Robert, and other MSB dwellers for Waffle Wednesdays and Pi Day celebrations, and thank you to the staff of TouchTank for the fun ~~diversion~~ *very serious business* of satirical oceanography zines. Sarah Dewey helped me navigate into the Arctic policy world, and Hally Stone helped me get there through many application reviews. I struggled through Inuktitut study with an amazing group of folks – Lizzy, Elena, Kelly, Ellen, and Kublu - that made even specific conditionals fun. And thank you to my community beyond Academia, especially Ronja, Jacob, Shelley, Colette, Bryce, Nat, and Andrew, for supporting me through 6+ long years. When I first started working in science at Purdue, I worked with Dr. Kari Clase who gave me advice that probably sums up graduate school: just keep going until someone tells you to stop. In Dr. Clase's lab I took my first steps into microbiology and followed around Soo Ha like a puppy trying to absorb everything from her, and, ultimately, Soo Jung Ha taught me everything I know.

Finally, thank you to my family: to my parents for instilling a love of learning and sense of adventure and independence that got me to this point, and working to give me the opportunity to get here; and to Andy, Carrie, and Cate for weekly quarantine meetings which continues 28 years as best friends.

Chapter 1.
An introduction to sea-ice carbon dynamics

1.1 The ocean as a carbon pool

With an estimated 38,000 Pg C, Earth's oceans hold one of the largest global reservoirs of carbon. Roughly 2% of this pool, about 660 Pg C, is in the form of dissolved organic carbon (DOC), the fraction of organic carbon that can pass through a 0.2 μm filter (Hansell *et al*., 2009). Though a small fraction of the total marine carbon pool, oceanic DOC serves as a fuel for microbial food webs and a connection between chemical (inorganic) and biological (organic) carbon cycles (Lønberg *et al*., 2020). Because marine DOC contains a mass of carbon similar to that of the atmosphere, small changes in DOC concentrations and cycles can have a large impact on global carbon cycling, particularly by affecting gaseous exchange with the atmosphere and carbon export to the deep sea (Lønberg *et al*., 2020).

Within high latitude seas, sea ice plays an important role in organic carbon cycling from its position at the interface between ocean and atmosphere. Acting as a semi-permeable lid, sea ice reduces gas exchange with the atmosphere compared to open-water systems. At the same time, sea ice alters exchanges between the surface and deep ocean, limiting inputs of light (and therefore reducing pelagic primary productivity) and concentrating DOC export into a seasonal pulse associated with spring ice melt (Vancoppenolle *et al*., 2013). Both of these processes, as with DOC cycling in the open ocean, are heavily influenced by microbial communities, which serve as a source of DOC through exudate, leakage, sloppy feeding, and lysis, as well as a sink as heterotrophic and mixotrophic organisms consume DOC to sustain activity and growth.

Sea ice is a microbial habitat by virtue of a network of interconnected liquid pockets (Deming, 2002). Salts segregated from ice crystals as seawater freezes become trapped and concentrated within this network, depressing the freezing point and allowing pockets of liquid water to persist within the ice. Governed by the interplay between temperature and salinity, these pockets, known as brine pores, become increasingly discrete and saline as temperature drops and ice continues to grow (Golden *et al*., 2007; Petrich and Eicken, 2017). Within these very cold, highly saline brine pores, microbial life also persists, adapted to the environmental crucible of low-temperature, high-salt conditions.

1.2 Sea-ice communities

Psychrophiles, microbes with an optimal growth temperature below 15˚C, and cold-adapted organisms in general have evolved means to circumvent the compound challenges of a low-temperature environment: reduced chemical reaction rates, altered protein flexibility, and reduced lipid fluidity (Morita, 1975; Deming, 2003; D'Amico, 2006; Ewert and Deming, 2013; 2014). Decreased enthalpic interactions of enzymes and proteins maintain flexibility and reaction rates, cold shock proteins stabilize genetic material for functionality, and increased fraction of unsaturated to saturated fatty acids in cell membranes confers greater membrane fluidity at low temperature (Gerday *et al*., 2000; D'Amico *et al*., 2002; Ermolennko and Makhatadze, 2002; Keto-Timonen *et al*., 2016). At the same time, organisms within sea ice experience hypersalinity or dramatic salinity shifts as ice thaws or refreezes, leading to osmotic pressure against the cell membrane while also challenging protein and enzyme confirmation and stability (Ewert and Deming, 2013). Well-adapted organisms within sea-ice brines are thus *halophiles*, organisms that grow optimally at or above seawater salinity, and demonstrate techniques of osmo-regulation (such

as the use of compatible solutes) and salt-adaptation in proteins (such as low iso-electric points featured in enzymes) (Ewert and Deming, 2014; DasSarma and DasSarma, 2015; Firth *et al*., 2016).

Algal communities within sea-ice brines are characterized by dense assemblages, most often diatoms, while heterotrophs dominate sea-ice bacterial communities, reaching densities of up to 10^8 cells mL^{-1} (Boetius *et al*., 2015). Paradigmatic thought suggests that heterotrophic organisms at low temperatures require higher concentrations of organic substrate to enable activity and growth (Pomeroy and Wiebe, 2001). In sunlit seasons such substrates are readily available, as net-autotrophic sea-ice microbial communities produce up to several hundred milligrams of carbon per meter squared per day. However, net-heterotrophic wintertime communities, lacking the necessary sunlight to support photosynthesis, must rely on organic matter trapped and concentrated during the freezing process (Cox and Weeks, 1983; Meiners and Michel, 2017).

This dissertation explores how bacteria within the extreme conditions of sea-ice brines access organic matter through winter, contributing to local organic carbon cycling and enabling survival and activity at low temperature and high salinity. Using a combination of laboratory techniques, field observations, and mathematical modelling, I investigate how bacteria move through their environment in search of DOC (Chapter 2), how they degrade sources of DOC once found (Chapter 3), and how interactions with their community – namely, their viruses or bacteriophage – could drive DOC recycling (Chapter 4). While each of these chapters represent distinct elements of microbial DOC cycling within sea-ice brines, together they demonstrate modes of bacterial interaction with the extracellular environment.

1.3 Sea ice and astrobiology

In addition to understanding how bacteria influence DOC cycling in terrestrial extreme environments, this dissertation deepens our understanding of potential life on other icy bodies within our solar system. Moons like Europa and Enceladus are known to possess cold, salty oceans with a very thick covering of salt-containing ice. Spectral analyses of ejecta from geysers passing through the kilometers-thick icy crust of Enceladus have indicated that many of the chemical requirements for life may be present within these oceans, making either of these bodies a strong candidate for the discovery of life beyond Earth (McKay *et al*., 2014; Hand *et al*., 2017; Waite *et al*., 2017). While the potential for life on Europa and Enceladus is discussed most commonly in the context of the underlying ocean, the ice layer provides more accessibility for sampling craft. By probing bacterial and viral activity under the most extreme ice conditions on Earth, this dissertation seeks to assess the potential existence of life within the ice layers of these moons.

The study of bacterial motility and taxis under cold to very cold temperature (5˚ to < –8˚C) conditions considered in Chapter 2 was originally conceived to help validate the use of motility as a biosignature on such icy moons (Deming, 2017). The same project deployed a novel digital holographic microscope in sea-ice environments on Earth as a demonstration of near *in situ* motility within sea ice, corroborating results seen in the laboratory (Lindensmith *et al*., 2016; Showalter & Deming, 2018). At the same time, understanding bacterial use of extracellular enzymes to degrade high molecular weight material under more extreme conditions, as presented in Chapter 3, suggests potential for bacterial activity in an extraterrestrial ice layer.

Chapter 4 seeks to assess the potential of a viral shunt, a process whereby viruses lyse bacteria and return DOC to the environment, within sea-ice brines. A potential virus shunt expands our understanding of potential habitability by presenting a mechanism for sustaining a microbial

population within saline ice through long time periods. Surface features on Europa observed by the Galileo probe imply probable occurrence of ice diapirs, pockets of mobile, deformable ice thought to convect through the crust because of a temperature differential, analogous to magmatic diapirs in Earth's crust. Diapirs are especially relevant to the study of possible life on icy moons, given their moderate conditions (250–270 K) and accessibility from the surface (Rathburn *et al*., 1998). These formations persist on time scales of hundreds of thousands of years (Ruiz *et al*., 2007), with any potential organic carbon, including life, trapped within the ice during the freezing process. Assuming that communities within this ice would be largely heterotrophic (as in terrestrial winter sea ice) and with no additional carbon inputs, would a Europan surface diapir contain active microbial communities? If microbial life from the underlying saline water can sustain activity in the frozen layer or upwelling diapirs by virtue of a viral shunt, future missions could forego logistically challenging ocean sampling in favor of ice features.

1.4 Sea ice across scales

Sea ice transcends multiple spatial and temporal scales. In the context of microbial ecology, sea ice is a regional environment of microliter-sized brine pores, dynamic across minutes and hours to months and years. On considering icy moons, planetary scale "sea" ice harboring potential microbial communities may operate on much longer scales, such as those on Earth with doubling times of hundreds to thousands of years (Price and Sowers, 2004). While this dissertation bridges terrestrial and extraterrestrial scales of sea ice, a comparative analysis of the dynamic sea-ice environment to relatively static sub-zero brines, such as in cryopeg brines which have been isolated in permafrost for >14,000 years, may yield a better understanding of how communities operate on slow temporal scales (Cooper *et al*., 2019; Zhang *et al*., 2020). In Appendix 2, I demonstrate values

of extracellular enzyme activity within cryopeg brines sampled near Utqiaġvik, Alaska, as a comparison to extracellular enzyme activity within sea ice presented in Chapter 3.

Bridging directly from microscale sea-ice features to planetary scale saline ice on icy moons also excludes an important intermediate scale of sea ice. The most common level of human interaction with sea ice is as a local or regional scale phenomenon. For those living in the Arctic, particularly indigenous Inuit, sea ice has been a factor of daily life for thousands of years, an extension of the land, an avenue of transport, and a source of sustenance (ICCC, 2008; ICC 2014). Conversely, non-Arctic communities interact with sea ice as a barrier, with a daily understanding extending only as far back as the satellite record and only as far forward as the first ice-free summer. In Appendix 3 of this dissertation, I present a brief review of how the health of Inuit communities is tied to sea ice, and how the negative health impacts of a changing climate are being countered by efforts of the Canadian government.

References

Cooper, Z. S., Rapp, J. Z., Carpenter, S. D., Iwahana, G., Eicken, H., Deming, J. W. (2019). Distinctive microbial communities in subzero hypersaline brines from Arctic coastal sea ice and rarely sampled cryopegs. *FEMS Microbiol Ecol*, *95*(12), 1–15. https://doi.org/10.1093/femsec/fiz166

Cox, G. F. N., & Weeks, W. F. (1983). Equations for determining the gas and brine volumes in sea ice samples. *J Glaciol*, *29*(102), 306–316.

D'Amico, S., Claverie, P., Collins, T., Georlette, D., Gratia, E., Hoyoux, A., *et al*. (2002). Molecular basis of cold adaptation. *Philos T R Soc B*, *357*(1423), 917–925. https://doi.org/10.1098/rstb.2002.1105

DasSarma, S., & DasSarma, P. (2015). Halophiles and their enzymes: Negativity put to good use. *Curr Opin Microbiol*, *25*(1), 120–126. https://doi.org/10.1016/j.mib.2015.05.009

Dawson, H. M., Heal, K. R., Boysen, A. K., Carlson, L. T., Ingalls, A. E., Young, J. N., Helmig, D., Arrigo, K. (2020). Potential of temperature- and salinity-driven shifts in diatom compatible solute concentrations to impact biogeochemical cycling within sea ice. *Elem Sci Anth*, *8*. https://doi.org/10.1525/elementa.421

De Maayer, P., Anderson, D., Cary, C., Cowan, D. A. (2014). Some like it cold: Understanding the survival strategies of psychrophiles. *EMBO Reports*, *15*(5), 508–517. https://doi.org/10.1002/embr.201338170

Deming, J. W. (2002). Psychrophiles and polar regions. *Curr Opin Microbiol*, *3*(5), 301–309. https://doi.org/Doi: 10.1016/s1369-5274(02)00329-6

Deming, J. W. (2019). Extremophiles: Cold environments. *Encyclo Microbiol*, 228–238. https://doi.org/10.1016/B978-0-12-809633-8.13045-6

Boetius, A., Anesio, A. M., Deming, J. W., Mikucki, J. A., Rapp, J. Z. (2015). Microbial ecology of the cryosphere: Sea ice and glacial habitats. *Nat Rev Microbiol*, *13*(11), 677–690. https://doi.org/10.1038/nrmicro3522

Ermolenko, D. N., & Makhatadze, G. I. (2002). Bacterial cold-shock proteins. *Cell Mol Life Sci*, *59*(11), 1902–1913. https://doi.org/10.1007/PL00012513

Ewert, M., & Deming, J. W. (2013). Sea ice microorganisms: Environmental constraints and extracellular responses. *Biology*, *2*(2), 603–628. https://doi.org/10.3390/biology2020603

Ewert, M., & Deming, J. W. (2014). Bacterial responses to fluctuations and extremes in temperature and brine salinity at the surface of Arctic winter sea ice. *FEMS Microbiol Ecol*, *89*(2). https://doi.org/10.1111/1574-6941.12363

Firth, E., Carpenter, S. D., Sørensen, H. L., Collins, R. E., Deming, J. W. (2016). Bacterial use of choline to tolerate salinity shifts in sea-ice brines. *Elem Sci Anth*, 1–15. https://doi.org/10.12952/journal.elementa.000120

Gerday, C., Aittaleb, M., Bentahir, M., Chessa, J. P., Claverie, P., Collins, T., *et al.* (2000). Cold-adapted enzymes: From fundamentals to biotechnology. *Trends Biotechnol*, *18*(3), 103–107. https://doi.org/10.1016/S0167-7799(99)01413-4

Golden, K. M., Eicken, H., Heaton, A. L., Miner, J., Pringle, D. J., Zhu, J. (2007). Thermal evolution of permeability and microstructure in sea ice. *Geophys Res Lett*, *34*(16), 2–7. https://doi.org/10.1029/2007GL030447

Hand, K. P., Chyba, C. F., Priscu, J. C., Carlson, R. W., Nealson, K. H. (2017). Astrobiology and the potential for life on Europa. *Europa*, *1*, 589–630. https://doi.org/10.2307/j.ctt1xp3wdw.32

Hansell, D. A., Carlson, C. A., Repeta, D. J., Schlitzer, R. (2009). Dissolved organic matter in the ocean a controversy stimulates new insights. *Oceanogr*, *22*(SPL.ISS. 4), 202–211. https://doi.org/10.5670/oceanog.2009.109

Inuit Circumpolar Council (ICC) (2014). The Sea Ice Never Stops: Circumpolar Inuit Reflections on Sea Ice Use and Shipping in Inuit Nunaat. *December*, 56. http://www.inuitcircumpolar.com/uploads/3/0/5/4/30542564/sea_ice_never_stops_-_final.pdf

Inuit Circumpolar Council-Canada (ICCC) (2008). The Sea Ice is Our Highway. *March*, 39. https://www.inuitcircumpolar.com/project/the-sea-ice-is-our-highway-an-inuit-perspective-on-transportation-in-the-arctic/

Lønborg, C., Carreira, C., Jickells, T., Álvarez-Salgado, X. A. (2020). Impacts of global change on ocean dissolved organic carbon (DOC) cycling. *Front Mar Sci*, *7*(June), 1–24. https://doi.org/10.3389/fmars.2020.00466

McKay, C. P., Anbar, A. D., Porco, C., Tsou, P. (2014). Follow the plume: The habitability of Enceladus. *Astrobiology*, *14*(4), 352–355. https://doi.org/10.1089/ast.2014.1158

Meiners, K.M., & Michel. C. (2017). Dynamics of nutrients, dissolved organic matter, and exopolymers in sea ice. In Thomas, D.N. (Ed.): *Sea Ice.* 415–432, https://doi.org/10.1016/B978-012374473-9.00637-8

Morita, R. (1975). Psychrophilic bacteria. *Bacteriol Rev*, 39(2): 144-167.

Petrich, C., & Eicken, H. (2017). Overview of sea ice growth and properties. In Thomas, D.N. (Ed.): *Sea Ice.* 1–41, https://doi.org/10.1016/B978-012374473-9.00637-8

Price, P. B., & Sowers, T. (2004). Temperature dependence of metabolic rates for microbial growth, maintenance, and survival. *Proc Natil Acad Sci USA*, *101*(13), 4631–4636. https://doi.org/10.1073/pnas.0400522101

Rathbun, J. A., Musser, G. S., Squyres, S. W. (1998). Ice diapirs on Europa: Implications for liquid water. *Geophys Res Lett*, *25*(22), 4157–4160. https://doi.org/10.1029/1998GL900135

Ruiz, J., Montoya, L., López, V., Amils, R. (2007). Thermal diapirism and the habitability of the icy shell of Europa. *Origins Life Evol B*, *37*(3), 287–295. https://doi.org/10.1007/s11084-007-9068-3

Showalter, G. M., & Deming, J. W. (2018). Low-temperature chemotaxis, halotaxis and chemohalotaxis by the psychrophilic marine bacterium *Colwellia psychrerythraea* 34H. *Environ Microbiol Rep*, *10*(1). https://doi.org/10.1111/1758-2229.12610

Vancoppenolle, M., Meiners, K. M., Michel, C., Bopp, L., Brabant, F., Carnat, G*., et al* (2013). Role of sea ice in global biogeochemical cycles: Emerging views and challenges. *Quaternary Sci Rev*, *79*, 207–230. https://doi.org/10.1016/j.quascirev.2013.04.011

Waite, J. H., Glein, C. R., Perryman, R. S., Teolis, B. D., Magee, B. A., Miller, G., *et al*. (2017). Cassini finds molecular hydrogen in the Enceladus plume: Evidence for hydrothermal processes. *Science*, *356*(6334), 155–159. https://doi.org/10.1126/science.aai8703

Zhong, Z.-P., Rapp, J. Z., Wainaina, J. M., Solonenko, N. E., Maughan, H., Carpenter, S. D., *et al*. (2020). Viral ecogenomics of Arctic cryopeg brine and sea ice. *MSystems*, *5*(3), 1–17. https://doi.org/10.1128/msystems.00246-20

Chapter 2.

Low-temperature chemotaxis, halotaxis and chemohalotaxis by the psychrophilic marine bacterium *Colwellia psychrerythraea* 34H

(This manuscript has been published previously as: Showalter, G.M., & Deming, J.W. (2018). Low-temperature chemotaxis, halotaxis and chemohalotaxis by the psychrophilic marine bacterium *Colwellia psychrerythraea* 34H. *Environmental Microbiology Reports, 10*(1), 92–101. doi: 10.1111/1758-2229.12610)

Abstract

A variety of ecologically important processes are driven by bacterial motility and taxis, yet these basic bacterial behaviors remain understudied in cold habitats. Here we present a series of experiments designed to test the chemotactic ability of the model marine psychrophilic bacterium *Colwellia psychrerythraea* 34H, when grown at optimal temperature and salinity (8°C, 35 ppt) or its original isolation conditions (–1°C, 35 ppt), towards serine and mannose at temperatures from –8 to 27°C (above its upper growth temperature of 18°C), and at salinities of 15, 35 and 55 ppt (at 8 and –1°C). Results indicate that *C. psychrerythraea* 34H is capable of chemotaxis at all temperatures tested, with strongest chemotaxis at the temperature at which it was first grown, whether 8 or –1°C. This model marine psychrophile also showed significant halotaxis towards 15 and 55 ppt solutions, as well as strong substrate-specific chemohalotaxis. We suggest that such patterns of taxis may enable bacteria to colonize sea ice, position themselves optimally within its extremely cold, hypersaline and temporally fluctuating microenvironments, and respond to various chemical signals therein.

2.1 Introduction

Motility and taxis are important survival strategies for many bacteria and critical to a variety of microbial processes, including biofilming (reviewed by Guttenplan & Kearns, 2013), pathogenicity (Josenhans & Suerbaum, 2002) and genetic competence (Meibom *et al.,* 2005). While much foundational knowledge of motility and taxis has been learned from mesophilic organisms like *Escherichia coli* (presented in detail by Berg, 2004) and *Pseudomonas alteromonas* (reviewed by Kato *et al.*, 2008), these processes are also considered to be widespread, if intermittent and of variable character, throughout the world's oceans based on seawater studies at temperatures of 15°C or warmer (Grossart *et al.*, 2001; Mitchell & Kogure, 2006).

Chemotaxis in particular has been hypothesized as an important process that allows bacteria to exploit the organic particles, point sources, and short-lived, patchy nutrient gradients that characterize the marine environment (Jackson, 1987; Kiørboe *et al*., 2001; Barbara *et al*., 2003; Stocker *et al*., 2008). Further studies have characterized the unique physical and ecological considerations for chemotaxis in the ocean (Stocker & Seymour, 2012; Taylor & Stocker, 2012). In laboratory studies of bacterial isolates, chemotaxis in seawater has been examined in the context of colonization, association, or nutrient consumption, for example with phytoplankton (*e.g.,* Bowen, *et al*., 1993; Barbara & Mitchell, 2002; Seymour *et al*., 2009; Smriga *et al.,* 2015). Studies of bacterial taxis *in situ* have shown that "infochemicals", for example DMSP, play an important role in driving chemotaxis and colonization of corals and other marine environments (Thurber *et al*., 2009; Raina *et al.*, 2010; Seymour *et al*., 2010; Garren *et al*., 2014; Tout *et al*., 2015a). For certain *Vibrio* populations, temperature (31°C) modulates their associations with corals, implying thermal effects on motility *(*Tout *et al.*, 2015b).

The majority of the world's ocean, however, is cold (5°C or below), and gradients encompassing more extreme (sub-zero) temperatures characterize the polar oceans. Gradients exist at the seawater/sea ice interface and the unfrozen brines within the ice, which also feature gradients in organic compounds and salt concentrations (Eicken, 2003; Krembs *et al*., 2011). Yet, the tactic behavior of bacteria in these environments is unknown. Only a few studies have examined taxis at cold temperatures. Chemotaxis at 5°C has been shown in *Pseudomonas fluorescens* (Lynch, 1980), *Colwellia maris* (Takada *et al*., 1993), and *Vibrio anguillarum* (Larsen *et al.*, 2004), while Hazeleger *et al*. (1998) demonstrated the ability of the enteric bacterium *Campylobacter jejuni* to chemotax at 4°C. The effects of even lower temperatures on bacterial chemotaxis or halotaxis, and certainly the sub-zero temperatures of sea-ice brines, are poorly understood.

There are many reasons to expect that temperature impacts the extent and efficiency of bacterial sensing and taxis. *E. coli* is known to use a robust, complex kinase cascade to propagate signals from surface chemoreceptors to the flagellum to direct chemotaxis (Alon *et al*., 1999; Bren & Eisenbach, 2000). The chemical reactions involved are individually very sensitive to temperature fluctuations, but kinetic parameters and enzyme synthesis in the chemotactic response cascade are temperature-compensated, leading to thermal robustness across the physiological range of *E. coli* (Oleksiuk *et al*., 2011). With both marine bacterial isolates and mesophilic *E. coli,* however, these pathways have been investigated only at relatively moderate temperatures (10–35°C) compared to those experienced by bacteria in cold seawater and within the brines of the sea-ice matrix, where temperatures can extend below –20°C (Junge *et al.,* 2004).

At cold temperatures, additional physical and physiological processes may reduce or inhibit the receipt of chemical signals that trigger bacterial chemotaxis, including fatty acid transition leading to lipid membrane rigidity (Lofgren and Fox, 1974), high salinities requiring

transport actions to maintain turgor pressure (Firth *et al*., 2016), and increased viscosity slowing diffusion (Schneider & Doetsch, 1974; Seymour & Stocker, 2012). Additionally, the fractal microstructure of sea-ice brine pores leads to high surface area to volume ratios (Krembs *et al.*, 2011), possibly favoring surface attachment over motility.

Studying motility and taxis at cold temperatures is challenging. Methods to study bacterial movement have focused primarily on mesophiles, with the recent inclusion of mesophilic marine bacteria and direct visualization using microscopy (reviewed by Son *et al.*, 2015). These studies often use microfluidic devices to observe individual and population responses to the introduction of gradients in nutrients, gases, repellents, *etc*. (Seymour *et al*., 2008; Ahmed *et al.*, 2010; Seymour *et al*., 2010). While these methods can produce rich and robust data sets, they can be expensive and difficult to adapt to cold temperatures which fog glass and cause small volumes of liquids to freeze easily. Previous studies have involved high resolution microscopes factory modified for sub-zero conditions, as well as cold rooms or freezers large enough to allow human operators to manipulate samples and microscopes (Junge *et al*., 2001, 2003). Although a cold stage on a microscope at room temperature (Bar Dolev *et al*., 2016) could be adapted for taxis studies, the traditional capillary tube assay, first used by Pfeffer (1884) and refined by Adler (1973), provides an imminently feasible and economic means to study bacterial taxis at cold temperature. This and similar techniques have already been adapted to marine bacteria (Larsen *et al*., 2004; Tout *et al.,* 2015a). In the classic assay, the chemotactic response of bacteria presented with a gradient in the attractant (or repellent) of interest is evaluated by enumerating those that swim into a capillary tube, the source of the high end of the diffusion-established gradient, relative to a control tube absent the target compound.

Colwellia psychrerythraea strain 34H (hereinafter *Cp*34H), was selected for this study as a model marine psychrophile (Methé et al., 2005). Originally isolated from Arctic marine sediments at –1°C (Huston, 2003), *Cp*34H has subsequently been found in other cold marine environments and is considered highly ice-adapted (Boetius *et al.*, 2015). *Cp*34H currently holds the low-temperature record for motility at –10°C, first observed in an analogue sea-ice brine (along with robust swimming at –8, –5 and –1°C; Junge *et al*., 2003), and since confirmed by digital holographic microscopy (Wallace *et al.,* 2015). At –1°C, *Cp*34H also transports compatible solutes (small molecular weight organic compounds) to tolerate salinity shifts inherent to sea-ice brines (Firth *et al*., 2016). Optimal (most rapid) growth occurs at 8°C and 35 ppt in organically rich media, with the growth range spanning –12°C to 22°C, and 15 to 70 ppt salinity (Huston, 2003; Wells & Deming, 2006). The responses of *Cp*34H, however, to the complex gradients in temperature, salinity, and nutrients presented by the sea-ice environment have yet to be characterized, leading to this work.

In preliminary work, we had observed thermotaxis by *Cp*34H; i.e., when grown at its optimal growth temperature of about 8°C (and salinity of 35 ppt) but placed at higher and lower temperatures, *Cp*34H swam towards its growth temperature (Showalter & Deming, Abstr. 115th Gen. Meet. Am. Soc. Microbiol. 2015). These observations of thermotaxis, coupled with previously published work showing optimal chemotaxis at optimal growth temperature for *E. coli* and *Vibrio anguillarum* (Takada *et al*., 1993; Larsen *et al.*, 2004; Oleksiuk, *et al.*, 2011), led us to hypothesize that *Cp*34H would behave similarly, with strongest chemotaxis occurring at its optimal growth temperature. We considered that at cold temperatures suboptimal for growth, the chemotactic response of *Cp*34H would be stronger to compounds able to provide a greater return of energy or to signal a more optimal environment. Given the co-occurring nutrient and salinity

gradients that characterize the sea-ice environment, we also hypothesized that when presented with chemoattractants under salinities higher and lower than seawater *Cp*34H would continue to exhibit chemotaxis, i.e. to exhibit *chemohalotaxis.*

Here we present the results of capillary tube experiments designed to characterize the chemotactic and halotactic behavior of *Cp*34H toward the amino acid serine (0.1 M to 1 M) and the sugar monomer mannose (1 M) across a range of temperatures (−8, −1, 8, 15, 22, and 27°C) and salinities (15, 35, and 55 ppt). Our goal was to provide foundational information on the potential for bacterial taxis within the gradients that characterize sea ice and its interface with seawater. Several factors suggested the use of serine as an experimental chemoattractant, including the finding that serine is the most dominant amino acid in sea ice, at likely millimolar concentrations in the brine (Yang, 1995). Serine is also commonly used as a chemoattractant in tests of laboratory isolates, in part because the *tsr* receptor, which senses serine, is among the most highly expressed chemoattractant receptors in *E. coli* (Feng *et al.,* 1997). Additionally, the *tsr* receptor is a component of thermosensory systems in *E. coli*, such that serine impacts how bacteria sense temperature gradients (Clarke & Koshland, 1979; Maeda & Imae, 1979). A survey of the *Cp*34H genome using the GenBank database (Clark *et al*., 2016) revealed that *Cp*34H contains methyl-accepting chemotaxis proteins similar to *tsr.* Mannose was chosen because it is a common monosaccharide found in sea ice (Aslam *et al*., 2016), often dominates the composition of exopolysaccharides produced by sea-ice bacteria (Underwood *et al.*, 2010), and might provide more energy (ATP) than serine if assimilated and catabolized. Mannose has also been used in temperate studies of marine chemotaxis in the context of coral reef bacteria, which demonstrated chemotaxis toward 100 μM mannose while bacteria not associated with reefs did not (Tout *et al.*, 2015a). Ultimately, we examined comparative tactic responses of our model organism when grown

at its optimal growth temperature (8°C) versus isolation temperature (–1°C), as the latter better represents polar waters and the sea-ice environment.

2.2 Materials and methods

2.2.1 Bacterial cultures

Cultures of *Colwellia psychrerythraea* strain 34H (*Cp*34H) were grown from glycerol-protected stocks stored at −70°C from the original isolate. The bacteria were grown in ½ strength 2216 Difco Marine Broth, adjusted to full-strength seawater salinity (35 ppt) using artificial seawater (ASW: 0.4 M NaCl, 9 mM KCl, 26 mM $MgCl_2$, 28 mM $MgSO_4$, and 5 mM TAPSO buffer) at their optimal growth temperature of approximately 8°C (Huston *et al*., 2003) in a cold room set at 8°C (± 1°C), with shaking at 220 hz. For test of cells grown below optimal growth temperature, they were grown similarly but at –1°C (± 1°C) in a temperature-controlled incubator (Caravell CIC65 Impulse Display Chiller), again with shaking. Bacteria were harvested for experiments in mid-log growth phase as determined by optical density (absorbance = 0.3–0.6, after approximately 3–5 days) and spot-checked using light microscopy to ensure samples displayed typical levels of motility. To harvest, cultures were centrifuged at x1000 g for 20 min in a temperature-controlled centrifuge (6–10°C) and resuspended in a chilled motility medium of ASW with a final salinity of 35 ppt (measured by refractometer), and 0.1 mM EDTA, added to chelate any free metals that inhibit motility as per the original motility protocol (Adler, 1973). The centrifugation and resuspension step was performed twice to remove dissolved organic compounds. In treatments below −1°C, an additional 5% glycerol w/v was added to the resuspension solution to prevent freezing without raising salinity. This addition does not alter

swimming speeds in *Cp*34H at subzero temperatures (Junge *et al.,* 2003), nor did tests for chemotaxis to glycerol elicit a response from *Cp*34H. For non-seawater salinity experiments, the resuspension medium contained ASW, diluted with distilled water (for 15 ppt treatment) or amended with 210 ppt NaCl (for 55 ppt treatment), and 0.1 mM EDTA.

2.2.2 Experimental set-up and treatments

Aliquots of the harvested bacteria in motility medium were distributed into Eppendorf tubes, each of which was then capped with parafilm. These sealed bacterial reservoirs (containing an average of $3.12 \pm 2.14 \times 10^7$ cells mL^{-1}, n = 10) were equilibrated at the desired experimental temperature for one hour prior to the introduction of chemoattractant; the chemoattractant solutions and control solutions of chemoattractant-free or, in the case of halotaxis, same-salinity motility medium were equilibrated similarly. After the equilibration period, sterile capillary tubes (30 µL Drummond Microcaps) were placed in the chemoattractant and control solutions to draw solution into the tube. The filled capillary tubes were then capped with a 2% agar plug to prevent evaporation or a change in fluid level within the tube during the experiment.

An experiment was initiated by placing a filled, temperature-equilibrated capillary tube into a bacterial reservoir, piercing the parafilm and allowing the tube to rest immersed in the reservoir. The set-up was then left to incubate at the desired temperature. For each experimental treatment, set-ups were prepared and incubated in triplicate: three biological replicates and three chemoattractant-free controls. Parallel cultures of *Cp*34H were always incubated at room temperature for each experiment as a check against possible bacterial contamination in the media or the cultures (none was ever detected). Because the presence of taxis above growth temperature was unexpected, experiments at 22°C and 27°C were repeated multiple times to confirm the attribution of chemotaxis to *Cp*34H above its upper growth temperature.

Chemotaxis was examined in set-ups incubated at −8, −1, 8, 15, 22, and 27°C for *Cp*34H grown at its optimal growth conditions of 8°C and 35 ppt. Additional experiments were conducted at −1, 8, and 15°C when the organism was grown instead at −1°C (and 35 ppt, optimal growth salinity at −1°C; Huston, 2003). Halotaxis was examined in *Cp*34H grown at 8°C and 35 ppt by presenting the bacteria with gradients determined by a different salinity, 15 or 55 ppt, in (chemoattractant-free) capillary tubes, incubated in set-ups at 8 and −1°C (35 ppt served as the control salinity). Chemohalotaxis was examined under the same conditions using capillary tubes filled with chemoattractant at the different salinities. For each set of temperature and salinity conditions tested, the bacteria were presented, in triplicate and separately, with gradients determined by 1 M serine and 1 M mannose in the capillary tubes, as well as the chemoattractant-free control.

Incubation times for the diffusion-based set-ups were selected so that the diffusion distance of chemoattractant would be approximately equal across the temperatures tested. Diffusion rates were calculated as a function of temperature and glycerol addition (altered viscosity) by approximating change in diffusion coefficient according to the Stokes-Einstein equation and then scaling relative to empirical data obtained at a reference temperature of 8°C. The selected incubation periods for temperatures of −8, −1, 8, 15, 22, and 27°C, were 6, 4, 2, 1.5, 1.5, and 1.5 hours, respectively. Diffusion coefficients do not scale linearly across these conditions, accounting for use of the same incubation times at warmer temperatures. Using more refined incubation periods to account for temperature-dependent diffusional differences more precisely at the warmer temperatures was not possible given unavoidable sample handling and processing time. Validation experiments were conducted at −8, 8, and 15°C using a low-molecular weight dye in place of chemoattractant for the calculated experimental periods (6, 2, and 1.5 hours, respectively). The

concentration of dye that had diffused into the reservoir after the treatment period was measured using spectrophotometry and was the same order of magnitude across all temperatures after the respective periods when compared to a standard curve.

Growth experiments were performed in parallel incubations, using cells treated as they were in chemotaxis experiments at −8, 8, and 15°C. Bacteria were counted manually using epifluorescence microscopy, as in previous studies (Marx *et al.*, 2009; Ewert & Deming, 2014). No significant (95% confidence level) growth was observed during the incubation periods equivalent to the experimental treatments.

After incubation, capillary tubes were removed from the reservoir and the capillary contents were expelled as droplets onto sterile parafilm. Aliquots of 20 μL were taken from the droplets and transferred directly to 4 mL of 0.2 μm-filtered ASW with 2% formaldehyde and 0.5% Triton-X. Fixed samples were stored in the dark at 4°C for a maximum of 12 hours until manual counting by epifluorescence microscopy, as in previous studies (Marx *et al.*, 2009; Ewert & Deming, 2014).

Bacteria were stained with a 20 μg ml^{-1} solution of 4',6'-diamidino-2-phenylindole (DAPI) in ASW and viewed with a Zeiss epifluorescence microscope, counting at least 200 cells per field and 20 fields per sample; counts were then scaled to the experimental volume.

The mean concentration of bacteria present in the treatment capillary tubes was compared to the mean concentration in the control tubes (triplicate set-ups in both cases) to evaluate the chemotaxis, halotaxis or chemohalotaxis response for a given set of conditions. The significance of the difference was determined by a student t test. The ratio of mean bacterial concentration in treatment versus control tubes was presented graphically (Figures 2.2–2.4) to depict the relative response between different test conditions.

2.3 Results and discussion

The results of our experiments, across the set of temperature and salinity conditions under which *Colwellia psychrerythraea* 34H was grown and tested for chemotaxis, halotaxis, and chemohalotaxis are presented in graphical form (Figures 2.1–2.4). To our knowledge, these results are unique in their demonstration of bacterial chemotaxis below 4°C, and they establish a new low-temperature record of –8°C (the lowest temperature we tested) for bacterial chemotaxis. They are also unique in demonstrating significant halotaxis and strong substrate-specific chemohalotaxis by a marine bacterium.

Obtaining internally consistent results across these conditions, which included warm, cold and sub-zero temperatures, required time-scaling and anti-freeze adjustments to the capillary tube assay, originally designed for room temperature work. Bacterial densities in the sets of treatment and control capillary tubes, with p-values for significance of the difference using a Student's t-test, are listed in Table 2.1. Significant ($p < 0.05$) results of two-way ANOVAs, used to examine interactions between experimental factors, are provided in the course of the discussion below.

2.3.1 Chemotaxis, when *Cp*34H was grown at 8°C

To first determine a suitable concentration of chemoattractant to use in this study, a dose-response experiment was conducted with 10 mM, 100 mM, and 1 M serine, commonly used concentrations in the pure-culture chemotaxis literature (*e.g.,* Alder, 1973; Takada *et al.*, 1993). *Cp*34H had been grown in nutrient-rich media (Difco Marine Broth 2216) at optimal growth temperature and salinity (8°C and 35 ppt), prior to rinsing and testing for chemotaxis at the same temperature and salinity. Negative controls of capillary tubes with no chemoattractant accounted for random motility. The organism's chemotactic response to 1 M serine was strong and significant

(Figure 2.1). The response to a lower concentration of 100 mM serine, though significant, was weaker, while the response to 10 mM serine was not significant (Figure 2.1). As similar results were obtained with mannose (not shown), a 1 M concentration of chemoattractant was used in all subsequent experiments. Organisms grown in nutrient-rich media may express low-sensitivity chemoreceptors because of heavy methylation of chemoreceptors (Terracciano & Canale-Parola, 1984), but the purpose of this study was to examine temperature and salinity conditions that could support chemotaxis, not to decipher receptor sensitivity in *Cp*34H.

In subsequent experiments, *Cp*34H demonstrated significant chemotaxis at all test temperatures (Figure 2.2): –8, –1, 8, 15, 22, and 27°C (all at salinity of 35 ppt; incubated for 8, 4, 2, 1.5, 1.5, and 1.5 hours, respectively), with strongest chemotaxis observed at the temperature at which the organism had been grown (8°C in Figure 2). Although the strongest response was to serine (at 8°C, with notable activity at –1°C), the temperature range for serine as chemoattractant was narrower than the range for mannose. No significant chemotaxis to serine was detected at the ends of the temperature test range, –8°C and 27°C; in contrast, chemotaxis to mannose was significant across the entire range (Figure 2.2). Mannose also tended to be the stronger chemoattractant at the warmer temperatures (Figure 2.2), including above maximal growth temperature (18°C, Huston, 2003), although insignificantly when compared to serine.

This pattern of a broad temperature range for chemotaxis with strongest taxis at optimal growth temperature, likely due to methylation of chemotaxis proteins, is generally consistent with results obtained for other bacteria, including two marine bacteria, *Vibrio anguillarum* (optimal growth and strongest chemotaxis at 25°C; Larsen *et al*., 2004) and *Colwellia maris* (optimal growth and strongest chemotaxis at 15°C; Takada *et al*., 1993). Also like *V. anguillarum* and *C. maris*, *Cp*34H remained significantly chemotactic at temperatures below optimal growth

temperature (8°C for *Cp*34H); i.e., at –1 and –8°C (Table 2.1). Both of these temperatures still fall within the growth range of *Cp*34H, which is bounded by –12°C and 18°C (Wells & Deming, 2006); we were not able to test for chemotaxis at or below the lower growth temperature.

Observations of chemotaxis at 27°C, 9°C above the upper growth temperature of *Cp*34H, suggest that *Cp*34H expends energy for high physiological activity beyond the bounds of growth. This phenomenon has been observed previously for chemotaxis when extending tests below the lower thermal bound for growth; e.g., Hazeleger *et al*. (1998) demonstrated chemotaxis in *Camplyobacter jejuni* as much as 30°C below its minimum growth temperature. Temperature-dependent motility responses have also been shown in *B. subtilis,* which produced proteins connected to flagellar synthesis and chemotaxis when shocked with low temperature (Graumann *et al*., 1996). For *Cp*34H, a strict psychrophile, we suggest that the chemotactic response at 27°C may indicate a short-term survival response to warm temperatures, a testable hypothesis in future experiments. Previous studies have demonstrated that proper membrane fluidity is required for chemotaxis (Lofgren *et al.*, 1974), likely due to membrane-embedded methyl-accepting chemotaxis proteins. The chemotactic responses of *Cp*34H demonstrate versatility in expressing the membrane rigidity required to respond chemotactically at 27°C, as well as the fluidity to respond at the sub-zero end of its temperature range. As the chemotaxis response of *Cp*34H above its upper growth temperature stands in contrast to previous work with *Colwellia maris*, where no chemotaxis was observed above its upper growth temperature (between 20 and 24°C; Takada *et al.*, 1993), more research on this aspect of chemotaxis is needed.

2.3.2 Chemotaxis, when *Cp*34H was grown at –1°C

*Cp*34H grown at the environmentally relevant temperature of –1°C demonstrated chemotaxis toward serine and mannose at similar magnitudes as when grown at optimal growth

temperature (8°C); the peak responses, however, were shifted from 8°C (Figure 2.2) to –1°C (Figure 2.3). This marine psychrophile thus appears to behave as the mesophile *E. coli* in showing thermal robustness for chemotaxis across its physiological growth range (Oleksiuk *et al*., 2011). As *Cp*34H is capable of growth at even colder temperatures (to –12°C; Wells & Deming, 2006), chemotaxis may be expected at such temperatures, as suggested by the significant response to mannose measured at –8°C (Figure 2.2). We observed that the chemotactic response to mannose at –1°C was significantly higher when *Cp*34H had been grown at –1°C (Figure 2.3) than when grown at 8°C (t test, $p = 0.002$; Figure 2.2). A two-way ANOVA comparing the effect of temperature and chemoattractant on chemotactic response of cells grown at –1°C indicated that experimental temperature was the main effect determining chemotactic response ($p = 1.06 \times 10^{-6}$). Comparing cells grown at –1°C and cells grown at 8°C indicated significant interaction between temperature and growth temperature at the 90% confidence level ($p = 0.0665$), implying that specific responses to serine versus mannose were connected to temperature.

Although the molecular-level mechanisms accounting for chemotactic and substrate-specific responses at sub-zero temperature remain to be determined, directed bacterial movements under the extreme temperatures we tested have both physiological and environmental implications, as discussed below.

2.3.3 Halotaxis and chemohalotaxis

As temperature gradients in sea ice and environs are accompanied by gradients in salinity and organic solutes, we included experiments to test for halotaxis and chemohalotaxis by *Cp*34H. When cultures grown under optimal conditions (8°C, 35 ppt) were presented with a salinity signal (absent organic chemoattractants) of either higher or lower salinity in the capillary tube, with the salts diffusing to create a gradient, *Cp*34H demonstrated significant halotaxis in each salinity

gradient at both test temperatures: 8°C (Figure 2.4A) and –1°C (Figure 2.4B). The strongest halotactic response was observed at –1°C in the gradient towards fresher salinity, simulating the melting of sea ice into –1°C seawater. Strong halotaxis near the freeze/thaw boundary for Arctic seawater (about –1.9°C) might indicate that bacteria use a change in salinity as a signal to colonize freezing sea ice in fall or to leave melting sea ice in spring (Figure 2.5). Future studies investigating bacterial taxis *in situ* at the sea ice/seawater boundary may provide tests of this hypothesis.

When a gradient in organic chemoattractant was presented simultaneously with the salinity gradient, significant chemohalotaxis was observed under all conditions (Figure 2.4A). Although patterns of response to the different chemoattractants were observed, a two-way ANOVA comparing effects of treatment temperature and chemoattractant indicated that temperature was the most important factor determining chemotaxis ($p = 0.0006$), whereas chemoattractant did not have a significant effect. The strongest chemohalotactic response was recorded at –1°C in a gradient towards higher salinity (55 ppt) and mannose (1 M) (Figure 2.4B). This result, and similar results from the earlier chemotaxis experiments, imply that under optimal growth conditions, *Cp*34H may chemotax more strongly to the nitrogen-containing chemoattractant serine (*e.g.*, at 8°C, the response to serine was greater than to mannose [$p = 1.90 \times 10^{-5}$]). When confronted with suboptimal or stressful conditions, however, the sugar monomer mannose was the stronger chemoattractant (*e.g.,* at –1°C and 15 ppt salinity [$p = 0.003$], and at –1°C and 55 ppt [$p = 0.003$]). From an energetic perspective, this finding is consistent with the hypothesis that *Cp*34H may seek substrate for maximum yield of ATP to counter suboptimal or stressful conditions (6-C mannose catabolism yields 2 ATP per unit, while 3-C serine catabolism yields 1 ATP per unit). In the context of the sea-ice environment, however, other explanations may pertain. Sea ice is an algae-rich habitat during the bloom season, and the concurrent production of extracellular polymeric

substances (EPS) by both algae and bacteria, including *Cp*34H (Marx *et al*., 2009), can lead to high concentrations of exopolysaccharides within sea-ice brine pockets and at the sea ice/seawater interface (Krembs *et al*., 2002; 2011), where such complex sugars serve as extracellular cryoprotectants, inhibiting ice formation near cells, and osmoprotectants, providing a hydrated buffer against salinity extremes (Krembs & Deming, 2008; Deming & Young, 2017). Algal EPS most commonly contain the monomers glucose and mannose, in varying concentrations (Aslam *et al.,* 2016), and though not yet possible to quantify on the relevant micrometer scale, gradients in such monomers due to EPS hydrolysis can be expected based on microscopic evidence (Krembs *et al*., 2011). The strong chemotactic response of *Cp*34H towards mannose may reflect the benefits of seeking algal EPS, which may serve as a source of energy, as protection against the extreme conditions of temperature and salinity that characterize sea ice (Ewert & Deming, 2014), or as a chemical signal to bacteria. The possibility that mannose may also serve as an intracellular osmoprotectant, once found and taken up by an organism, remains to be explored.

At the sea ice/seawater interface, salinity gradients are present both as the ice grows, rejecting high salinity brine into underlying seawater, and as the ice melts, releasing fresh or lower salinity water into the surface ocean (Figure 2.5). Our results suggest that *Cp*34H may have the capacity to respond to salinity gradients in both of these contexts, as halotaxis was demonstrated in response to salinities both higher and lower than seawater salinity, albeit under controlled laboratory conditions. These results are unique to *Cp*34H as compared to demonstrations of osmotaxis and halotaxis in *E. coli*, which prefers low concentrations of osmolyte under all tested conditions (Li *et al*., 1988). The difference in halotactic response of *Cp*34H at −1°C compared to 8°C suggests that temperature may influence the osmo-sensing ability, perhaps as a result of changes in membrane fluidity. Previous analysis of lipid membrane composition in *Cp*34H has

suggested that the organism is capable of homeoviscous acclimation at low temperatures (Methé *et al.,* 2005; Nunn *et al.*, 2014), and *Cp*34H has been shown to increase its number of monounsaturated fatty acids at −1°C as compared to 9°C (Huston, 2003). This change in membrane fluidity and fatty acid composition may modulate sensitivity or function of osmo-sensing proteins which are located in the bacterial membrane (Poolman *et al*., 2004; Los *et al*., 2004).

2.3.4 Implications for microbial life within sea ice

Although the results of this study may help to inform bacterial behavior at the sea ice/seawater interface, the scope of motility and chemotaxis within the ice is still an outstanding question for further investigation. Previous studies have shown that *Cp*34H is capable of motility in sea-ice brine analogues at and below −10°C (Junge *et al*., 2003; Wallace *et al*., 2015), but bacterial motility has not been visualized directly in natural sea ice. Here, we have demonstrated in laboratory experiments that *Cp*34H is capable not only of motility but also of chemotaxis between −8°C and 27°C and 15 to 55 ppt. In particular, *Cp*34H showed strong chemohalotaxis toward mannose at –1°C in a salinity gradient (upper bound set by 55 ppt) and chemotaxis toward mannose even at −8°C (in 35 ppt salt with 5% glycerol). These findings indicate that chemotaxis may be feasible within the sea-ice brine network (Figure 2.5). Indeed, 16S rRNA gene sequence data indicate that motile copiotrophic members of the *Gammaproteobacteria* and *Flavobacteria* commonly dominate sea-ice bacterial communities (Bowman *et al*., 2012; Boetius *et al*., 2015). Though untested, bacterial taxis toward mannose may allow colonization of sea ice, contributing to community differentiation from seawater.

Several factors, however, appear to argue against chemotaxis within sea-ice brines. More than 95% of the bacteria in sea ice reside in the brine fraction, but most of them are associated

with surfaces or EPS gels in the brine (Junge *et al*., 2001; 2004; Meiners *et al*. , 2008). Proteomic investigations of *Cp*34H have indicated loss of flagellar synthesis proteins after 24 hours at −10°C, possibly leading to surface association (Nunn *et al.,* 2015). Nunn *et al*. (2015) also demonstrated upregulation of chemosensing proteins at −10°C, which may indicate a "lie and wait" strategy by *Cp*34H, quickly returning to a chemotactic state upon sensing a lucrative chemical gradient. Indeed, Lindensmith *et al*. (2016) were able to stimulate taxis in non-motile bacteria in sea-ice brines by adding marine broth to the brines (Lindensmith *et al.,* 2016), implying the use of a similar 'lie and wait' strategy by bacteria *in situ*.

Future studies to determine environmental conditions that favor surface attachment and biofilming over motility and chemotaxis within sea ice will increase understanding of microbial ecology within sea ice. Recently, Bar Dolev *et al.* (2016) showed the production of a "molecular fishing hook" by *Marinomonas primoryensis*, allowing the organism to attach to the surface of ice crystals, while Carillo *et al*. (2015) and Casillo *et al*. (2017) showed that capsular and extracellular polysaccharides produced by *Cp*34H have ice-binding properties. If organisms such as *M. primoryensis* and *Cp*34H are capable of biofilming on ice as a surface, they may also experience enhanced horizontal gene transfer and variable viral infection dynamics, as in the well-known mesophilic *Vibrio* case (Meibom, 2005), which could improve understanding of the evolution and function of marine microbial communities in the cold. Tools to visualize bacteria within sea-ice brines directly, such as digital holographic microscopy (Wallace *et al*., 2015; Lindensmith *et al*., 2016), and to examine viral action directly (Brum & Sullivan, 2015), may allow the probing of these questions in a true environmental context in future studies. The results of this study lay groundwork by demonstrating that cold-adapted bacteria may be able to position themselves

within the sea-ice matrix by chemotaxis, halotaxis and chemohalotaxis, seeking optimal energy gains or responding to chemical signals prior to attachment.

Acknowledgements

We thank SD Carpenter for help with experimental procedures, JA Baross, R Woodgate, and JN Young for discussion of experimental design and analysis, and K Golden and R Woodgate for help with analyzing the mathematics of diffusion scaling. This research was supported by the Gordon and Betty Moore Foundation (GBMF) grant number 4037. The authors declare no conflict of interest.

References

Adler, J. (1973). A method for measuring chemotaxis and use of method to determine optimum conditions for chemotaxis by *E. coli*. *J Gen Microbiol 74,* 77–91.

Ahmed, T., Shimizu, T. S., Stocker, R. (2010). Microfluidics for bacterial chemotaxis. *Integr Biol 2*, 604–629.

Alon, U., Surette, M. G., Barkai, N., Leibler, S. (1999). Robustness in bacterial chemotaxis. *Nature 397,* 168–171.

Aslam, S. N., Michel, C., Niemi, A., Underwood, G. J. C. (2016). Patterns and drivers of carbohydrate budgets in ice algal assemblages from first year Arctic sea ice. *Limnol Oceanogr 61,* 919–937.

Barbara, G. M., & Mitchell, J. G. (2002). Bacterial tracking of motile algae. *FEMS Microbiol Ecol 44,* 79-87.

Barbara, G. M., & Mitchell, J. G. (2003). Marine bacterial organization around point-like source of amino acids. *FEMS Microbiol Ecol 43,* 99–109.

Bar Dolev, M., Bernheim, R., Guo, S., Davies, P. L, Braslavsky, I. (2016). Putting life on ice: Bacteria that bind to frozen water. *J R Soc Interface 13*.

Berg, H. (2004). *E. coli* in Motion. *Biological and Medical Physics, Biomedical Engineering.* Spring-Verlag, New York, USA.

Boetius, A., Anesio, A.M., Deming, J. W., Mikucki, J. A., Rapp, J. Z. (2015). Microbial ecology of the cryosphere: sea ice and glacial habitats. *Nat Rev Microbiol 13,* 677–690.

Bowen, J. D., Stolzenbach, K. D., Chisholm, S. W. (1993). Simulating bacterial clustering around phytoplankton cells in a turbulent ocean. *Limnol Oceanogr 38,* 36–51

Bowman, J. S., Rasmussen, S., Blom, N., Deming, J. W., Rysgaard, S., Sicheritz-Ponten, T. (2012). Microbial community structure of Arctic multiyear sea ice and surface seawater by 454 sequencing of the 16s RNA gene. *ISME J 6,* 11–20.

Bren, A., & Eisenbach, M. (2000). How signals are heard during bacterial chemotaxis: Protein-protein interactions in sensory signal propagation. *J Bacteriol 182*(24), 6865–6873.

Brum, J. R., & Sullivan, M. B. (2015). Rising to the challenge: Accelerated pace of discovery transforms marine virology. *Nat Rev Microbiol 13*, 147–159.

Carillo, S., Casillo, A, Pieretti, G., Parrilli, E., Sannino, F., Bayer-Giraldi, M. (2015). A unique capsular polysaccharide structure from the psychrophilic marine bacteria *Colwellia psychrerythraea* 34H that mimics antifreeze (glyco)proteins. *J Am Chem Soc 137*(1), 179–189.

Casillo, A., Parrilli, E., Sannino, F., Mitchell, D. E., Gibson, M. I., Marino, G., *et al.* (2017). Structure-activity relationship of the exopolysaccharide from a psychrophilic bacterium: A strategy for cryoprotection. *Carbohydr Polym 156*, 364–371.

Clark, K., Karsch-Mizrachi, I., Lipman, D. J., Ostell, J., Sayers, E. W. (2016). GenBank. *Nucleic Acids Res 4*(44), D67–D72.

Clarke, S., & Koshland, D. E. (1979). Membrane receptors for apstartate and serine in bacterial chemotaxis. *J Biol Chem 254*(19), 9695–9702.

Deming, J. W., & Eicken, H. (2007). Life in Ice. *Cambridge University Press, Cambridge, U.K.*

Deming, J. W., & Young, J. N. (2017). The role of exopolymers in microbial adaptation to sea ice. In Margesin, R., Schinner, F., Marx J. C., Gerday, C. (Eds.), *Psychrophiles: From biodiversity to biotechnology.* Berlin-Heidelberg, Springer Verlag.

Eicken, H. (2003). From the microscope to the macroscopic to the regional scale: Growth, microstructure and properties of sea ice. In Thomas, D.N. & Dieckmann, G.S. (Eds.), *Sea ice; an introduction to its physics, chemistry, biology and geology.* Blackwell Science, Oxford, United Kingdom.

Ewert, M., & Deming, J. W. (2014). Bacterial responses to fluctuations and extremes in temperature and brine salinity at the surface of Arctic winter sea ice. *FEMS Microbiol Ecol 89*, 476–489.

Feng, X., Baumgartner, J. W., Hazelbauer, G. L. (1997). High- and low-abundance chemoreceptors in *Escherichia coli*: Differential activities associated with closely related cytoplasmic domains. *J Bacteriol 179*(21), 6714–6720.

Firth, E., Carpenter, S. D., Sorensen, H. L., Collins, R. E., Deming, J. W. (2016). Bacterial use of choline to tolerate salinity shifts in sea-ice brines. *Elem Sci Anth* 4, p.000120.

Garren, M., Son, K., Raina, J., Rusconi, R., Menolascina, F., Shapiro, O. H., *et al*. (2014). A bacterial pathogen uses dimethylsulfoniopropionate as a cue to target heat-stressed corals. *ISME J 8*, 999–107.

Graumann, P., Schroder, K., Schmid, R., Marahiel, M. A. (1996). Cold shock stress-induced proteins in *Bacillus subtilis*. *J Bacteriol 178*(15), 4611–4619.

Grossart, H., Riemann, L., Azam, F. (2001). Bacterial motility in the sea and its ecological implications. *Aquat Microb Ecol 25*, 247–258.

Guttenplan, S. D., & Kearns, D. B. (2013). Regulation of flagellar motility during biofilm formation. *FEMS Microbiol Rev 37*(6), 849–871.

Hazeleger, W. C., Wouters, J. A., Rombouts, F. M., Abee T. (1998). Physiological activity of *Campylobacter jejuni* far below minimal growth temperature. *Appl Environ Microbiol 64*(10), 3917–3922.

Huston, A. L. (2003). Bacterial adaptation to the cold: in situ activities of extracellular enzymes in North Water polynya and characterization of a cold-active amino peptidase from *Colwellia psychrerythraea* strain 34H. [Doctoral Dissertation, University of Washington]. *ProQuest.*

Jackson, G. A. (1987). Simulating chemosensory response of marine microorganisms. *Limnol Oceanogr 32*, 1253–1266.

Josenhans, C., & Suerbaum, S. (2002). The role of motility as a virulence factor in bacteria. *Int J Med Microbiol 291*(8), 605–614.

Junge, K., Eicken, H., Deming, J. W. (2003). Motility of *Colwellia psychrerythraea* strain 34H at subzero temperatures. *Appl Environ Microbiol 69*(7), 4282–4284.

Junge, K., Eicken, H., Deming, J. W. (2004). Bacterial activity at –2°C to –20°C in Arctic wintertime sea ice. *Appl Environ Microbiol 70*(1), 550–557.

Junge, K., Krembs, C., Deming, J., Stierle, A., Eicken, H. (2001). A microscopic approach to investigate bacteria under in situ conditions in sea-ice samples. *Annals Glaciol 33*, 304–310.

Kato, J., Kim, H. E., Takiguchi, N., Kuroda, A., Ohtake., H. (2008). *Pseudomonas aeruginosa* as a model microorganism for investigation of chemotactic behaviors in ecosystem. *J Biosci Bioeng 106*(1), 1–7.

Kiørboe, T., & Jackson, G. A. (2001). Marine snow, organic solute plumes, and optimal chemosensory behavior of bacteria. *Limnol Oceanogr 46*, 1309–1318.

Krembs, C., & Deming, J. W. (2008). The role of exopolymers in microbial adaptation to sea ice. In Margesin, R., Schinner, F., Marx J.C., Gerday, C. (Eds.), *Psychrophiles: From biodiversity to biotechnology.* Heidelberg, Springer Verlag, 247–264.

Krembs, C., Eicken, H., Junge, K., Deming, J. W. (2002). High concentrations of exopolymeric substances in Arctic winter sea ice: implications for the polar ocean carbon cycle and cryoprotection of diatoms. *Deep Sea Res I 49*, 2163–2181.

Krembs, C., Eicken, J., Deming, J. W. (2011). Exopolymer alteration of physical properties of sea ice and implications for ice habitability and biogeochemistry in a warmer Arctic. *Proc Natl Acad Sci USA 108*(9), 3653–3658.

Larsen, M. H., Blackburn, N., Larsen, J. L., Olsen, J. E. (2004). Influences of temperature, salinity and starvation on the motility of chemotactic response of *Vibrio anguillarum*. *Microbiol 150*, 1283–1290.

Li, C., Boileau, A. J., Kung, C., Adler, J. (1988). Osmotaxis in *Escherichia coli*. *Proc Natl Acad Sci USA 85*, 9451-9455.

Lindensmith, C. A., Rider, S., Bedrossian, M., Wallace, J. K., Serbayn, E. Showalter, G. M., *et al.* (2016). A submersible, off-axis holographic microscope for detection of microbial motility and morphology in aqueous and icy environments. *PLoS ONE 11*(1), e0147700.

Lofgren, K. W., & Fox, C. F. (1974). Attractant-directed motility in *Escherichia coli*: Requirement for a fluid lipid phase. *J Bacteriol 118*(3), 1181–1182.

Los, D. A., & Murata, N. (2004). Membrane fluidity and its roles in the perception of environmental signals. *Biochim Biophys Acta 1666*, 142–157.

Lynch W. H. (1980). Effect of temperature on *Pseudomonas fluorescencs* chemotaxis. *J Bacteriol 143*(1), 338–342.

Maeda, K., & Imae, Y. (1979). Thermosensory transduction in *Escherichia coli*: Inhibition of the thermoresponse by L-serine. *Proc Natl Acad Sci USA 76*(1), 91-95.

Marx, J. G., Carpenter, S. D., Deming, J. W. (2009). Production of cryoprotectant extracellular polysaccharide substances (EPS) by the marine psychrophilic bacteria *Colwellia psychrerythraea* strain 34H under extreme conditions. *Can J Microbiol 55*, 63–72.

Meibom, K. L., Blokesch, M., Dolganov, N. A., Wu, C., Schoolnik, G. K. (2005). Chitin induces natural competence in *Vibrio cholerae*. *Science 310*, 1824–1827.

Meiners, K., Krembs, C., Gradinger, R. (2008). Exopolymer particles: Microbial hotspots of enhanced bacterial activity in Arctic fast ice (Chukchi Sea). *Aquat Microb Ecol 52*, 195–207.

Methé, B. A., Nelson, K. E., Deming, J. W., Momen, B., Melamud, E., Zhang, X., *et al.* (2005). The psychrophilic lifestyle as revealed by the genome sequence of *Colwellia psychrerythraea* 34H through genomic and proteomic analyses. *Proc Natl Acad Sci USA 102*(31), 10913–10918.

Mitchell, J. G., & Kogure, K. (2006). Bacterial motility: links to the environment and a diving force for microbial physics. *FEMS Microbiol Ecol 55*, 3–16.

Nunn, B. L, Slattery, K. V., Cameron, K. A., Timmins-Schiffman, E., Junge, K. (2014). Proteomics of *Colwellia psychrerythraea* at subzero temperatures – a life with limited movement, flexible membranes and vital DNA repair. *Env Microbiol 17*(7), 2139–2335.

Oleksiuk, O., Jakovljevic, V., Vladimirov, N., Carvahlo, R., Paster, E., Ryu, W.S., *et al*. (2011). Thermal robustness of signaling in bacterial chemotaxis. *Cell 145*(2), 312–321.

Pfeffer, W. (1884). Lokomotorische Richtungsbewegungen durch chemische Reize. *Untersuchungen aus dem Botanischen Institut in Tübingen 1,* 363–482.

Poolman, B., Spitzer, J. J., Wood, J. M. (2004). Bacterial osmosensing: roles of membrane structure and electrostatic in lipid-protein and protein-protein interactions. *Biochim Biophys Acta 1666*, 88–104.

Raina, J., Dinsdale, E. A., Willis, B. L., Bourne, D. G. (2009). Do the organic sulfur compounds DMSP and DMS drive coral microbial associations? *Cell Trends in Microbiol 18*(3), 101–108.

Schneider, W. R., & Doetsch, R. N. (1974). Effect of viscosity on bacterial motility. *J Bacteriol 117*(3), 696–701.

Seymour, J. R., Ahmed, T., Marcos, Stocker, R. (2008). A microfluidic chemotaxis assay to study microbial behavior in diffusing nutrient patches. *Limnol Oceanogr: Methods 6*, 447-488.

Seymour, J. R., Ahmed, T., Stocker, R. (2009). Bacterial chemotaxis towards the extracellular products of the toxic phytoplankton *Heterosigma akashiwo*. *J Plank Res 31*(12), 1557–1561

Son, K., Brumley, D. R., Stocker, R. (2015). Live from under the lens: exploring microbial motility with dynamic imaging and microfluidics. *Nat Microbiol Rev 13*, 761–775

Smriga, S., Fernandez, V. I., Mitchell, J. G., Stocker, R. (2015). Chemotaxis toward phytoplankton drives organic matter partitioning among marine bacteria. *PNAS 113*(6), 1576–158.

Stocker, R. (2012). Marine microbes see a sea of gradients. *Science 338,* 628–633.

Stocker, R., Seymour, J. R., Samadani, A., Hunt, D. E., Polz, M. F. (2008). Rapid chemotactic response enables marine bacteria to exploit ephemeral microscale nutrient patches. *Proc Natl Acad Sci USA 105*(11), 4209–4214.

Takada, Y., Hayashinaka, N, Hagihara-nukui, E., Fukunaga, N. (1993). Chemotaxis in a psychrophilic marine bacterium, *Vibrio* sp. strain ABE -1. *J Gen Appl Microbiol*, *39,* 371–379.

Taylor, J. R., & Stocker, R. (2012). Trade-offs of chemotactic foraging in turbulent water. *Science 338,* 675–679.

Terracciano, J. S., & Canale-Parola, E. (1984). Enhancement of chemotaxis in *Spirochaeta aurantia* grown under conditions of nutrient limitation. *J Bacteriol 159*(1), 173–178.

Thurber, R. V., Willner-Hall, D., Rodriguez-Mueller, B., Desnues, C., Edwards, R. A., Angly, F., *et al*. (2009). Metagenomic analysis of stressed coral holobionts. *Environ Microbiol 11*(8), 2148–2163.

Tout, J., Jeffries, T. C., Petrou, K., Tyson, G. W., Webster, N. S., Garren, M, *et al.* (2015a). Chemotaxis by natural populations of coral reef bacteria. *ISME J 9*, 764–1777.

Tout, J., Siboni, N., Messer, L. F., Garren, M., Stocker, R., Webster, N. S., *et al*. (2015b). Increased seawater temperature increases the abundance and alters the structure of natural *Vibrio* populations associated with the coral *Pocillopora damicornis*. *Frontiers in Microbiol 6,* 432.

Underwood, G. J. C., Fietz, S., Papadimitriou, S., Thomas, D. N., Dieckmann, G. S. (2010). Distribution and composition of dissolved extracellular polymeric substances (EPS) in Antarctic sea ice. *Mar Ecol Prog Ser 404,* 1–19.

Wallace, J. K., Rider, S., Serabyn, E., Kuhn, J., Liewer, K., Deming, J. W., *et al.* (2015). Robust, compact implementation of an off-axis digital holographic microscope. *Opt Express 23*(13), 17367–17378.

Wells, L. E., & Deming, J.W. (2006). Characterization of a cold-active bacteriophage on two psychrophilic marine hosts. *Aquat Microbiol Ecol 45,* 15–29.

Yang, H. (1995). Distributions of free amino acids in sea and lake ice cores from Antarctic with special reference to ice biota. *Proc NIPR Symp Polar Biol 8*, 114–125.

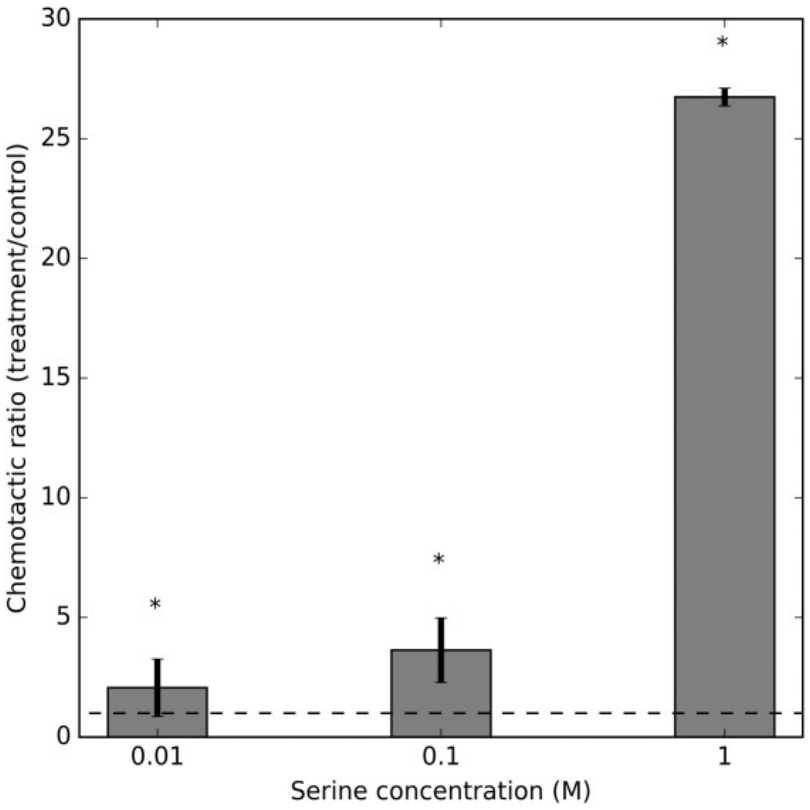

Figure 2.1 Chemotactic dose-response of *Colwellia psychrerythraea* 34H to serine at 8°C. *Cp*34H was grown and tested at 8°C and 35 ppt salinity, rinsed to remove dissolved organic compounds, and presented with 10 mM, 100 mM or 1 M serine as chemoattractant.

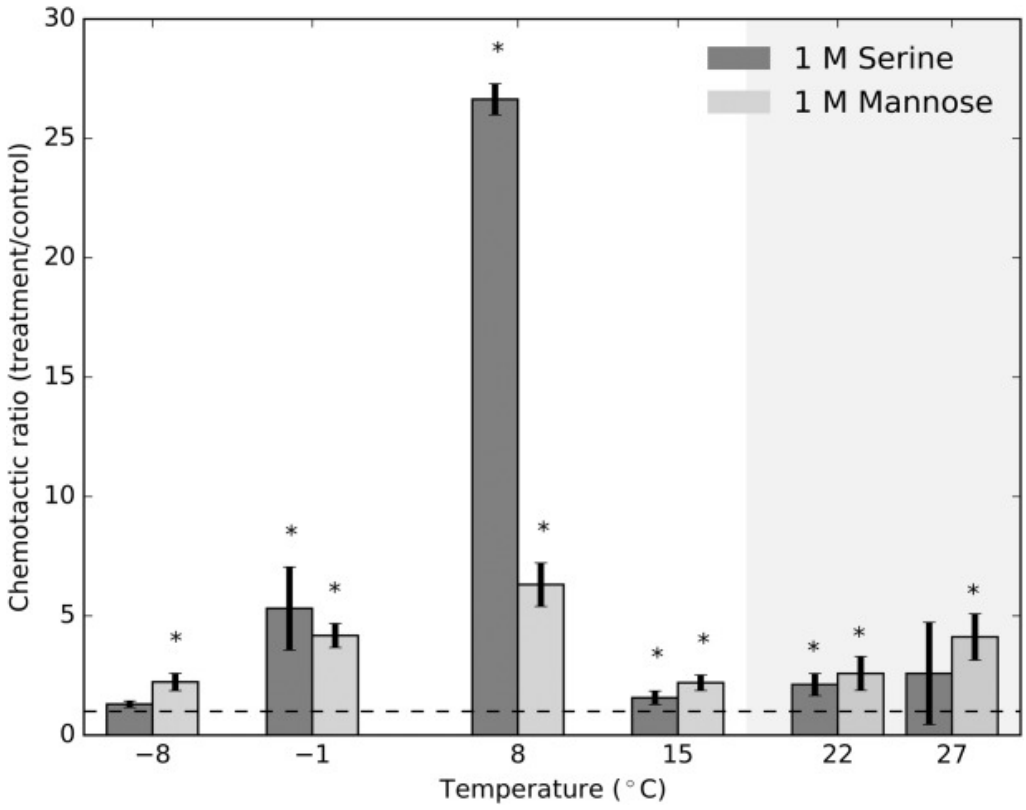

Figure 2.2 Chemotactic response of *Colwellia psychrerythraea* 34H at temperatures from −8°C to 27°C. *Cp*34H, when grown at 8°C, demonstrated significant taxis to serine at temperatures from −1°C to 22°C, and to mannose more broadly, at all test temperatures. Dark grey bars represent chemotaxis to 1 M serine; light grey bars, to 1 M mannose; shaded area indicates chemotactic responses above the upper growth temperature for *Cp*34H. Chemotactic response was calculated as the ratio of mean concentration of bacteria in the capillary tube with chemoattractant (treatment) to mean concentration of bacteria in the control tube. The dashed line indicates the normalized control value of 1, with values above the line indicating chemotaxis; asterisks indicate significant ($p < 0.05$) chemotaxis (see Table 2.1 for individual p values). Error bars indicate standard deviation of the mean ($n = 3$, except where indicated in Table 2.1).

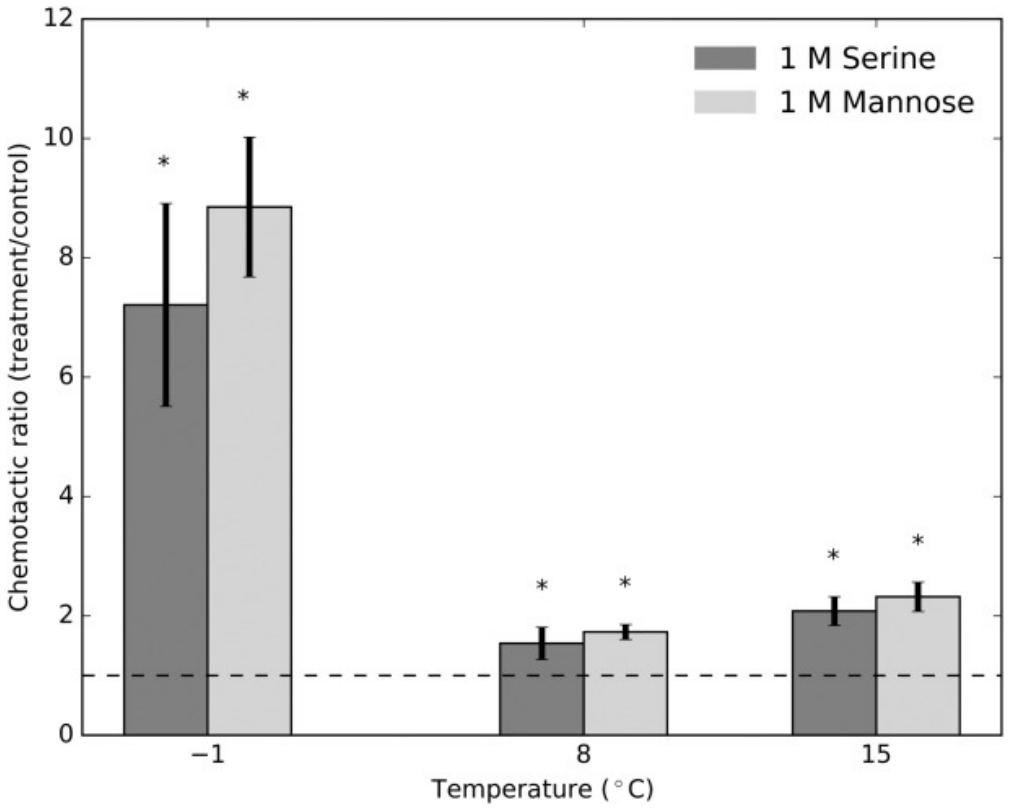

Figure 2.3 Chemotactic response of *Colwellia psychrerythraea* 34H when grown at −1°C. *Cp*34H grown showed strongest chemotaxis at its growth temperature, whether grown at −1°C (this figure) or at 8°C (Figure 2.1). Dark grey bars represent relative chemotaxis to 1 M serine; light grey bars, chemotaxis to 1 M mannose. The dashed line indicates the normalized control value of 1, with values above the line indicating chemotaxis; asterisks indicate significant ($p < 0.05$) chemotaxis (see Table 2.1 for individual p values). Error bars indicate standard deviation of the mean ($n = 3$).

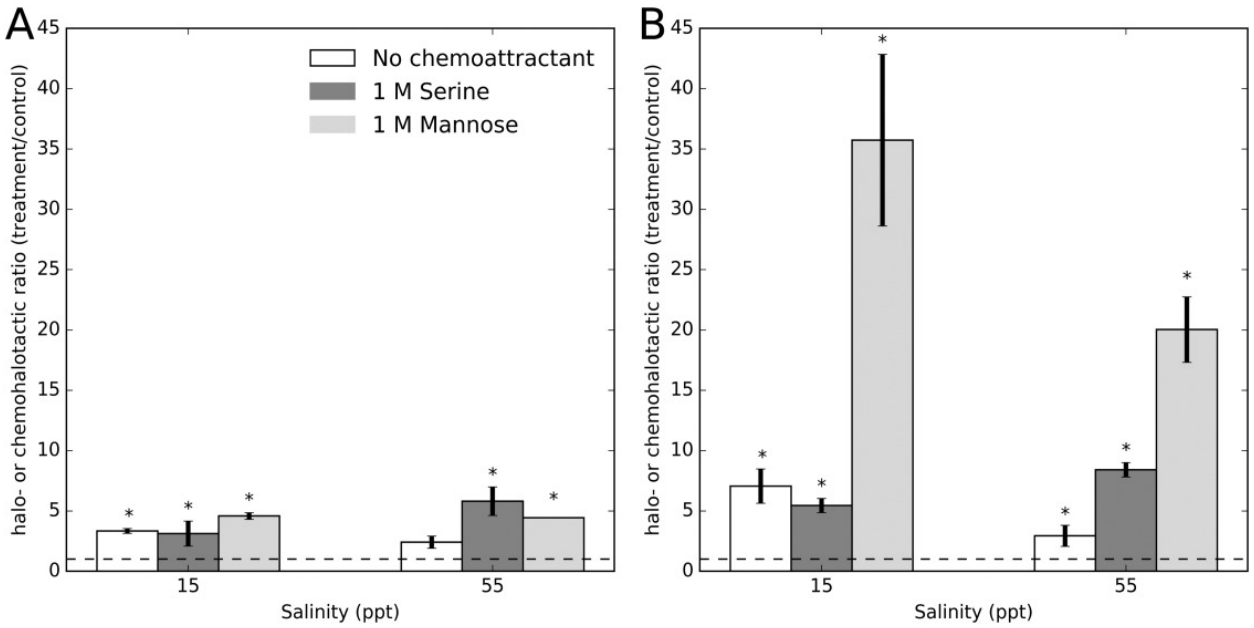

Figure 2.4 Halotactic and chemohalotactic response of *Colwellia psychrerythraea* 34H at 8°C and −1°C. A. At 8°C, *Cp*34H (grown at 8°C and 35 ppt) demonstrated significant halotaxis toward lower salinity (15 ppt) but not higher salinity (55 ppt) in the absence of chemoattractant (white bars). Significant chemohalotaxis was observed toward serine (dark grey bars) and toward mannose (light grey bars) and both lower and higher salinities. B. At −1°C, *Cp*34H (grown as in A) demonstrated significant halotaxis (white bars) toward lower salinity (15 ppt) and higher salinity (55 ppt), and significant chemohalotaxis to both serine (dark grey bars) and mannose (light grey bars) and both higher and lower salinities. The dashed line indicates the normalized control value of 1, with values above the line indicating chemotaxis; asterisks indicate significant ($p < 0.05$) chemotaxis (see Table 2.1 for individual p values). Error bars indicate standard deviation of the mean ($n = 3$).

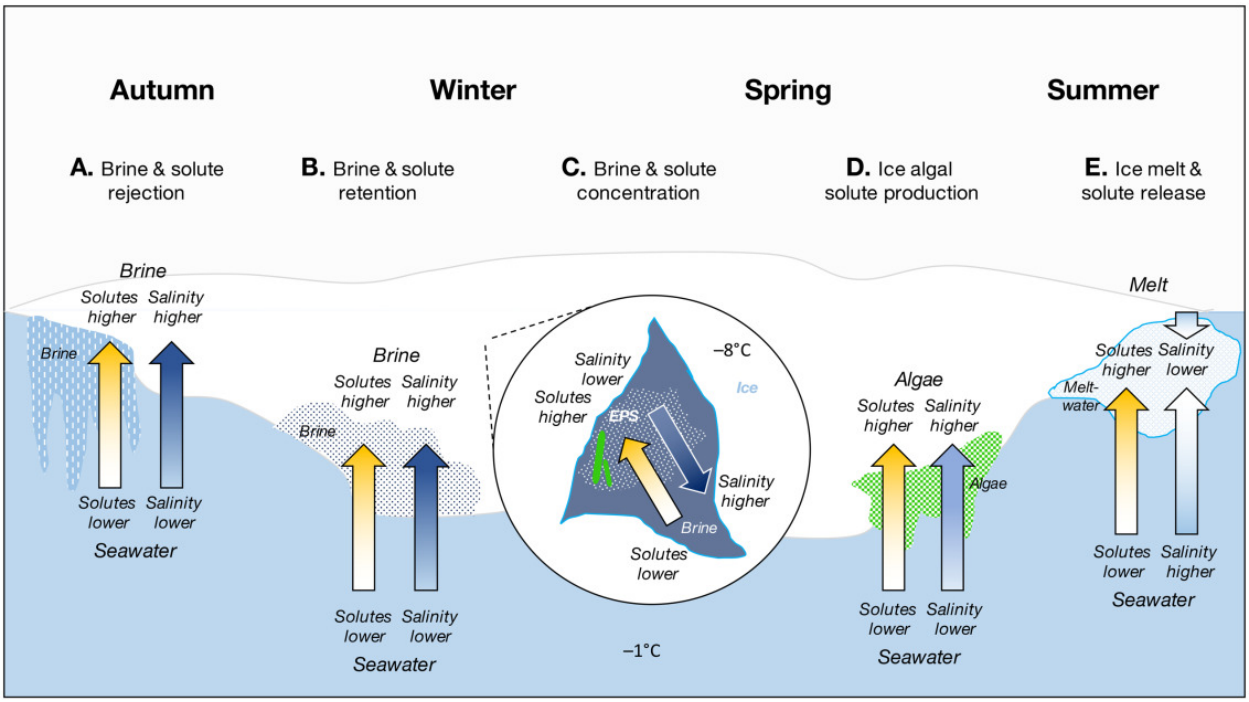

Figure 2.5 A schematic synthesis of suggested bacterial taxis in the context of the sea ice environment. Based on results from this study, we suggest that cold-adapted marine bacteria may use chemotaxis, halotaxis and chemohalotaxis to position themselves in response to environmental gradients encountered at the sea ice/seawater interface and within the sea-ice brine network. Chemohalotaxis by the model marine psychrophile *Colwellia psychrerythraea* 34H toward organic solutes (serine and mannose, in this study) at −1°C and salinities higher than seawater (55 ppt) suggest potential movement up gradients toward brine and solutes rejected from sea ice as it forms (A) or toward brine and solutes retained in the ice as it grows (B). Within the sea-ice brine network (C), chemohalotaxis and halotaxis by *Cp*34H at the subzero temperatures we tested (−1°C and −8°C) suggest that bacteria may be able to respond to chemical gradients produced by sea-ice algae (C and D, in green), EPS or other organic matter, as well as salinity gradients that change internally in the ice matrix as temperatures change. When sea ice melts (E), results of experiments with

*Cp*34H at −1°C suggest potential movement toward low-salinity melt waters and associated organics released from the ice. Arrows point in the direction of suggested bacterial movement. Gradients in yellow within arrows represent gradients of organic chemicals analogous to serine or mannose, while gradients in blue represent salt gradients; the highest concentration of chemoattractant or salt is represented by the darkest shade.

Table 2.1 Treatment conditions, resulting data and statistical significance for capillary tube experiments.

Experiment	Treatment conditions			Bacterial density in tube (number ± S.D. x 10^7 mL^{-1})		Significance [b] (p value)
	Temperature (°C)	Salinity (ppt)	Chemoattractant, concentration	Control [a]	Treatment	
Serine-dose response (Figure 2.1)	8	35	Serine, 10 mM	2.1 ± 1.2	4.3 ± 2.5	0.119
	8	35	Serine, 100 mM	2.1 ± 1.2	7.58 ± 2.8	**0.018**
	8	35	Serine, 1 M	2.1 ± 1.2	55.9 ± 0.8	**< 0.001**
Temperature profile, when grown at 8°C (Figure 2.2)	–8[c]	35	Serine, 1 M	4.65 ± 0.71	6.04 ± 0.65	0.057
	–8[c]	35	Mannose, 1 M	4.65 ± 0.71	10.4 ± 1.66	**0.003**
	–1	35	Serine, 1 M	1.17 ± 0.37	6.21 ± 2.03	**0.001**
	–1	35	Mannose, 1 M	1.17 ± 0.37	4.87 ± 0.59	**< 0.001**
	8	35	Mannose, 1 M	2.1 ± 1.2	13.2 ± 1.91	**0.021**
	15	35	Serine, 1 M	4.09 ± 1.10	6.42 ± 1.16	**0.020**
	15	35	Mannose, 1 M	4.09 ± 1.10	9.01 ± 1.31	**0.001**
	22	35	Serine, 1 M	3.2 ± 0.7	6.8 ± 1.46	**0.009**
	22	35	Mannose, 1 M	3.2 ± 0.7	8.3 ± 2.26	**0.018**
	27	35	Serine, 1 M	1.78 ± 0.40	4.60 ± 3.80	0.095
	27	35	Mannose, 1 M	1.78 ± 0.40	7.33 ± 1.71	**0.003**
Temperature profile, when grown at –1°C (Figure 2.3)	–1	35	Serine, 1 M	0.884 ± 0.027	6.37 ± 1.51	**0.008**
	–1	35	Mannose, 1 M	0.884 ± 0.027	7.82 ± 1.03	**0.001**
	8	35	Serine, 1M	7.54 ± 1.95	11.6 ± 2.0	**0.033**
	8	35	Mannose, 1 M	7.54 ± 1.95	13.0 ± 1.0	**0.006**
	15	35	Serine, 1 M	4.75 ± 1.60	9.87 ± 1.14	**0.005**
	15	35	Mannose, 1 M	4.75 ± 1.60	11.0 ± 1.2	**0.003**
Halotaxis and chemohalotaxis (Figure 2.4)	–1	15	none	1.17 ± 0.37	8.25 ± 1.65	**0.001**
	–1	55	none	1.17 ± 0.37	3.43 ± 1.02	**0.011**
	–1	15	Serine, 1 M	8.25 ± 1.65	6.21 ± 2.04	**< 0.001**
	–1	15	Mannose, 1 M	8.25 ± 1.65	41.8 ± 8.3	**0.001**
	–1	55	Serine, 1 M	3.43 ± 1.02	9.84 ± 0.70	**< 0.001**
	–1	55	Mannose, 1 M	3.43 ± 1.02	23.4 ± 3.2	**0.001**
	8	15	none	2.1 ± 1.2	7.03 ± 4.2	**0.006**
	8	55	none	2.1 ± 1.2	5.08 ± 1.08	0.100
	8	15	Serine, 1 M	7.03 ± 4.2	6.56 ± 2.19	**0.01**
	8	15	Mannose, 1 M	7.03 ± 4.2	9.63 ± 0.59	**< 0.001**
	8	55	Serine, 1 M	5.08 ± 1.08	12.2 ± 2.4	**0.001**
	8	55	Mannose, 1 M	5.08 ± 1.08	9.3 ± 0.0	**0.001**

[a] For chemotaxis experiments, same temperature and salinity as the treatment but no chemoattractant; for halotaxis experiments, same temperature and chemoattractant as the treatment but salinity of 35 ppt

[b] Determined using Student's t-test to compare bacterial concentration in the treatment capillary tube to that in the control tube; values considered significant ($p < 0.05$) are highlighted in bold; n = 3, except for −8°C treatments using serine (n = 2 due to freezing) and 8°C treatment (when grown at 8°C) using serine (n = 2 due to cracked capillary tubes)

[c] 5% glycerol solution added to prevent freezing

Chapter 3.

Extracellular enzyme activity in hypersaline, low-temperature conditions by *Colwellia psychrerythraea* strain 34H and *Psychrobacter* sp. strain 7E and in Arctic sea ice and surroundings

Abstract

Extracellular enzymes (EE) play an important role in the cycling of marine organic matter, breaking down large molecules into those small enough to be taken up across the microbial cell membrane. Within sea ice, physical concentration due to freezing increases concentrations of both bacteria and organic materials within brine pockets, which leads to higher encounter rates between extracellular enzymes and their substrates. Accordingly, EE may play an outsized role in recycling organic material within brines. However, whether EE are able to perform under the low temperature, high salinity conditions of wintertime brines is unknown. Here, we have characterized EE activity (EEA) of leucine aminopeptidase from two cold-active bacteria, *Colwellia psychrerythraea* strain 34H and *Psychrobacter* strain 7E under analogue sea-ice conditions using a standard fluorescence-based activity assay. Results demonstrated activity as low as –8˚C and up to 120 ppt salts, with enhanced activity when grown under sub-zero and high salinity conditions. Additionally, samples of sea-ice brine, under-ice water, and the sea-surface microlayer collected from the high Arctic were analyzed using the same assay to measure EEA subjected to a freeze-thaw cycle. Results showed EEA highest in sea-ice samples, with enzyme activity at as low as –10˚C and salinity as high as 142 ppt salts. These results indicate that EEA may be important in sea ice for the degradation of high molecular weight organics, both sustaining microbial communities in brine pores and altering the nature of organic material released at spring melt.

3.1 Introduction

As a result of brine concentration and active microbial communities, the interstitial network of brine channels and pores within sea ice contains concentrations of dissolved organic matter (DOM) that can greatly exceed those of underlying seawater (Thomas *et al*., 2001; Underwood *et al*., 2013; Arrigo, 2014; Aslam *et al*., 2016). Heterotrophic bacteria within sea ice rely on this organic material to sustain activity and growth, yet the majority of marine organic material is considered too large for cellular uptake (> 600 kDa; Chrost, 1991). To facilitate degradation of DOM to a utilizable size, bacteria commonly produce extracellular enzymes (EE), hydrolytic proteins within the periplasmic space of the cell, at the cell surface ("cell-attached EE"), or released into the environment ("free EE") (Chrost, 1990; 1991; Arnosti, 2011).

Extracellular enzyme activity (EEA) has long been recognized as the rate-limiting step in the bacterial cycling of high molecular weight organic material (Chrost, 1991; Meyer-Reil, 1991); understanding EEA is thus key to understanding broader organic cycling within the environment. While many studies have characterized bacterial EEA within varied marine environments, with high rates of organic hydrolysis demonstrated throughout the water column (Vetter & Deming, 1994; Christian & Karl, 1995; Hoppe & Ulrich, 1999; Fukada *et al*., 2000; Davey *et al*., 2001; Baltar *et al.*, 2009; Steen & Arnosti, 2013), especially on sinking aggregates (Huston & Deming, 2002; Grossart *et al*., 2007; Ziervogel *et al*., 2010; Kellogg & Deming, 2014), and within sediments (Arnosti, 1995; Boetius, 1995; Poremba, 1995; Arnosti & Jørgensen, 2003), fewer measurements have been made on sea ice (Helmke & Weyland, 1995; Huston *et al*., 2000; Deming, 2007; Yu *et al*., 2009) or on sea-ice isolates at *in situ* or near *in situ* conditions of cold temperature and hypersalinity (Groudieva *et al*., 2004; Huston *et al*., 2004; Wang *et al.,* 2005; Wang *et al*., 2018).

Sea ice experiences low temperatures from 0 to –40˚C, which slow chemical reactions and impart structural changes in proteins, limiting activity (Feller and Gerday, 2003). At the same time, organisms in sea ice can experience wide salinity ranges, from 0 to 250 ppt salts, altering protein interactions with surrounding water due to charge differences (Ortega *et al*., 2011). In combination, low temperature and high salt not only increase viscosity of sea-ice brine, limiting diffusional processes (Cox & Weeks, 1975), but also dramatically reduce water activity within the brines, a known challenge for enzymes (Karan *et al*., 2012). At the same time, enzymes in sea ice must contend with small-scale salinity changes as brine volume and salinity fluctuations on diel to seasonal cycles (Ewert & Deming, 2013). Extremophilic bacteria, such as psychrophiles (those with maximum growth rates below 15˚C; Morita, 1975) and halophiles (those growing optimally at salinities matching or above seawater; Kushner & Kamekura, 1988), have commonly been studied for their potential to produce enzymes that operate under extreme conditions relevant to both environmental and industrial processes. Such investigations have produced an understanding of enzymes that operate at freezing temperatures (Huston *et al.*, 2004) or up to saturating salt conditions (Ortega *et al*., 2011), but rarely have enzymes been investigated under concurrent salinity and temperature extremes (Karan *et al*., 2012), as would be experienced in sea-ice brines.

How EE function under such concurrent extremes and in response to freeze-thaw cycles can inform community ecology within sea-ice brines. Typically, sea-ice brines have higher concentrations of DOM than underlying seawater due to freeze-concentration as well as high primary productivity and exopolysaccharide production by algal assemblages within the bottom 5 cm of spring ice (for a review of sea-ice microbial communities, see Boetius *et al*., 2015). Previous studies have suggested that DOM within sea-ice brines contains a higher fraction of bio-available material compared to underlying seawater (Kähler *et al*., 1997; Amon *et al*., 2001; Jørgensen *et*

al., 2015); enzymatic degradation of DOM may contribute to increased bioavailability. Likewise, EEA in sea ice also has implications for DOM cycling within the seasonally ice-covered seas of both polar regions. At the air-sea interface where sea ice forms and melts sits the sea-surface microlayer (SML), a thin, gelatinous film within the top millimeter of the ocean, which serves as the collection reservoir for biopolymers from melting ice (Galgani *et al*., 2016; Wurl *et al*., 2017; Engel *et al*., 2018). EEA within sea-ice brines may thus influence the nature of organic material within the SML during ice melt by releasing more bioavailable material into the SML, while EE which retain activity through the temperature and salinity shifts of ice melt may continue to degrade such material within the SML.

To understand how concurrent temperature and salinity extremes and rapid changes of conditions due to freezing or thawing impact enzyme activity, we measured EEA of two psychrophilic bacteria, *Colwellia psychrerythraea* strain 34H (*Cp*34H) and *Psychrobacter* strain 7E (*P*7E) in laboratory experiments. These measurements were complemented by EEA experiments using natural communities from samples of Arctic seawater, SML, and sea-ice across co-varying temperature and salinity conditions. Taken together, these measurements survey the extremes of EEA within cold marine environments and depict how EEA may function at the freeze-thaw boundary of a polar ocean to influence organic matter composition.

3.2 Materials and methods

3.2.1 Cultured bacterial growth and harvest

Glycerol-protected stocks of *Cp*34H and *P*7E were reconstituted from –70˚C freezer storage. Strain *Cp*34H was originally isolated from Arctic marine sediments, but as strains of *Colwellia psychrerythraea* can be found in sea ice (Boetius *et al*., 2015), *Cp*34H is often used as

a model marine psychrophile (Huston, 2003; Methé *et al*., 2005; Czajka *et al*., 2018; Showalter *et al*., 2018), including in the context of cold-active enzymes (Huston *et al*., 2000; 2004; Bauvois *et al*., 2008). *Cp*34H has a growth range from –12 to 18˚C (at 35 ppt) and 17.5 to 70 ppt (at –1°C), *Cp*34H (Huston, 2000; Wells *and* Deming, 2006) while *P*7E, isolated from upper sea-ice brine, has a similar growth range in temperature (–8 to 25˚C) and but more extreme range in growth salinity (17.5 to 125 ppt) (Ewert *and* Deming, 2014).

Cells were grown in ½ strength 2216 Difco Marine Broth, adjusted to full-strength seawater salinity (35 ppt) using artificial seawater (ASW: 0.4 M NaCl, 9 mM KCl, 26 mM $MgCl_2$, 28 mM $MgSO_4$, and 5 mM TAPSO buffer) at the targeted experimental temperature (–8˚C, –4˚C, –1˚C, or 8˚C). For experiments manipulating growth salinity, full strength culture broth was amended with a NaCl solution in distilled water (DI) water to achieve the desired salt concentration (35, 55, or 70 ppt) while maintaining ½ strength organics. All cells for growth-condition experiments were sub-cultured twice under the desired conditions before using the cells for experiments by transferring 100 µL of turbid culture into fresh media. This approach represents at least eight generations for the cells and was taken to ensure that the cells used reflected those conditions.

When the cells had reached mid-log stage as determined by optical density (OD), verified previously by counts using epifluorescent microscopy (roughly 10^6 cells mL^{-1}), an aliquot of cells was removed and fixed with 2% final concentration formaldehyde for counting by epifluorescence microscopy, using a Zeiss epifluorescent microscope, counting at least 200 cells per field and 20 fields per sample. Counts were then scaled to the experimental volume. The remaining cells were centrifuged at slow speed (40 minutes at 400 x g, maintaining temperature between 2 and 6˚C) and the supernatant was then filtered using a 0.2-µm syringe filter to remove cells. Cell-free supernatant was confirmed by intermittent epifluorescence microscopy.

3.2.2 Laboratory enzyme activity assays

Extracellular enzyme activity rates were determined using a standard fluorogenic substrate assay as originally described by Hoppe (1983). Briefly, an artificial substrate with a fluorescent tag was added to samples and allowed to incubate under experimental conditions with periodic measurements of fluorescence. As extracellular enzymes cleave the artificial substrate, the fluorescent tag is released and the resulting change in fluorescence is measured to indicate rate of enzyme activity. We chose to measure leucine aminopeptidase activity using the fluorogenic substrate L-Leucine-7-amido-4-mtheylcoumarin hydrochloride (MCA-L, Sigma). MCA-L is a common artificial substrate for EEA assays in marine environments, with aminopeptidases often performing the most rapid, observable hydrolysis among field experiments. Additionally, the leucine aminopeptidase of *Cp*34H is well-characterized (Huston *et al*., 2004; Bauvois *et al*., 2008), and an NCBI BLAST survey using the sequence of leucine aminopeptidase of *Cp*34H suggests a similar enzyme is present in the genome of *P*7E. MCA-L was dissolved in methyl cellosolve (monomethyl ether, Sigma) to make a 10 mM stock solution from which further dilutions were made in DI water according to experimental plans.

Harvested cell-free supernatant was added to 96-well plates set on ice to prevent warming. Wells were pre-loaded with either DI water or a NaCl solution in DI water and with MCA-L in methyl cellosolve diluted in ASW such that these solutions together achieved desired experimental salinities (17.5, 35, 55, 70, 90, or 120 ppt salinity) and a saturating MCA-L concentration (250 µM, resulting in 2.5% v/v final concentration of methyl cellosolve in samples). The latter was determined by a saturation curve performed at each experimental temperature and for both *Cp*34H and *P*7E. Each treatment was performed in triplicate.

After the 96-well plate was loaded with three samples for each treatment, fluorescence was measured in triplicate using an OD spectrophotometer (Spectramax M2, Molecular Devices) set at optimal wavelength for the MCA tag (excitation 380 nm, emission 440 nm) and zeroed against a blank (cell supernatant without MCA-L). Free MCA compound (-amido-4-mtheylcoumarin hydrochloride) was observed in cell-free solution at all salinities and across endpoint temperatures to ensure there was no confounding drift in fluorescence. Time points were selected based on estimated rate of activity and confined to within a total of 24–48 hours. This sampling frame is commonly used among EEA assays that include the cell-attached fraction in order to ensure that no other metabolic response to artificial substrate obscures measurements; it was chosen to allow comparison of rates between these experiments, later field experiments, and literature. Plates were kept at their experimental temperatures until measured, then immediately returned to that temperature. Measurement time was short (< 3 minutes), but to ensure no significant warming had occurred, duplicates were made of selected treatments and left at their experimental temperature for end-point comparison.

3.2.3 Field experiments

Sea-ice cores were collected in the central Arctic Ocean at latitudes of 88–90°N during the MOCCHA expedition aboard the icebreaker *Oden* in August and September of 2018, as described by Torstensson *et al*. (2020). After collection, the bottom 10 cm of the cores were returned to the ship and were directly thawed at temperatures between 4–10 °C in a cold van, then the melted cores from one field site were pool (n = 2–3) and subsampled for EEA measurement within 24 hours. Sea-ice properties were characterized and can be found in Torstensson *et al*. (2020). Sea-ice core temperatures fell within the temperature range of 0 to –4.8˚C, with a narrower range of –

0.85 to –2.67 ˚C for the bottom 10 cm. Bulk salinity was measured using a handheld refractometer and ranged between 2 and 4 ppt.

For comparison to the sea-ice cores, surrounding ice-related environments were also sampled: seawater was collected from approximately 1 meter below the ice using a hand pump; and the sea-surface microlayer (SML) was sampled from an open lead near the ship using a glass plate technique, either by hand or using an automated catamaran (Ribas-Ribas *et al*., 2017). Both seawater and SML water were returned to the ship in dark, insulated containers and stored in a refrigerator at 4˚C before being sub-sampled for EEA within 12 hours. Sample salinity was again measured using a hand-held refractometer, with SML salinity at 8 ppt and seawater salinity between 31 and 33 ppt.

EEA was measured on the melted sea ice, SML, and seawater samples at temperatures near *in situ*, on warmed seawater samples, and on frozen SML and re-frozen sea-ice samples to investigate EEA after a freeze-thaw cycle. Sample aliquots were distributed into clean glass tubes and mixed with a saturating concentration of MCA-L (250 μL) which was determined from a saturation curve generated from sea-ice samples. Samples were incubated at near *in situ* temperatures (–1˚C for melted sea-ice sample and SML using an upright freezer, –1.8˚C for under-ice water using a temperature-controlled shipping container); refrozen (–1.8˚C for SML in the temperature-controlled shipping container, and –10˚C for sea ice and SML in an upright freezer), or warmed (6˚C for seawater, in a temperature-controlled shipping container). Fluorescence was measured using a Trilogy Laboratory Fluorometer (Turner) at 4–6 time points over a 24–48 hour period. For frozen samples, EEA was measured either as endpoints or over time points after freezing and then re-thawing. Endpoint samples were first spiked with MCA-L and measured for fluorescence, then thawed after a 10-day incubation period and measured to observe change in

fluorescence. Freeze-thaw samples were first frozen for 10 days, then thawed, distributed in aliquots, spiked with MCA-L, and measured for EEA over 24 hours. Prior to distributing aliquots for enzyme assay, subsamples from all samples were fixed with formaldehyde for subsequent bacterial counts to enable calculation of cell-specific EEA rates. For re-freezing experiments, the expected brine salinity was calculated based on Cox & Weeks (1983).

3.2.4 Rate calculation

Technical replicate fluorescence measurements were fit with a linear approximation using least squares regression to find average change in fluorescence Using these slopes, enzyme activity rates were calculated in units of nanomoles of MCA liberated per hour per cell by applying conversion values determined from a free-substrate concentration curve. These curves were measured at endpoint salinities (17.5 and 120 ppt) and temperatures (–8˚C and 15˚C) to investigate changes in fluorescence as a result of the experimental conditions; no such changes were observed. Rate values were scaled to bacterial concentration in the harvested culture pre-filtration to enable cell-specific comparisons across laboratory assays and between lab and field assays. A student's t-test was used to determine significant differences in rate where applicable using a p-value cutoff of 0.05.

3.2.5 Bacterial counts

Manual enumeration of bacteria was performed using epifluorescence microscopy as described in previous studies (Marx *et al.*, 2009; Ewert & Deming, 2014). Briefly, bacteria fixed with 2% final concentration formaldehyde were filtered over a black polycarbonate membrane filter (Sigma). Filters were stained with 4',6'-diamidino-2-phenylindole (DAPI) in ASW at 20 µg

mL^{-1} and then viewed on an epifluorescent microscope counting at least 200 cells per field and 20 fields per sample.

3.3 Results

3.3.1 EEA of *Cp*34H and *P*7E grown at optimal conditions

Free extracellular enzyme activity for *Cp*34H measured at –1˚C across a salinity profile (17.5, 35, 55, 75, 90, 120 ppt) after growth at maximum cell yield conditions (–1˚C, 35 ppt; Huston 2003) showed a dependence on salinity with the highest rate, 1.5 $x10^{-7}$ nM MCA-L hr^{-1} $cell^{-1}$, at 90 ppt and lowest rate, 0.65 $x10^{-7}$ nM MCA-L hr^{-1} $cell^{-1}$, at 17.5 ppt (Figure 3.1). The same assay performed on *P*7E resulted in a different pattern – not only was enzyme activity roughly an order of magnitude lower overall, with a maximum rate of activity around 0.2 x 10^{-7} nM MCA-L hr^{-1} $cell^{-1}$, but activity showed no apparent pattern in relation to salinity. EEA with *P*7E was negligible at 120 ppt, the highest salinity tested.

*P*7E demonstrated a stronger temperature dependence and higher overall activity than *Cp*34H when cells were grown at optimal conditions (–1˚C and 35 ppt) and assayed under the combined temperature and salinity conditions. While the overall EEA of both strains increased with increased temperature, the maximum EEA of *Cp*34H did not change significantly compared to –1˚C, but stayed within the range of 1.5 to 2.0 x 10^{-7} nM MCA-L hr^{-1} $cell^{-1}$ ($p > 0.05$). Maximum EEA of *P*7E, however, was significantly impacted by temperature: EEA jumped from 0.2 x 10^{-7} nM MCA-L hr^{-1} $cell^{-1}$ at –1˚C to 3.3 x 10^{-7} nM MCA-L hr^{-1} $cell^{-1}$ at 15˚C, a significant increase ($p = 0.03$) (Figure 3.2). Both strains showed maximum EEA at salinities above their optimal growth salinity: *Cp*34H at around 90 ppt, and *P*7E at around 55 ppt.

3.3.2 EEA of *Cp*34H grown at non-optimal conditions

EEA of *Cp*34H showed dependence on growth temperature. When cells were grown at optimal salinity (35 ppt) but different temperatures (either –8, –4, or 8˚C) and the resulting enzymes were assayed across a temperature and salinity range (–8, –4, –1, 8, and 15˚C; 17.5, 35, 55, 75, 90, 120 ppt), maximum EEA rates were observed when the enzymes were assayed at 15˚C but produced at either –8˚C (5.5 x 10^{-7} nM MCA-L hr^{-1} $cell^{-1}$) or 8˚C (4.6 x 10^{-7} nM MCA-L hr^{-1} $cell^{-1}$) (Figure 3.3).

When a similar experiment was repeated, growing *Cp*34H at optimal growth temperature (–1˚C) but non-optimal salinities (55 ppt or 70 ppt), maximal EEA was similarly observed when cells were grown at 70 ppt (Figure 3.4). Maximum rates of EEA produced by cells grown at 70 ppt (1.3 x 10^{-6} nM MCA-L hr^{-1} $cell^{-1}$, at 15˚C and 55 ppt) were roughly an order of magnitude higher than those of EEA produced by cells grown at 55 ppt (2.3 x 10^{-7} nM MCA-L hr^{-1} $cell^{-1}$, at 15˚C and 70 ppt) or at 35 ppt (as stated above, 1.5 x10^{-7} nM MCA-L hr^{-1} $cell^{-1}$ at 15˚C and 90 ppt).

3.3.3 EEA in environmental samples

Field measurements of EEA showed activity across all samples and conditions: under ice water (0.03–0.1 nM L^{-1} hr^{-1}), sea-surface microlayer (0.3–0.6 nM L^{-1} hr^{-1}), and sea ice (0.7–3.7 nM L^{-1} hr^{-1}). Sea ice and frozen SML EEA values are calculated to bulk volume rather than brine volume, and therefore EEA may be functionally higher *in situ* than listed here. Considering cell-specific values (those normalized to cell count), sea-ice core samples demonstrated the highest EEA rates (maximum of 6.4 x 10^{-6} nM MCA-L hr^{-1} $cell^{-1}$), measured at near *in situ* conditions (–1˚C, with a measured salinity of 19.5 ppt). The sea-ice EEA maximum was > 30 times higher than EEA in seawater at –1.8˚C and 32 ppt (0.2 x 10^{-6} nM MCA-L hr^{-1} $cell^{-1}$) and ~ 6 times higher than

EEA in SML at –1˚C and 8 ppt (1.0 x 10^{-6} nM MCA-L hr^{-1} $cell^{-1}$). Extracellular enzymes were assumed to partition into the brine fraction during freezing. Refrozen sea-ice cores, measured over a 10-day period at –10˚C and with a calculated brine salinity of 142 ppt, retained higher activity compared to re-frozen SML. However, the re-frozen core activity was still less than unfrozen (melted) ice cores, at 1.7 x 10^{-6} nM MCA-L hr^{-1} $cell^{-1}$. Warming increased the EEA rate of the underlying seawater (to 0.5 x 10^{-6} nM MCA-L hr^{-1} $cell^{-1}$), while refreezing and then re-thawing SML decreased EEA rate (0.8 x 10^{-6} nM MCA-L hr^{-1} $cell^{-1}$), which was near to that of warmed seawater. Finally, endpoint measurements of frozen SML (–10˚C, calculated brine salinity of 100 ppt) proved challenging; replicate tubes were lost shipboard and only one measurement was made, demonstrating a significantly decreased rate (0.1 x 10^{-6} nM MCA-L hr^{-1} $cell^{-1}$). A full list of field measurement rates, their errors, and significance values by a student's t test are given in Table 3.1.

3.4 Discussion

This study presents a new understanding of the limits of bacterial extracellular enzyme activity under low temperature, high salinity conditions. Primarily, these results have demonstrated the ability of psychrophilic bacteria to produce EE when grown at low temperature (–8˚C) or high salinity (70 ppt) and maintain activity under such conditions both in the laboratory and within field sea-ice, seawater, and sea-surface microlayer samples under manipulated conditions. EE production and activity under these conditions has implications for ecological processes and applications to biotechnology. Primarily, these data demonstrate that psychrophilic bacteria are likely able to maintain active digestion of large extracellular material under extremes of temperature and salinity by means of EE, which could support requirements for substrate in order to maintain metabolic activity or even growth in extreme environments. Free EE in the sea-ice

environment may also serve as a 'digestor' of large dissolved organic compounds within sea-ice brines and work to prime organic material for uptake by seawater communities at the onset of spring ice melt. Likewise, free EE which can operate under extreme conditions can be made useful for human applications, including industrial processes that require cold or high-salt conditions, and potentially industrial applications requiring use of an organic solvent that causes enzymes to experience low water activity, as they would in cold, hypersaline conditions.

Extracellular hydrolytic activity of psychrophilic and psychrotolerant organisms has been characterized previously in isolates from a variety of cold environments (Chanda Kasana, 2010; Bruno *et al*., 2019), including most commonly polar seawater and polar marine sediments (Kulakova *et al*., 1998; Srinivas *et al*., 2009; Martínez-Rosales & Castro-Sowinski, 2011; Prasad *et al*., 2014). While most of these studies take place in warm conditions relative to the original environment, often above 0˚C and more commonly above 4˚C, their rates of peptidase activity are comparable to those of our laboratory samples done in subzero temperatures. Conversely, *in situ* characterizations of enzyme activity are relatively uncommon in natural sea-ice communities (Helmke & Weyland, 1995; Huston *et al*., 2000; Deming, 2007; Yu *et al*., 2009) or with sea-ice isolates (Wang *et al*., 2005; Wang *et al*., 2018). Our results are comparable to previous observations of EEA rates from Helmke & Weyland (1995), which ranged between 0.1 and 51.1 nM L^{-1} hr^{-1}, and cell concentrations were of similar magnitude (mostly 10^4 cells mL^{-1}) though highly variable (Helmke and Weyland, 1995, at –1˚C). Our values were somewhat lower than those of Huston *et al*. (2000), which ranged between ~ 100 and 350 nM L^{-1} hr^{-1} (at 0–6˚C), although they reported similar differences in EEA rate between under-ice water and ice-core samples.

Notably, these values are also similar to EEA measurements from open water environments, which largely range between 5 and 80 nM L^{-1} hr^{-1} in open water (for a review, see Arnosti, 2011). However, the fluorescence-based activity assay used here (and in many other environmental studies) cannot distinguish the cause of differences in EEA, which may result from enhanced activity of individual enzymes (*i.e.*, the total EE concentration does not change as a result of growth conditions, but rather each enzyme is more active) or from greater overall concentration of enzymes (*i.e.*, the growth conditions stimulate production of more EE, which may mask individual enzyme efficiency). This distinction is especially important when comparing EEA from EE produced under different bacterial growth conditions, which often stimulates changes in concentration of EE produced (see below). Any observed differences in enzyme activity rate could be the result of higher or lower individual enzyme activity or higher or lower concentration of enzymes.

3.4.1 Patterns of activity suggesting psychrophilic nature

For both *Cp*34H and *P*7E the pattern of maximal rates of extracellular enzyme activity at supra-optimal growth temperatures is consistent with the well-established understanding of thermal dependence of enzyme activity. For *Cp*34H, previous characterizations of its leucine aminopeptidase when grown at 8˚C demonstrated maximum activity at 19˚C and reduced activity at lower temperatures (about 70% of maximum at 15˚C and ~ 15% of maximum at –1˚C; Huston *et al*., 2004), although characterization of an aminopeptidase from another sea-ice *Colwellia* showed a much higher temperature optimum (35˚C, Wang *et al*., 2005). A similar magnitude reduction in rate between 15˚C and –1˚C to that observed in Huston *et al*., 2004 is found in our study; both are consistent with reduction in enzyme activity due to temperature effects on chemical reactions when an Arrhenius equation is applied. Because the enzyme concentration was not

quantified in this experiment, accurate kinetic parameters cannot be deduced. However, assuming constant enzyme production under the same growth conditions, change in enzyme activity as a function of treatment temperature is consistent with Q10 thermal effects assuming a coefficient between 2 and 3. The pattern of EEA by *Cp*34H as a function of growth condition demonstrates that *Cp*34H is capable of producing functional extracellular enzymes when grown at a temperature as low as –8˚C (and 35 ppt), the lowest tested. Previous observations have similarly recorded increased EEA rates for *Cp*34H when grown at low temperatures (0–2˚C) compared to warmer temperatures (8˚C), possibly as the result of increased EE production (Huston *et al*., 2004).

Measurements of salinity effects on extracellular enzyme activity have been performed on EE produced by bacteria isolated from cold environments (*e.g.,* amylase by Qin *et al*., 2014; esterase, Tchigvintsev *et al*., 2015), including from sea ice (amylase, Wang *et al*., 2018), but fewer have been performed on cold-active leucine aminopeptidases or proteases (Lei *et al*., 2016; Salwan *et al.*, 2020). Patterns of halophilic enzyme sensitivity to salt from these studies, as well as studies of non-cold-active halophilic enzymes, are consistent with our observations of maximal EEA rates at supra-optimal salinities for both *Cp*34H and *P*7E (*i.e.*, at 55–90 ppt). Though enzymes can display a variety of salinity effects, moderately high salinity (*e.g*., between 0.5 and 2.0 M NaCl, as observed in Qin *et al*., 2014, and Wang *et al*., 2018) can enhance halophilic prokaryotic enzyme activity by stabilizing protein structures and interactions (Ortega *et* al., 2011; Sinha & Khare, 2014). The overall higher level of activity of enzymes produced by *Cp*34H when grown at supra-optimal salinities (55 and 70 ppt) suggests that the enzymes may indeed be charge-stabilized by the higher salinity. Conversely, salinities well beyond an organism's tolerance can have the effect of disrupting protein structure, reducing EEA rates. Such effects have been seen in other halophilic and halotolerant marine bacteria (Qin *et al*., 2014; Wu *et al*., 2015; de Santi *et al*., 2016; Wang *et*

al., 2018). This effect likely explains the lower rates of EEA observed at 120 ppt for *Cp*34H, which is beyond the maximum growth salinity of *Cp*34H, although the upper salinity bound for activity or survival of *Cp*34H is not known. Other organisms show monotonically decreasing enzyme activity with increased salt concentrations (Takenaka *et al*., 2018), such as observed with *P*7E, although our result is notable given the wide salinity range for growth of *P*7E. Given that our experiments assayed free EE, and not also attached EE, it is possible that *P*7E employs a different production strategy than *Cp*34H, favoring attached over free EE. Indeed, observations in marine systems have shown that the fraction of attached enzymes can vary greatly within an environment (Baltar, 2018).

As previously mentioned, the fluorescence assay used in this study cannot distinguish between enhanced EEA due to higher individual enzyme activity rates or higher concentration of enzymes. Enhanced EEA of *Cp*34H grown at –8˚C, which is well below the growth temperatures that maximize yield (–1˚C) or growth rate (8˚C), is likely the result of the latter; psychrophilic and psychotropic bacteria often reach maximal EE production at temperatures below their optimal growth temperatures (Buchon *et al*., 2000). Such behavior may represent a metabolic trade-off between growth and organic matter acquisition (Ramin and Allison, 2019). In cold marine environments, canonical thought suggests that bacteria require higher substrate concentration to enable activity and growth (Pomeroy and Wiebe, 2001). Previous studies have demonstrated that free extracellular enzymes can liberate enough organic substrate to sustain bacterial growth (Vetter *et al*., 1998; 1999). Thus enhanced enzyme production may help balance this resource need within sea-ice brines, where characteristic extremes of temperature and salinity already act to reduce growth rates.

3.4.2 EEA at the seawater/sea-ice interface

Observations from freeze-thaw cycle experiments showed increasing rates of EEA from seawater to SML to sea ice, likely reflective of the changing physical and biological constraints within each niche. Underlying seawater, which showed the lowest rates of activity, is the most dilute of these environments, whereas both sea ice and SML contain higher concentrations of organic matter. During growth in dilute nutrient (but non-starving) conditions, bacteria are less likely to produce extracellular enzymes (Cezairliyan & Ausubel, 2017). Previous investigations of the SML at temperate latitudes have confirmed EEA within this environment, but such measurements are sparse (Kuznetsova & Lee, 2001; Mustaffa *et al*., 2017; Perliński *et al*., 2017). Our study is unique for including the tracking of EEA in an Arctic SML through a freeze-thaw cycle that mimics natural conditions.

Though EEA rates among the natural samples were observed to be highest in sea ice in our work, the complexity of sea-ice brine complicates attribution of high activity to any one factor. For example, it is possible that EEA in sea ice is in part the result of the "living dead," i.e., free extracellular enzymes that persist unlinked to their producer (Baltar, 2018). Free enzymes can be released by bacteria as a result of changes in cell permeability (Chrost, 1990), which sea-ice bacteria commonly experience as a result of salinity changes due to freeze-thaw cycling in ice (Ewert & Deming, 2013). This process likely contributes to the elevated rates of EEA within our sea-ice samples which underwent thawing prior to rate measurement. Evidence suggests that diatoms and other phytoplankton, similar to those that can inhabit sea ice, also release extracellular enzymes (*e.g.,* Palenik & More, 1990; Paul & Pohnert, 2013; Luxmi *et al*., 2018). While not expressly considered here, it is possible that algal enzymes may contribute to measured EEA in our field samples.

Extracellular enzymes likely retain activity through the freezing and concentration process, even if the bacteria producing these enzymes do not. Free enzymes are known to persist in cold water (Steen & Arnosti *et al*., 2011) and be stabilized by bacterial EPS (Huston *et al*., 2004), which can be selectively entrained into sea ice during formation (Ewert & Deming, 2011). EPS are also copiously produced in sea ice by algae (Krembs *et al*., 2002) and by bacteria, as shown in simulated sea-ice brines when temperature was decreased to –8°C (Marx *et al*., 2009), potentially extending the life-time of enzymes present in the ice. These factors, in addition to ongoing EE production, may lead to accumulation of free EE, especially EE unlinked to the bacteria that produced them.

Within brines, enzymes experience increased viscosity as temperatures drop and salinity increases (Cox & Weeks 1975), limiting diffusion while affecting strategies of extracellular enzyme production. By their nature, extracellular enzymes are a community good: degraded substrate will diffuse to benefit the closest cell (Vetter *et al*., 1998). In models of well-mixed, low-viscosity environments, this effect leads to extinction of EE-producing cells and the proliferation of cheater cells, those which do not produce EE but reap the benefit. Conversely, while under a high-viscosity regime with spatial structuring, a mixed community of producer and cheater cells proliferates (Nowak & May, 1992; Wakano *et al*., 2009; Allison *et al*., 2014). Given observed EEA in sea ice, a mixed community of cheaters and enzyme producers therefore seems likely in this environment. This interpretation implies active production of extracellular enzymes within sea ice, a conclusion corroborated by our observation of EEA in cultures of *Cp*34H grown at –8˚C. However, the diffusion regime suggests that free EE have a low return for producers and cheaters alike because of high viscosity conditions, especially for motile cells (Traving *et al*., 2015). Given that motility has been observed under near *in situ* conditions for sea-ice brines (Lindensmith *et al*.,

2016) and for *Cp*34H under analogue brine conditions (Junge *et al*., 2003; Wallace *et al*., 2015; Showalter & Deming 2018), attached EE are likely to be a more beneficial strategy in sea ice.

3.4.3 Environmental implications

While EEA is often considered the rate-limiting step for organic carbon cycling within open ocean environments, results of this study indicate that EEA may not be rate-limiting within sea-ice brines. Slower bacterial growth and metabolic activity rates preclude a need for rapid hydrolysis of large-sized organic material, especially if free enzymes are abundant due to freeze-in and slow decay rates. Rather, enzyme activity in sea-ice brines may be most ecologically relevant when considering the composition of organic material and phase transitions during ice growth and melt.

Much organic matter within sea ice is carbohydrate, largely as a result of EPS production, although sea-ice brine pockets can also be enriched in proteinaceous material (Thomas *et al*., 2001; Underwood *et al*., 2010; Stedmon *et al*., 2011; Müller *et al*., 2013). While the aminopeptidases measured in this study would not measure degradation of carbohydrate-rich materials, the bacterial production of active enzymes under extreme conditions suggests that sea-ice communities likely have the ability to produce carbohydrate-degrading enzymes as well. Data suggest that freezing promotes aggregation of DOM in sea ice, leaving a small portion of OM in sea ice as dissolved (Passow, 2002; Meiners *et al*., 2003; Müller *et al*., 2011; Müller *et al*., 2013; Jørgensen *et al*., 2015; Longnecker, 2015; see Krembs *et al*., 2002 for an opposing view). Active hydrolysis, typically enhanced on aggregates compared to surrounding environments, could thus increase the relative proportion of low molecular weight organics to the benefit not only of sea-ice communities but also SML and seawater communities during ice melt. In effect, high rates of EEA within sea-ice brines could define sea ice as a "digestor," particularly for members of the community less well

adapted to extreme temperatures or salinities. This role may be especially important at high latitudes where genome streamlining may have led to highly specific enzymes (Steen & Arnosti, 2014); long periods of enzymatic digestion in sea-ice brines could circumvent this limitation and decrease community response time to organic input during melt season. Indeed, organic material from sea ice less than 100 kDa in size has been shown to promote rapid growth in seawater bacteria after ice melt (Underwood *et al*., 2019).

Conversely, SML, which also contains higher concentrations of organic matter than underlying seawater, is enriched in amino acids (Engel *et al*,. 2018). While carbohydrase, lipase, and peptidase activities in the SML have been confirmed by past studies, they were measured at relatively warm temperatures (> 4˚C, Kuznetsova & Lee, 2001) or unspecified temperatures (Mustaffa *et al*., 2017; Perliński *et al*., 2017). Our work demonstrates that active EEA in the SML proceeds both at sub-zero temperatures and immediately following thawing of frozen samples, suggesting that EE produced by SML communities can survive the thaw-freeze transition and retain EEA within sea ice. EEA within the SML at low temperatures may also have atmospheric implications: organic material from the ocean's surface has been found to serve as ice-nucleating material when of the proper size (Chance *et al*., 2018). The ice-nucleating potential of the SML is especially relevant in the Arctic, where future cloud cover is a large unknown (Kay *et al*., 2016).

Further characterizations of enzyme activity in extreme environments are warranted. As highlighted by Arnosti (2011), the standard method of EEA measurement (Hoppe, 1983) presents an incomplete picture of environmental processes with respect to substrate specificity and degradation of complex compounds such as EPS. Furthermore, quantification of enzyme production under such conditions may enhance our understanding of which organisms actively produce enzymes under specific environmental conditions and which organisms reap the benefit.

The results presented here show extracellular enzyme production and activity in low temperature, high salinity conditions, presenting an expanded understanding of bacterially mediated carbon cycling within sea ice. In demonstrating EEA to –8˚C and 120 ppt salts in the laboratory, and activity to –10˚C and up to 142 ppt salts in field samples, we present a potential mechanism for DOC degradation within winter sea ice, potentially serving as a primer for spring communities at the onset of ice melt by increasing the fraction of low molecular weight organic matter readily available for uptake.

Acknowledgements

The field work detailed in this chapter was performed aboard the Swedish icebreaker *IB Oden* during the 2018 Arctic Ocean MOCCHA expedition and assisted by Anders Torstensson, Walker Smith, and Andrew Margolin, and the crew of *Oden*. SML samples were collected by Brandy Robinson and Michaela Haack under the direction of Oliver Wurl. We thank Ginger Armbrust for use of her fluorometer while aboard *Oden* and Shelly Carpenter for assistance in bacterial counts and cruise logistics and discussion in experimental planning.

References

Allison, S. D., Lu, L., Kent, A. G., Martiny, A. C. (2014). Extracellular enzyme production and cheating in *Pseudomonas fluorescens* depend on diffusion rates. *Front Microbiol*, *5*(APR), 1–8. https://doi.org/10.3389/fmicb.2014.00169

Amon, R. M. W., H.-P. Fitznar, R. Benner. (2001). Linkages among the bioreactivity, chemical composition, and diagenetic state of marine dissolved organic matter. *Limnol Oceanogr 4*6, 287–297. https://doi.org/10.4319/lo.2001.46.2.0287

Arnosti, C. (1995). Measurement of depth- and site-related differences in polysaccharide hydrolysis rates in marine sediments. *Geochim Cosmochim Acta, 59*, 4247–4257.

Arnosti C., & Jørgensen, B. B. (2003). High activity and low temperature optima of extracellular enzymes in Arctic sediments: implications for carbon cycling by heterotrophic microbial communities. *Mar Ecol Prog Ser 249,* 15–24.

Arnosti, C. (2011). Microbial extracellular enzymes and the marine carbon cycle. *Ann Rev Mar Sci*, *3*(1), 401–425. https://doi.org/10.1146/annurev-marine-120709-142731

Arrigo, K. R. (2014). Sea ice ecosystems. *Ann Rev Mar Sci*, *6*. https://doi.org/10.1146/annurev-marine-010213-135103

Aslam, S. N., Michel, C., Niemi, A., Underwood, G. J. C. (2016). Patterns and drivers of carbohydrate budgets in ice algal assemblages from first year Arctic sea ice. *Limnol Oceanogr*, *61*(3), 919–937. https://doi.org/10.1002/lno.10260

Baltar, F. (2018). Watch out for the "living dead": Cell-free enzymes and their fate. *Front Microbiol*, *8*(JAN), 1–6. https://doi.org/10.3389/fmicb.2017.02438

Baltar, F., Arístegui, J., Sintes, E., Van Aken, H. M., Gasol, J. M., Herndl, G. J. (2009). Prokaryotic extracellular enzymatic activity in relation to biomass production and respiration in the meso- and bathypelagic waters of the (sub)tropical Atlantic. *Environ Microbiol*, *11*(8), 1998–2014. https://doi.org/10.1111/j.1462-2920.2009.01922.x

Bauvois, C., Jacquamet, L., Huston, A. L., Borel, F., Feller, G., Ferrer, J. L. (2008). Crystal structure of the cold-active aminopeptidase from *Colwellia psychrerythraea*, a close structural homologue of the human bifunctional leukotriene A4 hydrolase. *J Biol Chem*, *283*(34), 23315–23325. https://doi.org/10.1074/jbc.M802158200

Boetius, A. (1995). Microbial hydrolytic enzyme activities in deep-sea sediments. *Helgoland Mar Res*, *49*(1–4), 177–187. https://doi.org/10.1007/BF02368348

Bruno, S., Coppola, D., di Prisco, G., Giordano, D., Verde, C. (2019) Enzymes from marine polar regions and their biotechnological applications. *Marine Drugs, 17*(544). https://doi.org/10.3390/md17100544

Buchon, L., Laurent, P., Gounot, A. M., & Guespin-Michel, J. F. (2000). Temperature dependence of extracellular enzymes production by psychrotrophic and psychrophilic bacteria. *Biotech Lett*, *22*(19), 1577–1581. https://doi.org/10.1023/A:1005641119076

Cezairliyan, B., & Ausubel, F. M. (2017). Investment in secreted enzymes during nutrient-limited growth is utility dependent. *Proc Natl Acad Sci USA 114*(37), E7796–E7802. https://doi.org/10.1073/pnas.1708580114

Chance, R. J., Hamilton, J. F., Carpenter, L. J., Hackenberg, S. C., Andrews, S. J., Wilson, T. W. (2018). Water-soluble organic composition of the Arctic sea surface microlayer and association with ice nucleation ability. *Environ Sci Technol*, *52*(4), 1817–1826. https://doi.org/10.1021/acs.est.7b04072

Chand Kasana, R. (2010). Proteases from psychrotrophs: An overview. *Crit Rev Microbiol*, *36*(2), 134–145. https://doi.org/10.3109/104084-10903-485525

Christian, J. R., & Karl, D. M. (1995). Bacterial ectoenzymes in marine waters: activity ratios and temperature responses in three oceanographic provinces. *Limnol Oceanogr 40*:1042–49

Chróst, R. J. (1990). Microbial ectoenzymes in aquatic environments. In Overbeck, J., & Chróst, R. J. (Eds.), *Aquatic Microbial Ecology, Biochemical and Molecular Approaches*, New York, NY: Springer, 47–78.

Chróst, R. J. (1991). Environmental control of the synthesis and activity of aquatic microbial ectoenzymes. In Chróst, R.J. (ed.). *Microbial Enzymes in Aquatic Environments*, (New York: Springer-Verlag), 84–95.

Cox, G. F. N., & Weeks, W. F. (1975). Brine Drainage and Initial Salt Entrapment in Sodium Chloride Ice. *US Army Corps Eng Cold Reg Res Eng Lab Res Rep*, *345*.

Cox, G. F. N., & Weeks, W. F. (1983). Equations for determining the gas and brine volumes in sea ice samples. *J Glaciol*, *29*(102), 306–316.

Davey, K. E., Kirby, R. R., Turley, C. M., Weightman, A. J., Fry, J. C. (2001). Depth variation of bacterial extracellular enzyme activity and population diversity in the northeastern North Atlantic Ocean. *Deep-Sea Res II 48,* 1003–17.

Deming, J. W. (2007) Life in ice formations at very cold temperatures. In Gerday, C. and Glansdorff, N. (Eds.), *Physiology and Biochemistry of Extremophiles*, ASM Press.

De Santi, C., Leiros, H. K. S., Di Scala, A., de Pascale, D., Altermark, B., & Willassen, N. P. (2016). Biochemical characterization and structural analysis of a new cold-active and salt-tolerant esterase from the marine bacterium *Thalassospira sp*. *Extremophiles*, *20*(3), 323–336. https://doi.org/10.1007/s00792-016-0824-z

Engel, A., Sperling, M., Sun, C., Grosse, J., Friedrichs, G. (2018). Organic matter in the surface microlayer: Insights from a wind wave channel experiment. *Front Mar Sci*, *5*(JUN). https://doi.org/10.3389/fmars.2018.00182

Ewert, M., & Deming, J. W. (2011). Selective retention in saline ice of extracellular polysaccharides produced by the cold-adapted marine bacterium *Colwellia psychrerythraea* strain 34H. *Ann Glaciol*, *52*, 111–117. https://doi.org/10.3189/172756411795931868

Ewert, M., & Deming, J. W. (2013). Sea ice microorganisms: Environmental constraints and extracellular responses. *Biol*, *2*(2), 603–628. https://doi.org/10.3390/biology2020603

Ewert, M., & Deming, J. W. (2014). Bacterial responses to fluctuations and extremes in temperature and brine salinity at the surface of Arctic winter sea ice. *FEMS Microbiol Ecol*, *89*(2). https://doi.org/10.1111/1574-6941.12363

Feller, G., & Gerday, C. (2003). Psychrophilic enzymes: Hot topics in cold adaptation. *Nat Rev Microbiol*, *1*(3), 200–208. https://doi.org/10.1038/nrmicro773

Fukuda, R., Sohrin, Y., Saotome, N., Fukuda, H., Nagata, T., Koike, I. (2000). East-west gradient in ectoenzyme activities in the subarctic Pacific: possible regulation by zinc. *Limnol Oceanogr 45,* 930–39.

Galgani, L., Piontek, J., Engel, A. (2016). Biopolymers form a gelatinous microlayer at the air-sea interface when Arctic sea ice melts. *Sci Rep*, *6*(April), 1–10. https://doi.org/10.1038/srep29465

Grossart, H. P., Tang, K. W., Kiørboe, T., Ploug, H. (2007). Comparison of cell-specific activity between free-living and attached bacteria using isolates and natural assemblages. *FEMS Microbiol Lett*, *266*(2), 194–200. https://doi.org/10.1111/j.1574-6968.2006.00520.x

Groudieva, T., Kambourova, M., Yusef, H., Royter, M., Grote, R., Trinks, H., & Antranikian, G. (2004). Diversity and cold-active hydrolytic enzymes of culturable bacteria associated with Arctic sea ice, Spitzbergen. *Extremophiles*, *8*(6), 475–488. https://doi.org/10.1007/s00792-004-0409-0

Helmke, E., & Weyland, H. (1995). Bacteria in sea ice and underlying water of the eastern Weddell Sea in midwinter. *Mar Ecol Prog Ser*, *117*(1–3), 269–288. https://doi.org/10.3354/meps117269

Hoppe, H-G. (1983). Significance of exoenzymatic activities in the ecology of brackish water: measurements by means of methylumbelliferyl-substrates. *Mar Ecol Prog Ser, 11*, 299–308.

Hoppe, H-G., & Ullrich, S. (1999). Profiles of ectoenzymes in the Indian Ocean: phenomena of phosphatase activity in the mesopelagic zone. *Aquat Microbiol Ecol, 19,* 139–148.

Huston, A. L., Krieger-Brockett, B. B., Deming, J. W. (2000). Remarkably low temperature optima for extracellular enzyme activity from Arctic bacteria and sea ice. *Environ Microbiol 2*(4), 383–388. https://doi.org/10.1046/j.1462-2920.2000.00118.x

Huston, A. L., & Deming, J. W. (2002). Relationships between microbial extracellular enzymatic activity and suspended and sinking particulate organic matter: Seasonal transformations in the North Water. *Deep-Sea Res II 49*(22–23), 5211–5225. https://doi.org/10.1016/S0967-0645(02)00186-8

Huston, A. L. (2003). Bacterial adaptation to the cold: in situ activities of extracellular enzymes in the North Water Polynya and characterization of a cold-active aminopeptidase from *Colwellia psychrerythraea* strain 34H. Doctoral Dissertation, *University of Washington, Seattle.*

Huston, A. L., Methe, B., Deming, J. W. (2004). Purification, characterization, and sequencing of an extracellular cold-active aminopeptidase produced by marine psychrophile *Colwellia psychrerythraea* strain 34H. *Appl Environ Microbiol*, *70*(6), 3321–3328. https://doi.org/10.1128/AEM.70.6.3321-3328.2004

Jørgensen, L., Stedmon, C. A., Kaartokallio, H., Middelboe, M., Thomas, D. N. (2015). Changes in the composition and bioavailability of dissolved organic matter during sea ice formation. *Limnol Oceanogr*, *60*(3), 817–830. https://doi.org/10.1002/lno.10058

Junge, K., Eicken, H., Deming, J. W. (2003). Motility of *Colwellia psychrerythraea* strain 34H at Subzero. *Microbiol Ecol 69*(7), 8–11. https://doi.org/10.1128/AEM.69.7.4282

Kähler, P., P. K. Bjørnsen, K. Lochte, A. Antia. (1997). Dissolved organic matter and its utilization by bacteria during spring in the Southern Ocean. *Deep-Sea Res II 44,* 341– 353. https://doi.org/10.1016/S0967-0645(96)00071-9

Karan, R., Capes, M. D., DasSarma, S. (2011). Function and biotechnology of extremophilic enzymes. *Biochem (Moscow)*, *76*(6), 686–693. https://doi.org/10.1134/S0006297911060095

Kay, J. E., L'Ecuyer, T., Chepfer, H., Loeb, N., Morrison, A., & Cesana, G. (2016). Recent advances in Arctic cloud and climate research. *Curr Climate Change Reps*, *2*(4), 159–169. https://doi.org/10.1007/s40641-016-0051-9

Kellogg, C. T. E., Deming, J. W. (2014). Particle-associated extracellular enzyme activity and bacterial community composition across the Canadian Arctic Ocean. *FEMS Microbiol Ecol*, 89(2), 360–375. https://doi-org.offcampus.lib.washington.edu/10.1111/1574-6941.12330

Krembs, C., Eicken, H., Junge, K., Deming, J. W. (2002). High concentrations of exopolymeric substances in Arctic winter sea ice: Implications for the polar ocean carbon cycle and cryoprotection of diatoms. *Deep Sea Res I, 49*(12), 2163–2181. https://doi.org/10.1016/S0967-0637(02)00122-X

Kulakova, L., Galkin, A., Kurihara, T., Yoshimura, T., Esaki, N. (1999). Cold-active serine alkaline protease from the psychrotrophic bacterium *Shewanella* strain Ac10: Gene cloning and enzyme purification and characterization. *Appl Enivron Microbiol, 65*(2), 611–617. https://doi.org/10.1128/aem.65.2.611-617.1999

Kushner, D.J., & Kamekura, M. (1988) Physiology of halophilic eubacteria. In: Rodríguez-Valera, F. (Ed.) *Halophilic Bacteria*. CRC, Boca Raton.

Kuznetsova, M., & Lee, C. (2001). Enhanced extracellular enzymatic peptide hydrolysis in the sea-surface microlayer. *Mar Chem*, *73*(3–4), 319–332. https://doi.org/10.1016/S0304-4203(00)00116-X

Lei, F., Zhao, Q., Sun-Waterhouse, D., Zhao, M. (2017). Characterization of a salt-tolerant aminopeptidase from marine *Bacillus licheniformis* SWJS33 that improves hydrolysis and debittering efficiency for soy protein isolate. *Food Chem*, *214*, 347–353. http://dx.doi.org/10.1016/j.foodchem.2016.07.028

Lindensmith, C. A., Rider, S., Bedrossian, M., Wallace, J. K., Serabyn, E., Showalter, G. M., Deming, J. W., Nadeau, J. L. (2016). A submersible, off-axis holographic microscope for detection of microbial motility and morphology in aqueous and icy environments. *PLoS ONE*, *11*(1). https://doi.org/10.1371/journal.pone.0147700

Longnecker, K. (2015). Dissolved organic matter in newly formed sea ice and surface seawater. *Geochim Cosmochim Acta*, *171*, 39–49. https://doi.org/10.1016/j.gca.2015.08.014

Luxmi, R., Blaby-Haas, C., Kumar, C., Rauniyar, N., King, S. M., Mains, R. E. *et al.* (2018). Proteases shape the *Chlamydomonas* secretome: Comparison to classical neuropeptide processing machinery. *Proteomes*, *6*(36). https://doi.10.3390/proteoms6040036

Madern, D., Ebel, C., Zaccai, G. (2000). Halophilic adaptation of enzymes. *Extremophiles*, *4*(2), 91–98. https://doi.org/10.1007/s007920050142

Martínez-Rosales, C., Castro-Sowinski, S. (2011). Antarctic bacterial isolates that produce cold-active extracellular proteases at low temperature but are active and stable at high temperature. *Polar Res, 30*, 7123. https://doi.org/10.3402//polar.v30i0.7123

Marx, J. G., Carpenter, S. D., Deming, J. W. (2009). Production of cryoprotectant extracellular polysaccharide substances (EPS) by the marine *Colwellia psychrerythraea* strain 34H under extreme conditions. *Can J Microbiol 55*, 63–72.

Meiners, K., Gradinger, R., Fehling, J., Civitarese, G., Spindler, M. (2003). Vertical distribution of exopolymer particles in sea ice of the Fram Strait (Arctic) during autumn. *Mar Ecol Prog Ser*, *248*, 1–13. https://doi.org/10.3354/meps248001

Meyer-Reil, L. A. (1991). Ecological aspects of enzyme activity in marine sediments. In Chróst, R.J. (Ed.), *Microbial Enzymes in Aquatic Environments*, New York: Springer-Verlag, 84–95.

Morita, R. (1975). Psychrophilic bacteria. *Bacteriol Rev*, *39*(2), 144–167.

Müller, S., Vähätalo, A. V., Granskog, M. A., Autio, R., Kaartokallio, H. (2011). Behaviour of dissolved organic matter during formation of natural and artificially grown Baltic Sea ice. *Ann Glaciol*, *52*(57), 233–241. https://doi.org/10.3189/172756411795931886

Müller, S., Vähätalo, A. V., Stedmon, C. A., Granskog, M. A., Norman, L., Aslam, S. N., *et al*. (2013). Selective incorporation of dissolved organic matter (DOM) during sea ice formation. *Mar Chem*, *155*, 148–157. https://doi.org/10.1016/j.marchem.2013.06.008

Mustaffa, N. I. H., Striebel, M., Wurl, O. (2017) Enrichment of extracellular carbon anhydrase in the sea surface microlayer and its effect on air-sea CO_2 exchange. *Geophys Res Letts*, *44*(12), 324–330. doi: 10.1002/2017GL075797

Nowak, M. A., & May, R. M. (1992). Evolutionary games and spatial chaos. *Nature*, *359*, 826–829.

Ortega, G., Laín, A., Tadeo, X., López-Méndez, B., Castaño, D., Millet, O. (2011). Halophilic enzyme activation induced by salts. *Sci Rep*, *1*, 1–6. https://doi.org/10.1038/srep00006

Palenik, B., & Morel, F. M. M. (1990) Comparison of cell-surface L-amino acid oxidases from several marine phytoplankton. *Mar Ecol Prog Ser, 59*, 195–201.

Passow, U. (2002). Transparent exopolymer particles (TEP) in aquatic environments. *Prog Oceanogr*, *55*(3–4), 287–333. https://doi.org/10.1016/S0079-6611(02)00138-6

Paul, C., & Pohnert, G. (2013). Induction of protease release of the resistant diatom *Chaetoceros didymus* in response to lytic enzymes from an algicidal bacterium. *PLoS One, 8*(3) e57577. https://doi.10.137/journal.pone.0057577

Perliński, P., Mudryk, Z. J., Antonowicz, J. (2017). Enzymatic activity in the surface microlayer and subsurface water in the harbour channel. *Estuar Coast Mar Sci*, *196*, 150–158. https://doi.org/10.1016/j.ecss.2017.07.001

Pomeroy, L. R., & Wiebe, W. J. (2001). Temperature and substrates as interactive limiting factors for marine heterotrophic bacteria. *Aquat Microb Ecol*, *23*(2), 187–204. https://doi.org/10.3354/ame023187

Poremba, K. (1995). Hydrolytic enzymatic activity in deep-sea sediments. *FEMS Microb Ecol*, *16*(3), 213–221. https://doi.org/10.1016/0168-6496(94)00085-B

Prasad, S., Manasa, P., Buddhi, S., Tirunagari, P., Begum, Z., Rajan, S., *et al*. (2014). Diversity and bioprospective potential (cold-active enzymes) of cultivable marine bacteria from the subarctic glacial fjord Kongsfjorden. *Curr Microbiol*, *68*, 233–238. https://doi.org/10.1007/s00284-013-0467-6

Qin, Y., Huang, Z., Liu, Z. (2014). A novel cold-active and salt-tolerant α-amylase from marine bacterium *Zunongwangia profunda*: Molecular cloning, heterologous expression and biochemical characterization. *Extremophiles*, *18*(2), 271–281. https://doi.org/10.1007/s00792-013-0614-9

Ramin, K. I., & Allison, S. D. (2019). Bacterial tradeoffs in growth rate and extracellular enzymes. *Front Microbiol*, *10*, 1–10. https://doi.org/10.3389/fmicb.2019.02956

Ribas-Ribas, M., Mustaffa, N. I. H., Rahlff, J., Stolle, C. Wurl, O. (2017). Sea Surface Scanner (S^3): a catamaran for high-resolution measurements of biochemical properties of the sea surface microlayer. *J Atmos Ocean Technol, 34*, 1433–1448. https://doi.org/10.1175/JTECH-D-17-0017.1

Salwan, R., Sharma, V., Chand Kasan, R., Gulati, A. (2020). Bioprospecting psychrotrophic bacteria for serine-type proteases from the cold areas of the Western Himalayas. *Curr Microbiol*, *77*, 795–806. https://doi.org/10.1007/s00284-020-01876-w

Serreze, M. C., & Stroeve, J. (2015). Arctic sea ice trends, variability and implications for seasonal ice forecasting. *Phil T R Soc A*, *373*(2045). https://doi.org/10.1098/rsta.2014.0159

Showalter, G. M., & Deming, J. W. (2018). Low-temperature chemotaxis, halotaxis and chemohalotaxis by the psychrophilic marine bacterium *Colwellia psychrerythraea* 34H. *Environ Microbiol Rep*, *10*(1). https://doi.org/10.1111/1758-2229.12610

Sinha, R., & Khare, S. K. (2014). Protective role of salt in catalysis and maintaining structure of halophilic proteins against denaturation. *Front Microbiol*, *5*(APR), 1–6. https://doi.org/10.3389/fmicb.2014.00165

Srinivas, T. N. R., Nageswara Rao, S. S. S., Vishnu Vardha Reddy, P., Pratibha, M. S., Sailaja, B., Kavya, B., *et al*. (2009). Bacterial diversity and bioprospecting for cold-active lipases, amylases and proteases, from culturable bacteria of Kongsfjorden and Ny-Ålesund, Svalbard, Arctic. *Curr Microbiol, 59*, 537–547. https://doi.org/10.1007/s00284-009-9473-0

Steen, A. D., & Arnosti, C. (2011). Long lifetimes of β-glucosidase, leucine aminopeptidase, and phosphatase in Arctic seawater. *Mar Chem*, *123*(1–4), 127–132. https://doi.org/10.1016/j.marchem.2010.10.006

Steen, A. D., & Arnosti, C. (2013). Extracellular peptidase and carbohydrate hydrolase activities in an Arctic fjord (Smeerenburgfjord, Svalbard). *Aquat Microb Ecol*, *69*(2), 93–99. https://doi.org/10.3354/ame01625

Steen, A. D., & Arnosti, C. (2014). Picky, hungry eaters in the cold: Persistent substrate selectivity among polar pelagic microbial communities. *Front Microbiol*, *5*(OCT), 1–5. https://doi.org/10.3389/fmicb.2014.00527

Stedmon, C. A., Thomas, D. N., Papadimitriou, S., Granskog, M. A., Dieckmann, G. S. (2011). Using fluorescence to characterize dissolved organic matter in Antarctic sea ice brines. *J Geophys Res: Biogeosci*, *116*(3), 1–9. https://doi.org/10.1029/2011JG001716

Takenaka, S., Yoshinami, J., Kuntiya, A., Techapun, C., Leksawasdi, N., Seesuriyachan, P., *et al*. (2018). Characterization and mutation analysis of a halotolerant serine protease from a new isolate of *Bacillus subtilis*. *Biotechnol Lett*, *40*, 189–196. https://doi.org/10.1007/s10529-017-2459-2

Tchigvintsev, A., Tran, H., Popovic, A., Kovacic, F., Brown, G., Flick, R., *et al*. (2015). The environment shapes microbial enzymes: five cold-active and salt-resistant carboxylesterases from marine metagenomes. *Appl Microbiol Biotechnol*, *99*, 2165–2178.

Thomas, D. N., Kattner, G., Engbrodt, R., Giannelli, V., Kennedy, H., Haas, C., *et al*. (2001). Dissolved organic matter in Antarctic sea ice. *Ann Glaciol*, *33*, 297–303. https://doi.org/10.3189/172756401781818338

Torstensson, A., Margolin, A. R., Showalter, G. M., Smith, W. O., Shadwick, E. H., Carpenter, S. D., *et al*. (2020) Sea-ice microbial communities in the central Arctic Ocean: limited responses to short-term pCO_2 perturbations. *Limnol Oceanogr* (accepted)

Underwood, G. J. C., Aslam, S. N., Michel, C., Niemi, A., Norman, L., Meiners, K. M., Laybourn-Parry, J., *et al*. (2013). Broad-scale predictability of carbohydrates and exopolymers in Antarctic and Arctic sea ice. *Proc Natl Acad Sci USA*, *110*(39), 15734–15739. https://doi.org/10.1073/pnas.1302870110

Underwood, G. J. C., Fietz, S., Papadimitriou, S., Thomas, D. N., & Dieckmann, G. S. (2010). Distribution and composition of dissolved extracellular polymeric substances (EPS) in Antarctic sea ice. *Mar Ecol Prog Ser*, *404*, 1–19. https://doi.org/10.3354/meps08557

Underwood, G. J. C., Michel, C., Meisterhans, G., Niemi, A., Belzile, C., Witt, M., *et al*. (2019). Organic matter from Arctic sea-ice loss alters bacterial community structure and function. *Nat Climate Change*, *9*(2), 170–176. https://doi.org/10.1038/s41558-018-0391-7

Vetter, Y.-A., & Deming, J. W. (1994). Extracellular enzyme activity in the Arctic northeast water polynya. *Mar Ecol Prog Ser*, *114*(1–2), 23–34. https://doi.org/10.3354/meps114023

Vetter, Y.-A., & Deming, J. W. (1999). Growth rates of marine bacterial isolates on particulate organic substrates solubilized by freely released extracellular enzymes. *Microb Ecol, 37*, 86–94. https://doi.org/10.1007/s002489900133

Vetter, Y.-A., Deming, J. W., Jumars, P. A., Krieger-Brockett, B. B. (1998). A predictive model of bacterial foraging by means of freely released extracellular enzymes. *Microb Ecol 36*(1), 75–92. https://doi.org/10.1007/s002489900095

Wakano, J. Y., Nowak, M. A., Hauert, C. (2009). Spatial dynamics of ecological public goods. *Proc Natl Acad Sci USA*, *106*(19), 7910–7914. https://doi.org/10.1073/pnas.0812644106

Wallace, J. K., Rider, S., Serabyn, E., Kühn, J., Liewer, K., Deming, J., Showalter, G., Lindensmith, C., Nadeau, J. (2015). Robust, compact implementation of an off-axis digital holographic microscope. *Optics Express*, *23*(13), 17367. https://doi.org/10.1364/OE.23.017367

Wang, Q. F., Miao, J. L., Hou, Y. H., Ding, Y., Wang, G. D., Li, G. Y. (2005). Purification and characterization of an extracellular cold-active serine protease from the psychrophilic bacterium *Colwellia* sp. NJ341. *Biotechnol Lett*, *27*(16), 1195–1198. https://doi.org/10.1007/s10529-005-0016-x

Wang, X., Kan, G., Ren, X., Yu, G., Shi, C., Xie, Q., *et al*. (2018). Molecular cloning and characterization of a novel alpha-amylase from Antarctic sea ice bacterium *Pseudoalteromonas* sp. M175 and its primary application in detergent. *BioMed Res Intl.* https://doi.org/10.1155/2018/3258383

Wells, L. E., & Deming, J. W. (2006). Effects of temperature, salinity and clay particles on inactivation and decay of cold-active marine Bacteriophage 9A. *Aquat Microb Ecol*, *45*(1), 31–39. https://doi.org/10.3354/ame045031

Wheeler, P. A., Watkins, J. M., Hansing, R. L. (1997). Nutrients, organic carbon and organic nitrogen in the upper water column of the Arctic Ocean: Implications for the sources of dissolved organic carbon. *Deep-Sea Res II, 44*(8), 1571–1575. https://doi.org/10.1016/S0967-0645(97)00051-9

Wu, G., Zhang, X., Wei, L., Wu, G., Kumar, A., Mao, T., Liu, Z. (2015). A cold-adapted, solvent and salt tolerant esterase from marine bacterium *Psychrobacter pacificensis*. *Intl J Biol Macro*, *81*, 180–187. https://doi.org/10.1016/j.ijbiomac.2015.07.045

Wurl, O., Ekau, W., Landing, W. M., Zappa, C. J. (2017). Sea surface microlayer in a changing ocean - A perspective. *Elem Sci Anth*, *5*(31). https://doi.org/10.1109/TCOMM.2005.855022

Yu, Y., Li, H., Zeng, Y., Chen, B. (2009). Extracellular enzymes of cold-adapted bacteria from Arctic sea ice, Canada Basin. *Polar Biol*, *32*(10), 1539–1547. https://doi.org/10.1007/s00300-009-0654-x

Zäncker, B., Bracher, A., Röttgers, R., Engel, A. (2017). Variations of the organic matter composition in the sea surface microlayer: A comparison between open ocean, coastal, and upwelling sites off the Peruvian coast. *Front Microbiol*, *8*(DEC), 1–17. https://doi.org/10.3389/fmicb.2017.02369

Ziervogel, K., Steen, A. D., Arnosti, C. (2010). Changes in the spectrum and rates of extracellular enzyme activities in seawater following aggregate formation. *Biogeosci*, *7*(3), 1007–1015. https://doi.org/10.5194/bg-7-1007-2010

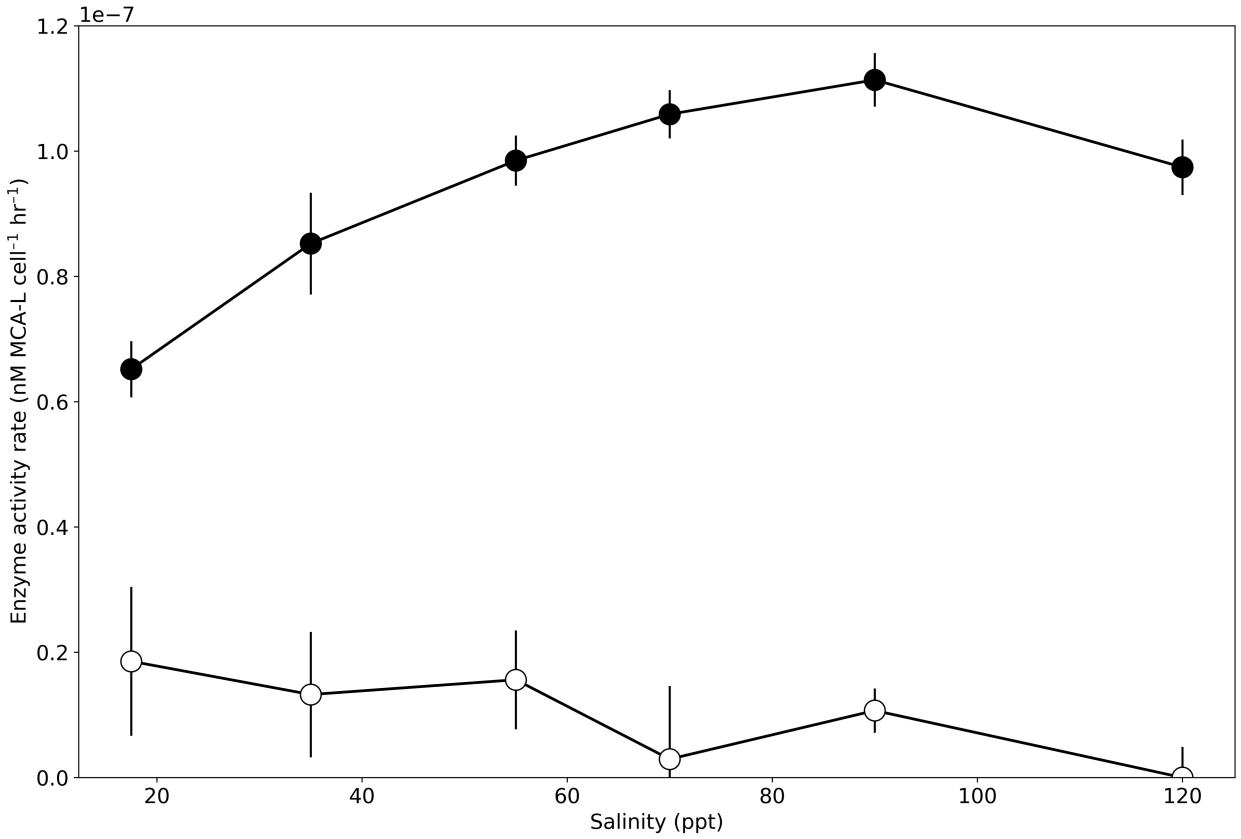

Figure 3.1 Extracellular enzyme activity rate as a function of salinity at –1°C. Data represent the average rate of EEA for both *Cp*34H (filled circles) and *P*7E (open circles) at each salinity with the standard deviation of replicate samples indicated by error bars (n = 3).

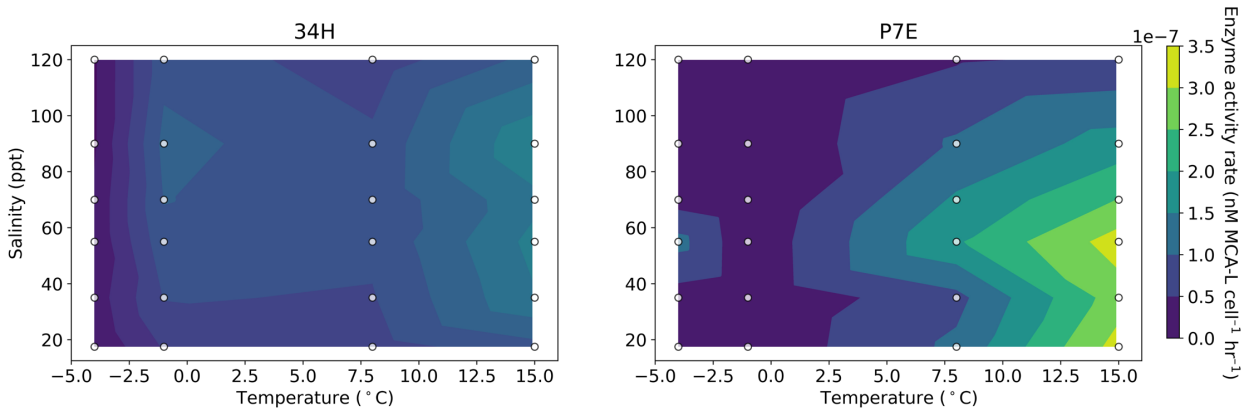

Figure 3.2 Rate of EEA in temperature and salinity space. Data represent the EEA measurements for both *Cp*34H (left panel) and *P*7E (right panel) across a temperature spectrum from –4˚C to 15˚C and salinity spectrum from 17.5 to 120 ppt when the organisms were grown (produced EE) at –1°C and 35 ppt. Open circles represent measurements (n = 3), with contours representing average rate as linearly interpolated using Python3. Integrated across all salinities, *Cp*34H showed significantly higher average activity at –1˚C than *P*7E ($p = 0.0001$), while *P*7E showed significantly higher activities at 8˚C ($p = 0.04$) and 15˚C ($p = 0.03$) according to a student's t-test.

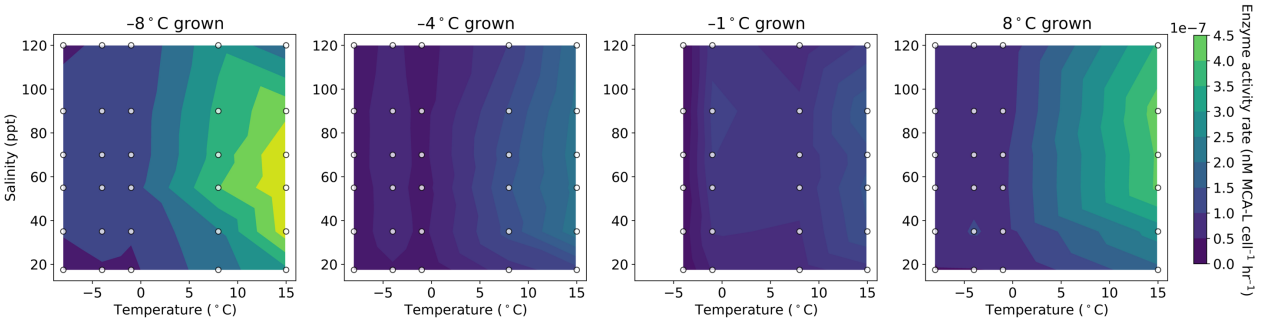

Figure 3.3 Rate of EEA in temperature and salinity space as a function of growth temperature. Data represent EEA measurements for *Cp*34H across a temperature spectrum between –8˚C to 15˚C and salinity spectrum from 17.5 to 120 ppt after growth at 35 ppt and –8˚C (far left panel), –4˚C (second panel), or 8˚C (far right panel). Open circles represent measurements (n = 3), with contours representing average rate as linearly interpolated using Python3. Contour of EEA when *Cp*34H was grown at –1˚C (third panel; Figure 3.2) is included for visual comparison. Cells grown at –8˚C showed significantly higher activity than cells grown at other temperatures when assayed at –8, –4, and 8˚C ($p < 0.05$).

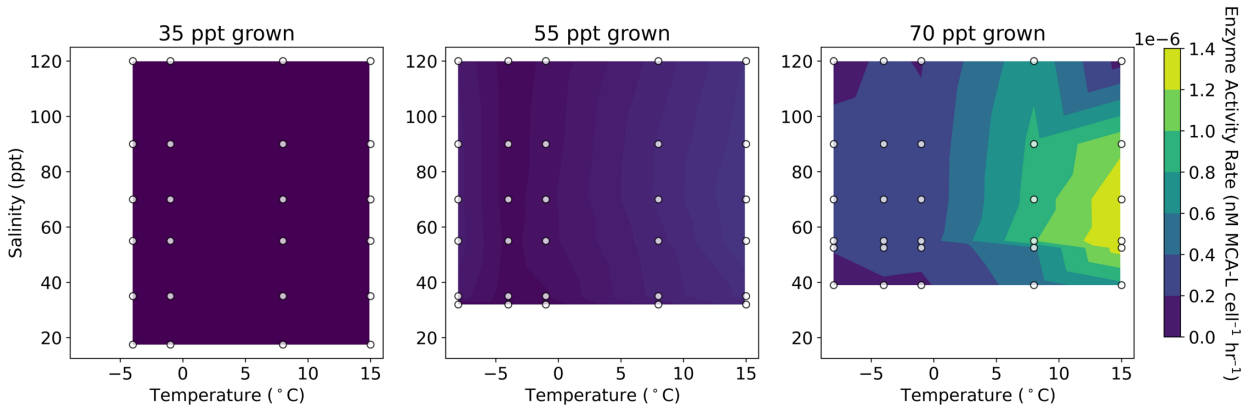

Figure 3.4 Rate of EEA in temperature and salinity space as a function of growth salinity. Data represent EEA measurements for *Cp*34H across a temperature spectrum between –8˚C to 15˚C and salinity spectrum between 17.5 to 120 ppt after growth at –1˚C and 55 ppt (center panel) or 70 ppt (right panel). Open circles represent measurements (n = 3), with contours representing average rate as linearly interpolated using Python3. Contour of EEA when *Cp*34H was grown at –1°C and 35 ppt (left panel) is included for visual comparison; note that EEA was detected but at relatively low levels compared to results for higher growth salinities. Difference in minimum test salinity at 55 and 70 ppt growth conditions are an result of maintaining constant organic content through dilution. At all temperatures measured except –4˚C, 35 ppt-grown cells showed significantly lower EEA than cells grown at 55 or 70 ppt ($p < 0.003$). At all temperatures measured, 70 ppt grown cells showed significantly higher EEA than either 35 or 55 ppt grown cells ($p < 0.004$ for all). Structure in the contours at scales smaller than the data points are artifacts of the interpolation scheme.

Table 3.1 EEA data from field samples. The averages of measured EEA rates (n = 3, unless noted) in samples of sea ice, under-ice water, and the sea-surface microlayer are displayed alongside experimental temperatures and salinities. Student t-tests were performed on pairs indicated by superscript letters and found to be statistically significant: (a, d-f) $p < 0.0001$, (b) $p = 0.031$, (c) $p = 0.0169$.

Sample type	Temperature (˚C)	Salinity (ppt)	Enzyme activity rate (x 10^{-6} nM MCA-L hr^{-1} $cell^{-1}$)
Sea-ice bottom	–1	19.5	$6.41 \pm 0.15^{a,d,e}$
Sea-ice bottom, frozen	–10	142[1]	$1.66 \pm 0.04^{a,f}$
Under-ice water	–1.8	32	$0.150 \pm 0.18^{b,d}$
Under-ice water	6	32	0.532 ± 0.09^{b}
Sea-surface microlayer	–1	8	$1.01 \pm 0.02^{c,e}$
Sea-surface microlayer, frozen	–1.8	8	$0.832 \pm 0.076^{c,f}$
Sea-surface microlayer frozen, endpoints	–10	100[1]	0.15[2]

[1]Salinities on these two frozen samples were calculated by applying the equations of Cox and Weeks (1983) to bulk salinity measurements of unfrozen (melted) samples.

[2] Only one sample was recovered for this experiment, so no statistics were performed.

Chapter 4.
Modeled viral dynamics: potential controls on infection and production rates within sea-ice brines

Abstract

Observations indicating high concentrations of viruses within sea-ice brines relative to bacteria indicate that bacteriophage may play an outsized role in shaping host community structure and recycling organic matter within sea ice. However, while these high virus-to-bacteria ratios may be a function of active viral production and release, they may also be the result of slow virion decay due to the low temperature, high salinity conditions of sea-ice brines. Here, we present a mathematical model of virus–host interactions within sea-ice brines, one that uses viral and bacterial abundance data to interpret which mechanisms may most influence population dynamics. We also assess the existence and potential impact of a viral shunt within sea ice. Data from both field samples and laboratory isolates were used to achieve most likely parameter distributions for *in situ* communities, constraining the model to observed dynamics. A simple model of phage-host interaction networks was adapted to demonstrate the impact of potential phage promiscuity suspected to be higher under sea-ice brine conditions than in seawater. Deeper understanding of the viral impact on sea-ice communities and the recycling of dissolved organic carbon within the ice will help to understand how these largely heterotrophic communities maintain activity under extreme conditions and further constrain Arctic carbon budgets through the seasons.

4.1 Introduction

Extremes of temperature (from near –40˚C to 0˚C) and salinity (from near 240 ppt to 0 ppt salts) characterize the entrapped brine network of sea ice, yet active sea-ice microbial communities persist within this habitat year-round (Ewert & Deming, 2013; Boetius *et al*., 2015). While phototrophs, largely diatoms, contribute the most biomass to these communities in sunlit seasons, heterotrophic bacteria, largely *Flavobacteria* and *Gammaproteobacteria* (up to 75% of the community), can achieve high densities in sea ice, up to 10^7 cells per milliliter of brine (Boetius *et al*., 2015). Evidence suggests that heterotrophic bacteria at low temperatures such as those experienced in sea ice require high concentrations of organic substrate to maintain activity and sustain growth (Pomeroy and Wiebe, 2001). In sunlit seasons, organic carbon is readily available, because net autotrophic sea ice microbial communities produce up to hundreds of milligrams of carbon per meter squared per day (Mikkelsen *et al*., 2008; Boetius *et al*., 2013). However, wintertime SIMCOs, dominated by heterotrophic bacteria (Deming, 2010; Boetius *et al*., 2015), must rely on organic substrates trapped and concentrated in the brine during the freezing process (Thomas *et al*., 1995; 2001; Meiners & Michel, 2017). In marine environments, organic substrate cycling is understood through the framework of the *microbial loop*, by which bacteria incorporate dissolved organic carbon (DOC) into biomass, facilitating trophic transfer. Bacteriophage, viruses that infect bacteria, “short circuit” this loop in a process known as the *viral shunt*, whereby viruses lyse bacteria and return DOC to the environment (Wilhelm & Suttle, 1999; Weitz & Wilhelm, 2012). In open-water marine environments, the viral shunt is suggested to recycle as much as 25% of all carbon fixed by autotrophs (Wilhelm & Suttle, 1999). How viruses may influence organic matter recycling within sea-ice brines, especially in bacterially dominated sea ice, is unknown.

Field observations of viral and bacterial abundances in the form of virus-to-bacteria ratios within sea ice, which approach a ratio of 10,000-to-1, can greatly exceed those of source seawater (Collins & Deming, 2011; Figure 4.1), which often range between 1 and 100 viruses per bacterium (Knowles *et al*., 2016; Wigington, *et* al., 2016; Parikka *et al*., 2017). These very high ratios have in turn led to the suggestion that viruses must be produced within sea-ice brines at rates well beyond those observed in seawater (Collins & Deming, 2011). The primary argument supporting this suggestion is that tight physical coupling between virus and host within a brine pore favors increased infection rates. Indeed, as a result of the physical freeze-concentration effect and reduced viscosity of subzero brines, the relative contact rate of viruses and bacteria within brines has been calculated to be up to 1,000 times greater than in seawater, depending on temperature (Wells & Deming, 2006a).

While high virus-to-bacteria ratios in sea ice could be interpreted as indicators of active or rapid viral production, few data on *in situ* viral production rates exist to verify this interpretation (Wells & Deming, 2006a; Paterson & Laybourn-Parry, 2012). Indeed, the virus-to-bacteria ratio increasingly is considered a poor indicator of production rate, as many factors influence the measurement, such a slow decay rates or processes such a pseudolysogeny which can regularly release individual viruses from still-living cells (Weitz *et al*., 2016). Within sea ice, slower bacterial growth rates as a result of high salinity and low temperature, including those of psychrophiles, may inhibit viral production (Kottmeier *et al*., 1987; Smith *et al*., 1989; Nedwell, 1999; Nichols *et al*., 1999; Huston, 2003). Likewise, slow decay of free viral particles (virions) under low-temperature conditions (Wells & Deming, 2006c) may drive a high virus-to-bacteria ratio, even in the absence of enhanced viral production (Köstner *et al*., 2017). Taken together,

these factors imply that the cause of the high virus-to-bacteria ratios as observed in sea ice remains unclear, and may be due to high production, low decay, or a combination of both factors.

Simple mathematical models can help to resolve mechanisms driving population dynamics within natural systems, and have often been deployed to understand virus-host interactions within the marine environment (for a review of such models, see Mateus, 2017). While these models are limited to a hypothetical understanding of interactions, they have been useful in understanding important ecological features such as community composition and nutrient cycling (Middelboe, 2000; Weitz *et al*., 2005; 2015). From a model using a simple series of differential equations, as employed here, insights have been gained into viral influence on basic population dynamics of marine systems (Middelboe, 2000), the coevolutionary "arms-race" between phage and host in marine systems (Weitz *et al.,* 2005), trophic transfer in a complex marine food web (Weitz *et al*., 2015), and states of host population dynamics which favor lytic or lysogenic invasion strategies by phages (Weitz & Dushoff, 2008). Such models are particularly useful for understanding potential modes of viral life strategy to reproduce observed patterns, for example toggling lytic cycles, in which viruses are reproduced and burst forth from the cell, and lysogenic cycles, in which viruses incorporate into the host genome (*e.g.*, Weitz *et al*., 2019).

To probe the underlying mechanisms of virus-host dynamics within sea ice, we present a mathematical model that adapts existing marine virus-host population models to sea-ice brine pores, approximated as a closed system of heterotrophic bacteria. The model incorporates field and laboratory observations with the goal of replicating observed virus-to-bacteria ratios and to interpreting which mechanisms may drive these observations, namely physical effects, growth and infection rates, lysogeny/lytic ratios, or phage-host specificity.

4.2 Materials and methods

4.2.1 Model framework

A simple model built with a series of differential equations built in the manner of Weitz (2015) served as the framework for several numerical experiments which considered sea-ice brines as a closed system. The model was initiated with a pool of nutrients (N) in the form of dissolved organic carbon (DOC) taken up by bacteria (B) and utilized for growth and respiration (Nguyen & Maranger, 2011). In turn, these bacteria exude DOC as a fraction of the uptake of nutrients. Viruses (V) infect the bacteria and contribute to the dissolved organic pool through lysis. To account for temperature-dependent concentration and viscosity effects, starting concentrations of N, B, and V were scaled to brine concentrating factor, a value representing the physical concentration effect of freezing (Cox and Weeks, 1983). Additionally, virus-host interactions were scaled according to relative contact rate (Wells and Deming, 2006a). These interactions were represented as a system of ordinary differential equations for N, B, and V which counted uptake and recycling (N; Eq. 4.1), growth, infection, and death (B; Eq. 4.2), and lysis, infection and death (V; Eq. 4.3) as the processes driving change. Equations are listed below, with additional explanation presented in Appendix 1.

Organic carbon: $$\dot{N} = -\alpha B \frac{N}{N+\xi} + \varrho \alpha B \frac{N}{N+\xi} + \upsilon \sigma B V \quad \textit{Eq. 4.1}$$

Bacterial concentration: $$\dot{B} = \mu \frac{N}{N+\xi} - \varphi B V - dB \quad \textit{Eq. 4.2}$$

Viral concentration: $$\dot{V} = \beta \varphi B V - \varphi B V - mB \quad \textit{Eq. 4.3}$$

Values for model parameters were taken from published values or extracted from datasets found in literature using the Metropolitan-Hastings fitting algorithm described in Thamatrakoln *et al*. (2019). Upon initiation of each model run, values of temperature-dependent parameters of interest (growth rate, μ; adsorption rate, φ; and burst size, β) were selected from distributions in an effort to account for biological variability; these distributions were constructed with published values or values extracted from published figures. A full list of values used for the model parameters and their sources is presented in Table 4.1. Given the unlikelihood that observations of virus-to-bacteria ratios in samples of natural sea ice represent steady-state systems, time-dependent model runs (*i.e.*, not necessarily reaching steady state) were also used to approximate observed virus-to-bacteria ratios by varying the focal parameters, i.e., the decay rate (m), and the lytic fraction (γ). All equations were coded in Python 3.1 and are available on GitHub.

4.2.2 Model analysis

The non-trivial steady-state solutions were found by setting the differential equations dNdt, dBdt, and dVdt to zero and solving for state variables (N, B, and V). The steady-state solution was then used to determine sensitivity of steady-state concentrations of bacteria and viruses to changes in the focal parameters of growth rate (μ), adsorption rate (φ), and burst size (β) and the additional parameter of viral decay rate (m). A Sobol' global variability analysis, which deconvolutes variance of model output to determine relative parameter control, was performed on the non-trivial steady-state solution in Python. Values were selected from parameter space using Saltelli sampling from a uniform distribution, log-normalized where applicable, and encoded using SAlib in Python 3.1 (Herman and Usher, 2017). A sensitivity cut-off of 0.05 was used to determine significant effect. Model parameters were iterated over a range of values taken from the literature extremes

and modeled VBR values were compared to the collection of previously observed VBR values given in Collins and Deming (2011; shown in Figure 4.1) using a t-test.

Lytic fraction, the percent of viruses in the system that leads to burst after infection, was approximated by applying a constant (γ) to the virus production term similar to the manner of Record *et al*. (2016). Lytic fraction was co-varied with the above parameters as a constant or as dependent on temperature, nutrient concentration, or growth conditions to investigate potential lytic-lysogenic triggers within the system (Jiang & Paul, 1996; Weinbauer *et al*., 2003; Evans & Brussaard, 2012; Payet & Suttle, 2013; Howard-Varona *et al*., 2017). The parameter values that return the best approximations to observed data were determined by comparing final bacterial and viral concentrations using a student's t-test with a cut-off value of $p = 0.05$.

After approximation of optimal parameter values, the model was used to probe the role of viruses in driving concentration of recycled dissolved organic carbon (represented by state variable D in the model). Two sources were considered for recycled material within the system: cellular material from lysis (lytic-derived), modeled as a fraction of DOC per lysis event, and cellular material from exudate released by living cells (i.e., exudate-derived), modeled as a fraction of carbon uptake per cell. These two sources were co-varied between end-point values to determine the relative importance of lytic- or exudate-derived DOC as function of temperature.

To capture multi-strain dynamics and the influence of phage-host specificity, these equations were also applied to an adapted phage-host evolution model (Beckett & Williams, 2013), which includes genotype-specific infection by assigning arbitrary genotype designations to bacterial and viral populations as a value between 0 and 1 (equations given in Appendix 1). Using a modified adsorption coefficient that includes a specificity constant, the proximity of viral and bacterial genotypes dictate infection rate as a Gaussian function. In adapting this model to sea ice,

two major changes were made beyond addition of temperature effects (represented by relative contact rate, brine concentrating factor, and parameter values). First, 100 bacterial populations with unique genotypes were seeded using a Pareto distribution in order to capture a population distribution more similar to natural populations (Hong *et al*., 2006). In addition, the phage-host specificity parameter, *s*, was assigned as a genotype property rather than a community property, such that each population of viruses had an independent specificity. This step was taken to approximate more closely a system in which multiple modes of specificity are likely (Flores *et al*., 2011; Flores *et al*., 2013; Koskella & Meaden, 2013). Model equations are presented in Appendix 1.

4.2.3 Model assumptions and simplifications

Several simplifying assumptions were made when developing this model. Physically, the system is approximated as a closed brine pore, for within natural sea-ice systems brine pockets are largely discrete below –5˚C (Golden *et al*., 2007). Brine pumping, gravity drainage, brine migration, and flushing from melt ponds can lead to changes in the physical structure or connectivity of the pores, particularly as the ice warms (Petrich *et al.,* 2006; Pringle *et al*., 2009; Polashenski *et al*., 2012; Griewank & Notz, 2013; Polashenski *et al*., 2017), but these processes can be considered negligible in winter brines or any seasonal brines where cold temperature (below –5°C) reduces connectivity of brine pores to near zero.

The biological system assumes no significant contribution of algae or their viruses. While algae, especially diatoms, are common near the sea-ice/seawater interface, genetic and other analyses of upper and wintertime sea-ice communities have demonstrated dominance of heterotrophic bacteria (Deming, 2010; Boetius *et al*., 2015). Some evidence of bacterial proteorhodopsins within Antarctic sea-ice brine communities suggests potential autotrophy even

in the absence of diatoms and other algal cells (Koh *et al*., 2010; Feng *et al*., 2013; Burr *et al*., 2017); however, as light-dependent energy acquisition is unlikely to persist through polar night, the importance of proteorhodopsins is considered negligible in this model. Additionally, bacterial nitrification within sea ice may provide a non-negligible source of energy to wintertime communities (Priscu *et al*., 1990; Fripiat, *et al*., 2014; 2015; Bowman, 2015). However, this process has scantly been quantified in ice and was excluded from model consideration (Baer *et al*., 2015; Firth *et al*., 2016). Future iterations of a model including this process may offer a more refined understanding the influence of bacterial metabolism and growth on viral population dynamics in sea ice.

The mathematical system within the model is also a streamlined version of true processes. When adapting the model equations, we sought to create the simplest representation that still reflects observed community dynamics in order to avoid computational excess and over-modeling the system. This model aligns best to other simplified published models that also do not explicitly consider an infected class of bacteria or a latent period of viral infection. This choice minimized use of parameters that are poorly constrained by experimental or field observations; e.g., fraction of adsorbed viruses leading to host infection and burst size dictated by that (unknown) value. Rather, the model assumes that any adsorption of virus to host leads to infection and that burst is dictated by the value of adsorption rate.

4.3 Results and discussion

This work represents the first application of a quantitative phage-host ecological model to the sea-ice ecosystem. It presents both unique insights as well as several limitations of modeling population dynamics within an extreme environment. In corroborating published, high virus-to-

bacteria ratios, which inspired creation of this model, the results as discussed below suggest that viruses may indeed play an outsized role in sea-ice brine ecology through both community structuring and organic matter recycling.

4.3.1 Steady-state solution and Sobol' analysis

Steady-state analysis provides opportunity to determine sensitivity to parameters while remaining agnostic to their exact value. One pair of non-trivial steady-state solutions was found for bacterial and viral concentrations. The solutions demonstrated a dependence on adsorption rate, growth rate, and burst size, as well as viral decay rate. The steady-state solutions for bacterial concentration (B) and viral concentration (V) are given in Equation 4.1.

$$B = \frac{m}{\varphi(\gamma\beta - 1)} \qquad V = \frac{\mu\frac{N}{N+Q} - d}{\varphi\gamma} \qquad [4.1]$$

A Sobol' global sensitivity analysis, which co-varies parameters of interest to determine relative influence on variance, showed that steady-state virus-to-bacteria ratio had significant dependence on viral decay rate (index = 0.169) and bacterial growth rate (index = 0.066), while burst size (index 0.017) and adsorption rate (index approaching 0) were below the designated significance cut-off value of 0.05. Second-order sensitivities showed the strongest interaction between growth rate and viral decay rate (index = 0.244), while burst size and growth rate, burst size and decay rate, and growth rate and adsorption rate also had significant interactions.

This analysis makes clear that neither rapid virus production nor slow viral decay is the sole contributor to high virus-to-bacteria ratios within sea-ice brines; however, slow viral decay has a stronger effect on the final ratio. Both low temperature and high salinity have been shown to

slow the rate of viral decay in sea-ice brine analogues, with the isolated cold-active virus *Colwelliaphage* 9A surviving for several weeks at subzero conditions, including in high salinities (up to 161 ppt) (Wells and Deming, 2006c). Likewise, wintertime sea ice is largely free of the ultraviolet light known to contribute to rapid viral decay in the open ocean (Suttle and Chen, 1992). However, data from benthic communities, another slow-growing, spatially restricted marine environment, suggest that bacterial extracellular enzymes may act on viral particles, leading to enhanced viral decay rate (Danovaro *et al*., 2016). Measurements of extracellular proteases *in situ* and in analogue sea-ice brines show enzyme activity within the same order of magnitude as rates measured in open seawater and benthic environments (see Chapter 2). One may therefore hypothesize that enzyme activity within sea-ice brines could contribute to viral decay rates in sea ice; however, experimental measurements of enzymatic degradation of free virions in subzero brines would be required to confirm or reject this hypothesis.

4.3.2 Parameter estimation and tuning

Scant experimental measurements of virus-host parameters, such as burst size or adsorption rate, provided an underlying challenge for this model, as few have been made in cold systems (below 4˚C: Elder & Tanner, 1928; Spencer, 1963; Chen *et al.,* 1966; Valentine *et al*., 1966; Olsen, 1967; Olsen, 1968; Kulpa & Olsen, 1971; Whitman & Marshall, 1971b; Delisle & Levin, 1972a, b; Greer, 1983; Middelboe *et al*., 2002; Sillankorva *et al*., 2004), and even fewer are specific to sea ice (Borriss *et al*., 2003; Wells & Deming, 2006b; Luhtanen *et al*., 2014; Senčilo *et al*., 2015; Yu *et al*., 2015; Luhtanen *et al*., 2018). Of these, only two studies (Borriss *et al*., 2003; Wells & Deming, 2006b) have measured or calculated values for the parameters used in our model, contributing to wide uncertainties in parameter values. Data available in the literature on cold-active phage-host pairings demonstrate a wide range of parameter values at low temperature, as

shown in Table 4.1, likely the result of niche differentiation among mesophilic, psychrophilic, and psychrotolerant bacteria in seawater versus sea ice. Temperature-dependent distributions of the parameter values used to sample this variability thus showed wide standard deviation intervals. This variability is particularly notable when comparing adsorption values extracted from *in situ* and near *in situ* sea-ice observations using the Met-Hastings model fitting algorithm and adsorption values published for the isolated cold active *Colwelliaphage* 9A (Wells & Deming 2006a; Collins & Deming, 2011). Whereas algorithm-derived values suggested absorption rates on the order of 10^{-7} cells^2 mL^{-1} hr^{-1}, in line with other published values including in warmer systems, previous laboratory experiments with 9A showed much lower adsorption rates (too low to accurately quantify; Wells, 2006). In both instances, adsorption rate is calculated rather than explicitly measured, which may obfuscate processes or mechanisms more complex than non-reversible adsorption and lead to much variability between the values. This issue pertains especially to field studies, where data on processes like lysogeny and pseudolysogeny, superinfection, lysis from without, viral adsorption to sediment particles or extracellular polysaccharides, and virus digestion by extracellular enzymes are simply unavailable and thus wholly unaccounted for in our parameter estimation model. This uncertainty for lack of data influenced the decision to use temperature-dependent distributions of parameters rather than single parameter values for the model as an attempt to capture possible variability and therefore lead to more meaningful results.

Non-steady-state model runs covarying the focal parameters and viral decay rate demonstrated that the observed data were best replicated when growth rate and adsorption rates were reduced by 3 to 5 orders of magnitude compared to literature-obtained distributions, while burst size had minimal impact on model fit. Parameter optimization can be visualized in Figures 4.2–4.6, which show panels representing parameter sweeps for bacterial growth rate (μ; Figure

4.2), burst size (β; Figure 4.3), viral decay rate (m; Figure 4.4), adsorption rate (φ; Figure 4.5), and lytic fraction (γ, co-varied with adsorption rate; Figure 4.6). In each of these figures, panels show the distribution of observed VBRs from literature overlain with modeled VBRS (100 runs), with each panel representing a scaling factor of the varied parameter. Visual goodness of fit can be observed when modeled VBRs most closely overlay the contour distribution of observed values, which was used to confirm statistical goodness of fit as determined by t-tests.

A reduced growth rate corroborates the widely-held assumption that culture-derived estimates of bacterial growth and activity often represent maximum possible values because of culture homogeneity, environmental stability, and nutrient-replete conditions. Likewise, culture studies of psychrophiles under challenging conditions often represent the best-adapted organisms, whereas a natural community will cover a spectrum of activities and growth rates. In sea ice, the fraction of metabolically active bacteria varies greatly, between < 1 to > 30% (Junge *et al*., 2004; Martin *et al*,. 2008; Martin *et al*., 2012; Cooper *et al*., 2019). The reduced growth rates that allow the model to best simulate observed values range between 10^{-4} and 10^{-2} per hour, or doubling times of roughly 100 to 10,000 hours, which likely captures the variability of activity and growth rate in natural communities. Experimental measurements of doubling rates within sea-ice communities or psychrophilic bacteria taken from a literature survey spanned a range of 0.006 to 0.15 hr^{-1}, compared to modeled values of 0.0001 to 0.01 (Table 4.1).

Lower than expected adsorption rate also minimizes the model error as indicated by smaller statistical difference between modeled VBR and the observed given in Collins and Deming (2011). As described above, literature and algorithm-derived values show great variability in adsorption rate, between 10^{-12} and 10^{-6} $cells^2$ mL^{-1} hr^{-1}, while model output was optimized at adsorption rates closer to 10^{-12} $cells^2$ mL^{-1} hr^{-1}. Within sea-ice brine pores, reduced adsorption rates may be a

function of low temperature, reducing the chemical reaction rates or altering molecular conformations which drive adsorption (Moldovan *et al*., 2007), or of high salinity, which may inhibit binding conformations (Whitman & Marshal, 1971b), although high salinity often works to the opposite effect (Kukkaro & Bamford, 2009). More likely, however, a discrepancy in adsorption rate values is the result of several biological processes implicit in the single value of adsorption rate: contact efficiency, injection of genetic material, and evasion of host defenses. Such processes are likely affected by the extreme conditions of sea ice. For example, the model psychrophile *Colwellia psychrerythraea* strain 34H is known to exude copious amounts of extracellular polysaccharides (EPS) as temperature drops below freezing (Marx *et al*., 2009), yet whether EPS works to inhibit or enhance viral infection is unclear. Suspecting that EPS reduces contact rate by increasing viscosity and decreasing access to cell surfaces may seem logical; however, within sea ice, EPS has been shown to be a 'microbial hotspot' to which many bacteria attach and increase in activity (Meiners *et al*., 2008). Similarly, sea-ice brine pores often contain sediment particles, and bacterial association with these particles increases as temperature drops (Junge *et al*., 2004), potentially reducing contact rate. Widespread observations within other marine and cryospheric environments have shown that viruses are highly susceptible to adsorption to sediments which may lead to inactivation (e.g., Carlson *et al*., 1968; Bitton & Mitchell, 1974; LaBelle & Gerba, 1980; Maat *et al*., 2019), and similar results have been observed in analogue sea-ice brines (Wells & Deming, 2006c). Many of the viruses within sea ice may never successfully adsorb to their host, instead adsorbing to other organic material or surfaces. Finally, the nature of anti-phage defense mechanisms within cold environments is underexplored, but temperature or salinity-dependent effects could systematically change bulk community infection efficiency.

4.3.3 Lytic fraction estimate

When accounting for lysogenic viruses, model runs demonstrated closer fidelity to observed values. With lytic fraction modeled either as constant (with 10 or 1% of all viruses being lytic) or variable (inversely-correlated with temperature or correlated to growth rate), no obvious best fit was evident; however, when lytic fraction was covaried with adsorption rate, a high adsorption rate and temperature-dependent lytic fraction replicated observed bacterial and viral concentration within the designated statistical acceptance.

The relative importance of lytic and lysogenic viral lifestyles has not yet been reliably quantified for sea-ice ecosystems; as such, these results present novel support for mixed communities of lytic and lysogenic viruses. Consistent with the model, new metagenomic data identifying marker genes have shown that both lytic and lysogenic viruses exist within sea ice (J. Rapp *et al*., 2019). However, what toggles a lytic or lysogenic lifestyle among sea-ice viruses remains undetermined. Culture studies of a model psychrophilic bacterium found in sea ice, *Colwellia psychrerythraea*, indicate potential existence of a heat-induced lysogen (Wells, 2006), while investigation of a lytic-lysogenic switch in open-water polar systems has led to speculation that nutrient stress may trigger a lytic lifestyle among cold-active bacteriophage (Brum *et al*., 2015). Non-polar studies of marine bacteria corroborate nutrient stress for lysogen induction (Morris *et al*., 2020). Density-dependent triggers, such as systems based on quorum-sensing thresholds (Laganenka *et al*., 2019), or ecological theories akin to the Piggyback-the-Winner Hypothesis, in which lysogeny is the dominate viral strategy at high host densities (Knowles *et al*., 2016; 2017), may be especially important within sea-ice brines, where the brine concentration factor leads to higher concentrations of bacteria than commonly observed in seawater. Most likely, unique virus-host pairs also have unique lytic-lysogenic switches as a manifestation of niche

differentiation. Our model seems to support this hypothesis, as the multispecies model (below) replicated observed values only with a growth-rate-dependent lytic fraction, which is also implicitly dependent on nutrient concentration, cell density, and temperature.

4.3.4 DOC recycling

Covarying the fraction of recycled material from viral lysis and cellular exudate in model runs suggested a temperature-dependent relationship between these two governing sources. At the highest and lowest temperatures modeled (–1 and –15˚C), cellular exudate was a larger source of recycled DOC in the system, indicated by a contour slope less than –0.45 (Figure 4.7). In between these temperatures, viral lysis was a more important source of recycled DOC, indicated by a contour slope greater than –0.45. This pattern likely represents a balance between uptake, which increases with temperature and is proportionally linked to exudate volume, and viral production, which is linked to temperature and directly linked to lysis. At –2˚C, for example, bacterial growth rates allow for uptake and therefore exudate volume to outpace viral lysis, while at the colder temperatures (e.g., –12˚C), slow viral diffusion and production reduces lysis. Within the zone of intermediate temperatures (–4 to –10˚C) slower bacteria production reduces exudate volume, but viral lysis is increased due to higher relative contact rate. The total amount of recycled organic carbon also showed temperature dependence, with the lowest maximum value at –6˚C (4.0 µg C) and the highest at –1˚C (28 µg C). These values represent the maximum possible carbon recycling given the modeled conditions; however, the occurrence of such conditions and maximized rates within sea-ice brines is unlikely due to natural inefficiencies in the system.

While data corroborate the idea that a high fraction of organic material would be released to the environment by lysis, as little carbon is funneled into virions themselves (Jover *et al*., 2014), the release of a similar fraction of carbon due to cellular exudate seems unlikely. Model

psychrophile *Colwellia psychrerythraea* strain 34H has been shown to upregulate the most probable source of cellular exudate, extracellular polysaccharides (EPS), at temperatures below –2°C, reaching maximum concentrations of approximately 2 x 10^{-8} µg glucose equivalents $cell^{-1}$, or about 8 x 10^{-9} µg C $cell^{-1}$, after seven days (Marx *et al*., 2009). Order-of-magnitude calculations assuming constant production suggest that this value is still < 1% of modeled uptake (~ 2 x 10^{-9} µg C hr^{-1} $cell^{-1}$). The most likely scenarios in organic carbon recycling within sea ice, then, are represented by high fraction of lytic material (nearing a value of 1) and low fraction of cellular exudate (nearing a value of 0).

In pelagic systems, the viral shunt is thought to recycle up to 25% of organic material within the microbial loop (Wilhelm and Suttle, 1999). While evidence predicts existence of a similar microbial loop in sea ice in which microalgae help sustain activity of heterotrophic bacteria through leakage and exudation of DOM (Martin *et al*., 2008; 2012), potential for a viral shunt within sea-ice brines not yet been verified or measured. Given the high concentration of viruses within the system and limited input of algal DOM in upper Arctic or wintertime sea ice, viruses likely play an especially important role in this system. Marine sediments offer an example of a microbial loop in which viral lysis may play an important role (Danovaro *et al*., 2016). Similarities between deep marine sediments and very cold sea-ice ecosystems, both characterized by spatially restricted pores with limited organic input and low microbial activity compared to the surface ocean, corroborate model results demonstrating that viral lysis is also important in sea-ice brines. The organic material derived from viral lysis within brine pores may play an important role in maintaining activity of psychrophiles through the winter, as canonical thought has suggested that bacteria in cold temperature waters require high concentrations of organic material in order to be active (Pomeroy & Wiebe, 2001). However, quantification of carbon uptake in cold-active

communities has not confirmed this idea (Yager and Deming, 1999), and much of the organic material released by lysis may first require degradation by extracellular enzymes to allow microbial uptake.

This model does not include bacterial respiration and production as independent carbon sinks, a choice which may be significant given previous characterizations of bacterial production as highly variable compared to relatively steady, and quantitatively important, respiration (albeit measured at 2–4°C; Nguyen & Maranger, 2011). Future iterations of this model which are constrained by observed carbon dynamics within sea ice could further refine our understanding of how viruses influence DOC cycling.

4.3.5 Multispecies interactions

The multispecies model adapted from Beckett and Williams reproduced community compositions similar to observed values from coastal sea ice (Cooper *et al*., 2019); however, large margins of variability were observed when averaging values of multiple runs. As with the single species model described above, high variability in output is likely the result of large variability among parameter values described in literature. As more investigations of cold-active phages or field observations of viruses are performed, future iterations of this model may be able to reduce error if values such as phage adsorption rate or burst size converge. However, the high variability within these observations may also reflect the known biological heterogeneity of sea ice microbial communities (Collins *et al*., 2008), and thus be inherent to the system rather than an artifact of the model.

A clear result of the model is a correlation between higher phage-host specificity and increased diversity as measured by a calculated Shannon Index, a commonly used measure of community diversity which considers both richness (how many unique populations exist) and

evenness (how abundant each unique population is). When considering phage-host specificity as a constant for each community (rather than specific to each host) at a static temperature (–5˚C), average Shannon Index increased from 0.27 to 0.65 across specificity factor increases from 250 to 1000 (n = 10 for each specificity value). At the highest phage-host specificity tested (s = 1000), Shannon diversity was significantly higher in a two-tailed t-test than at the lowest specificity factor (s = 250) with a cut-off of p = 0.05 (p = 0.04, n =10), and was higher than all other specificity factors tested with a cut-off of p = 0.1. Notably, the model consistently produced Shannon Index values which were lower than those observed in sea-ice brines, with modeled values ranging between 0.3 and 2.5, compared to observed values nearing 3 or 4, although as phage-host specificity increased, these values approached some of the lower observations of Shannon Index from Antarctic pack ice (Brinkmeyer *et al*., 2003; Bowman *et al*., 2012; Hatam *et al*., 2016). Low Shannon Index within the model was likely an artifact of the program's architecture, which has limited capacity for microbial diversity owing to the pre-determined maximum number of species (100). Similarly, as described above, average Shannon diversity calculations had large variability. Future iterations of the model with more runs may reduce this error to within reasonable limits and produce a significant trend.

The true pattern of phage-host specificity within sea-ice brines is likely more complicated than can be modeled easily within a system of differential equations. Analysis of culture-based phage-host systems has suggested that patterns of specificity within a single environment are most often nested, *i.e.,* that the most difficult-to-infect hosts are infected by generalist phages, while easily infected hosts are infected by both generalist and specific phages (Flores *et al*., 2011). Such behaviors are difficult to replicate within this model, which may obscure true dynamics. However, we were able to run the model with unique phage-host specificity factors for each virus genotypes,

and in doing so simulate some variability among phage-host specificity within the system. When the model was run with phage-host specificity inversely dependent on phage genotype adsorption rate, as a trade-off between specificity and adsorption has often been assumed (reviewed by Koskella & Meaden, 2013), the Shannon Index increased. This effect was strongest at low temperatures; i.e., at –15˚C modeled average Shannon Index was 2.2 ± 0.4 (n = 10). Beyond the local scale, which favors nested phage-host interaction networks, virus-host communities may tend more toward modular networks of interaction (Flores *et al*., 2013). An investigation of phage-host interaction networks across multiple scales of brine space, such as disconnected brine pockets or comparable sub-zero, hypersaline brines, may reveal such a pattern.

Previous investigations of microbial communities in cold or sub-zero, hypersaline conditions have suggested that these environments may experience enhanced evolution and horizontal gene transfer mediated by viruses as a result of long residence times, increased lysogeny, tight spatial coupling, or reduced host immunity due to environmental stress (Anesio *and* Bellas, 2011; Deming, 2017; Cooper *et al*., 2020). Recently, Zhong *et al*. (2020) demonstrated metagenomic evidence for virally-mediated transfer of a fatty acid desaturase gene among *Proteobacteria* members within sea ice, and another among *Bacteroidetes*. The results found here, which suggest sea-ice communities have high phage-host specificity, offer counter-evidence to wide spread horizontal gene transfer (HGT) within sea-ice brines, though suggested rates of high lysogeny demonstrated in the single-species model could increase HGT values. However, neither metagenomic studies nor modelling work can directly observe active HGT; future studies should seek to measure these HGT rates among cold-active viruses and psychrophilic communities experimentally and *in situ*.

4.4 Conclusions

The model presented here provides a novel attempt at quantifying phage-host population dynamics within sea-ice brines using mathematical equations with parameter values rooted in field and laboratory observations. Perhaps the most important result of this model is the suggestion that viruses within sea-ice brines, despite having low production rates, may play a more important role in recycling DOC than in underlying seawater, supporting the hypothesis of a viral shunt within sea ice. Acknowledgement of the important role of viruses within sea ice DOC cycling may focus future investigations in the environment.

This work also lays out several avenues of experimental investigation for future studies of sea-ice brines. Primarily, future work to characterize the fundamental parameters of phage-host isolate systems from sea-ice brines, quantifying important values such as adsorption rate and burst size, could advance accuracy of population models. While this characterization can be aided by metagenomic or transcriptomic work, the very challenging work of quantifying parameters experimentally would likely provide the best understanding of the underlying mechanisms of phage-host dynamics. Additionally, work characterizing the lytic-lysogenic life styles of viruses within sea-ice brines, or other life styles, would almost certainly improve future models, as would investigations that aim to understand the role of algal viruses within this system, e.g. increasing DOC through algal lysis, which could influence our understanding of VBR values in the ice.

Future iterations of this model may help to refine the conclusions reached above and provide a better hypothesis-generating tool to direct experimental and ‘omic investigations of field samples. Work including the algal component of primary production within sea-ice brines and the role of algal viruses would expand the application of this model to environments near the seawater/sea-ice interface. This model could also serve as the basis for a comparative model

between sea-ice communities and those inhabiting cryopegs, an environment of sub-zero, hypersaline brines of marine origin isolated within permafrost brines for millennia (Cooper *et al*., 2019).

Acknowledgements

We thank David Talmy at the University of Tennessee, Knoxville, for help in establishing the systems of equations for this model and directing focus for model development, as well as Stephen Beckett for sharing the MATLAB code of Beckett and Williams (2013) which, though ultimately not used, was the inspiration for the multispecies model.

References

Anesio, A. M., & Bellas, C. M. (2011). Are low temperature habitats hot spots of microbial evolution driven by viruses? *Trends Microbiol*, *19*(2), 52–57. https://doi.org/10.1016/j.tim.2010.11.002

Anesio, A. M., Mindl, B., Laybourn-Parry, J., Hodson, A. J., Sattler, B. (2007). Viral dynamics in cryoconite holes on a high Arctic glacier (Svalbard). *J Geophys Res: Biogeosciences*, *112*(4), 1–10. https://doi.org/10.1029/2006JG000350

Baer, S. E., Connelly, T. L., Bronk, D. A. (2015). Nitrogen uptake dynamics in landfast sea ice of the Chukchi Sea. *Polar Biol*, *38*(6), 781–797. https://doi.org/10.1007/s00300-014-1639-y

Beckett, S. J., & Williams, H. T. P. (2013). Coevolutionary diversification creates nested-modular structure in phage – bacteria interaction networks. *Interface Focus*, *3*(6). https://doi.org/10.1098/rsfs.2013.0033

Bitton, G., & Mitchell, R. (1974). Effect of colloids on the survival of bacteriophages in seawater. *Water Res*, *8*(4), 227–229. https://doi.org/10.1016/0043-1354(74)90159-6

Boetius, A., Albrecht, S., Bakker, K., Bienhold, C., Felden, J., Fernández-Méndez, M., … Felden, J. (2013). Export of algal biomass from the melting arctic sea ice. *Science*, *339*(6126), 1430–1432. https://doi.org/10.1126/science.1231346

Boetius, A., Anesio, A. M., Deming, J. W., Mikucki, J. A., Rapp, J. Z. (2015). Microbial ecology of the cryosphere: Sea ice and glacial habitats. *Nat Rev Microbiol*, *13*(11), 677–690. https://doi.org/10.1038/nrmicro3522

Borriss, M., Helmke, E., Hanschke, R., Schweder, T. (2003). Isolation and characterization of marine psychrophilic phage-host systems from Arctic sea ice. *Extremophiles* 7:377–384.

Bowman, J. S., Rasmussen, S., Blom, N., Deming, J. W., Rysgaard, S., Sicheritz-Ponten, T. (2012). Microbial community structure of Arctic multiyear sea ice and surface seawater by 454 sequencing of the 16S RNA gene. *ISME J*, *6*(1), 11–20. https://doi.org/10.1038/ismej.2011.76

Bowman, J. S. (2015). The relationship between sea ice bacterial community structure and biogeochemistry: A synthesis of current knowledge and known unknowns. *Elem Sci Anth*, *3*, 1–20. https://doi.org/10.12952/journal.elementa.000072

Bratbak, G., & Dundas, I. (1984). Bacterial dry matter content and biomass estimations. *Appl Environ Microbiol*, *48*(4), 755–757. https://doi.org/10.1128/aem.48.4.755-757.1984

Brailsford, F. L., Glanville, H. C., Golyshin, P. N., Johnes, P. J., Yates, C. A., Jones, D. L. (2019). Microbial uptake kinetics of dissolved organic carbon (DOC) compound groups from river water and sediments. *Sci Reports*, *9*(1), 11229. https://doi.org/10.1038/s41598-019-47749-6

Brinkmeyer, R., Knittel, K., Jürgens, J., Weyland, H., Amann, R., Helmke, E. (2003). Diversity and structure of bacterial communities in Arctic versus Antarctic pack ice. *Appl Environ Microbiol*, *69*(11), 6610–6619. https://doi.org/10.1128/AEM.69.11.6610-6619.2003

Braun, S., Morono, Y., Littmann, S., Kuypers, M., Aslan, H., Dong, M., Jørgensen, B. B., Lomstein, B. A. (2016). Size and carbon content of sub-seafloor microbial cells at Landsort

Deep, Baltic Sea. *Front Microbiol*, *7*(AUG), 1–13. https://doi.org/10.3389/fmicb.2016.01375

Brum, J. R., Hurwitz, B. L., Schofield, O., Ducklow, H. W., Sullivan, M. B. (2016). Seasonal time bombs: Dominant temperate viruses affect Southern Ocean microbial dynamics. *ISME J*, *10*(2), 437–449. https://doi.org/10.1038/ismej.2015.125

Burr, D. J., Martin, A., Maas, E. W., Ryan, K. G. (2017). In situ light responses of the proteorhodopsin-bearing Antarctic sea-ice bacterium, *Psychroflexus torques*. *ISME J*, *11*(9), 2155–2158. https://doi.org/10.1038/ismej.2017.65

Carlson, G. F. Jr., Woodard, F. E., Wentworth, D. F., Sproul, O. J. (1968). Virus inactivation on clay particles in natural waters. *J Water Pollut Control Fed* 40:R89–R10.

Chen, P. K., Citarella, R. V., Salazar, O., Colwell, R. R. (1966). Properties of two marine bacteriophages. *J Bacteriol* 91:1136–1139.

Chua, M. J., Campen, R. L., Wahl, L., Grzymski, J. J., Mikucki, J. A. (2018). Genomic and physiological characterization and description of *Marinobacter gelidimuriae* sp. nov., a psychrophilic, moderate halophile from Blood Falls, an Antarctic subglacial brine. *FEMS Microbiol Ecol*, *94*(3), 1–15. https://doi.org/10.1093/femsec/fiy021

Collins, R. E., Carpenter, S. D., Deming, J. W. (2008). Spatial heterogeneity and temporal dynamics of particles, bacteria, and pEPS in Arctic winter sea ice. *J Mar Sys*, *74*(3–4), 902–917. https://doi.org/10.1016/j.jmarsys.2007.09.005

Collins, R.E., Rocap, G., Deming, J. W. (2010). Persistence of bacterial and archaeal communities in sea ice through an Arctic winter. *Environ Microbiol*, *12*(7), 1828–1841. https://doi.org/10.1111/j.1462-2920.2010.02179.x

Collins, R. E., & Deming, J. W. (2011). Abundant dissolved genetic material in Arctic sea ice Part II: Viral dynamics during autumn freeze-up. *Polar Biol*, *34*(12), 1831–1841. https://doi.org/10.1007/s00300-011-1008-z

Connelly, T. L., Baer, S. E., Cooper, J. T., Bronk, D. A. (2014). Urea uptake and carbon fixation by marine pelagic bacteria and archaea during the Arctic summer and winter seasons. *Appl Environ Microbiol*, *80*(19), 6013–6022. https://doi.org/10.1128/AEM.01431-14

Cooper, Z. S., Rapp, J. Z., Carpenter, S. D., Iwahana, G., Eicken, H., Deming, J. W. (2019). Distinctive microbial communities in subzero hypersaline brines from Arctic coastal sea ice and rarely sampled cryopegs. *FEMS Microbiol Ecol*, *95*(12), 1–15. https://doi.org/10.1093/femsec/fiz166

Cox, G. F. N., & Weeks, W. F. (1983). CRREL Report 82-30, Equations for Determining the Gas and Brine Volumes in Sea Ice Samples. *J Glaciol*, *29*(102), 306–316.

Danovaro, R., Corinaldesi, C., Dell'Anno, A., Fabiano, M., Corselli, C. (2005). Viruses, prokaryotes and DNA in the sediments of a deep-hypersaline anoxic basin (DHAB) of the Mediterranean Sea. *Environ Microbiol*, *7*(4), 586–592. https://doi.org/10.1111/j.1462-2920.2005.00727.x

Danovaro, R., Dell'anno, A., Corinaldesi, C., Rastelli, E., Cavicchioli, R., Krupovic, M., … Prangishvili, D. (2016). Virus-mediated archaeal hecatomb in the deep seafloor. *Sci Adv*, *2*(10), 1–10. https://doi.org/10.1126/sciadv.1600492

Delisle, A. L., & Levin, R. E. (1972a). Characteristics of three phages infectious for psychrophilic fishery isolates of *Pseudomonas putrefaciens. A van Leeuw Microbiol* 38:1–8

Delisle, A. L., & Levin, R. E. (1972b). Effect of temperature on an obligately psychrophilic phage-host system of *Pseudomonas putrefaciens. A van Leeuw Microbiol* 38:9–15

Deming, J. W. (2010). Sea ice bacteria and viruses. In Thomas, D.N. and Dieckman, G.S. (Eds.), *Sea Ice – An Introduction to its Physics, Chemistry, Biology and Geology*, 2nd Ed. Blackwell Science Ltd, Oxford, 247–282.

Elder, A. L., & Tanner, F. W. (1928). Action of bacteriophage on psychrophilic organisms. *J Infect Dis* 43:403–406.

Evans, C., & Brussaard, C. P. D. (2012). Regional variation in lytic and lysogenic viral infection in the southern ocean and its contribution to biogeochemical cycling. *Appl Environ Microbiol, 78*(18), 6741–6748. https://doi.org/10.1128/AEM.01388-12

Ewert, M., & Deming, J. W. (2013). Sea ice microorganisms: Environmental constraints and extracellular responses. *Biol*, *2*(2), 603–628. https://doi.org/10.3390/biology2020603

Feng, S., Powell, S. M., Wilson, R., & Bowman, J. P. (2013). Light-stimulated growth of proteorhodopsin-bearing sea-ice psychrophile *Psychroflexus torquis* is salinity dependent. *ISME J*, *7*(11), 2206–2213. https://doi.org/10.1038/ismej.2013.97

Flores, C. O., Meyer, J. R., Valverde, S., Farr, L., Weitz, J. S. (2011). Statistical structure of host-phage interactions. *P Natl Acad Sci USA*, *108*(28). https://doi.org/10.1073/pnas.1101595108

Flores, C. O., Valverde, S., Weitz, J. S. (2013). Multi-scale structure and geographic drivers of cross-infection within marine bacteria and phages. *ISME J*, *7*(3), 520–532. https://doi.org/10.1038/ismej.2012.135

Fripiat, F., Sigman, D. M., Fawcett, S. E., Rafter, P. A., Weigand, M. A., Tison, J.-L. (2014). New insights into sea ice nitrogen biogeochemical dynamics from the nitrogen isotopes. *Global Biogeochem Cycles*, *28*, 115–130. https://doi.org/10.1002/2014GB004832

Fripiat, F., Sigman, D. M., Masse, G., Tison, J. L. (2015). High turnover rates indicated by changes in the fixed N forms and their stable isotopes in Antarctic landfast sea ice. *J Geophys Res: Oceans*, *120*, 3079–3097. https://doi.org/10.1002/2014JC010485

Fukuda, R., Ogawa, H., Nagata, T., Koike, I. (1998). Direct determination of carbon and nitrogen contents of natural bacterial assemblages in marine environments. *Appl Environ Microbiol 64*(9), 3352–3358.

Golden, K. M., Eicken, H., Heaton, A. L., Miner, J., Pringle, D. J., Zhu, J. (2007). Thermal evolution of permeability and microstructure in sea ice. *Geophys Res Lett*, *34*(16), 2–7. https://doi.org/10.1029/2007GL030447

Granato, E. T., Meiller-Legrand, T. A., Foster, K. R. (2019). The Evolution and Ecology of Bacterial Warfare. *Curr Biol*, *29*(11), R521–R537. https://doi.org/10.1016/j.cub.2019.04.024

Greer, G.G. (1983). Psychrotrophic *Brocothrix thermosphacta* bacteriophages isolated from beef. *Appl Environ Microbiol* 46:245–25.

Griewank, P. J., & Notz, D. (2013). Insights into brine dynamics and sea ice desalination from a 1-D model study of gravity drainage. *J Geophys Res: Oceans*, *118*(7), 3370–3386. https://doi.org/10.1002/jgrc.20247

Guixa-Boixareu, N., Calderón-Paz, J. I., Heldal, M., Bratbak, G., Pedrós-Alió, C. (1996). Viral lysis and bacterivory as prokaryotic loss factors along a salinity gradient. *Aquatic Microbial Ecology*, *11*(3), 215–227. https://doi.org/10.3354/ame011215

Hatam, I., Lange, B., Beckers, J., Haas, C., Lanoil, B. (2016). Bacterial communities from Arctic seasonal sea ice are more compositionally variable than those from multi-year sea ice. *ISME J*, *10*(10), 2543–2552. https://doi.org/10.1038/ismej.2016.4

Heldal, M., & Bratbak, G. (1991). Production and decay of viruses in aquatic environments. *Mar Ecol Progr Ser*, *72*(3), 205–212. https://doi.org/10.3354/meps072205

Herman, J., & Usher, W. (2017). SALib: An open-source Python library for sensitivity analysis. *J Open Source Software*, 2(9). doi:10.21105/joss.00097

Hong, S. H., Bunge, J., Jeon, S. O., Epstein, S. S. (2006). Predicting microbial species richness. *P Natl Acad Sci USA*, *103*(1), 117–122. https://doi.org/10.1073/pnas.0507245102

Howard-Varona, C., Hargreaves, K. R., Abedon, S. T., Sullivan, M. B. (2017). Lysogeny in nature: Mechanisms, impact and ecology of temperate phages. *ISME J*, *11*(7), 1511–1520. https://doi.org/10.1038/ismej.2017.16

Huston, A. L. (2003). Bacterial adaptation to the cold: in situ activities of extracellular enzymes in the North Water polynya and characterization of a cold-active aminopeptidase from *Colwellia psychrerythraea* strain 34H. Ph.D. thesis, University of Washington, Seattle.

Jiang, S. C., & Paul, J. H. (1996). Occurrence of lysogenic bacteria in marine microbial communities as determined by prophage induction. *Mar Ecol Prog Ser*, *142*(1–3), 27–38. https://doi.org/10.3354/meps142027

Jover, L. F., Effler, T. C., Buchan, A., Wilhelm, S. W., Weitz, J. S. (2014). The elemental composition of virus particles: Implications for marine biogeochemical cycles. *Nat Rev Microbiol*, *12*(7), 519–528. https://doi.org/10.1038/nrmicro3289

Jörgensen, F., & Kurland, C. G. (1987). Death rates of bacterial mutants. *FEMS Microbiol Lett*, *40*(1), 43–46. https://doi.org/10.1111/j.1574-6968.1987.tb01979.x

Junge, K., Eicken, H., Deming, J. W. (2004). Bacterial Activity at –2 to –20°C in Arctic Wintertime Sea Ice. *Appl Environ Microbiol*, *70*(1), 550–557. https://doi.org/10.1128/AEM.70.1.550-557.2004

Kim, J. W., & Kathariou, S. (2009). Temperature-dependent phage resistance of Listeria monocytogenes epidemic clone II. *Appl Environ Microbiol*, *75*(8), 2433–2438. https://doi.org/10.1128/AEM.02480-08

Kirchman, D. L., Malmstrom, R. R., Cottrell, M. T. (2005). Control of bacterial growth by temperature and organic matter in the Western Arctic. *Deep-Sea Research Part II*, *52*(24–26), 3386–3395. https://doi.org/10.1016/j.dsr2.2005.09.005

Kirchman, D. L., Morán, X. A. G., Ducklow, H. (2009). Microbial growth in the polar oceans - Role of temperature and potential impact of climate change. *Nature Rev Microbiol*, *7*(6), 451–459. https://doi.org/10.1038/nrmicro2115

Koh, E. Y., Atamna-Ismaeel, N., Martin, A., Cowie, R. O. M., Beja, O., Davy, S. K., … Ryan, K. G. (2010). Proteorhodopsin-bearing bacteria in Antarctic sea ice. *Appl Environ Microbiol*, *76*(17), 5918–5925. https://doi.org/10.1128/AEM.00562-10

Köstner, N., Scharnreitner, L., Jürgens, K., Labrenz, M., Herndl, G. J., Winter, C. (2017). High viral abundance as a consequence of low viral decay in the Baltic Sea redoxcline. *PLoS ONE*, *12*(6), 1–21. https://doi.org/10.1371/journal.pone.0178467

Kottmeier, S. T., Grossi, S. M. G., Sullivan, C. W. (1987). Sea ice microbial communities. VIII. Bacterial production in annual sea ice of McMurdo Sound, Antarctica. *Mar Ecol Prog Series*, *35*(1984), 175–186. https://doi.org/10.3354/meps035175

Koskella, B., & Meaden, S. (2013). Understanding bacteriophage specificity in natural microbial communities. *Viruses*, *5*(3), 806–823. https://doi.org/10.3390/v5030806

Köstner, N., Scharnreitner, L., Jürgens, K., Labrenz, M., Herndl, G. J., Winter, C. (2017). High viral abundance as a consequence of low viral decay in the Baltic Sea redoxcline. *PLoS ONE*, *12*(6), 1–21. https://doi.org/10.1371/journal.pone.0178467

Knowles, B., Silveira, C. B., Bailey, B. A., Barott, K., Cantu, V. A., Cobian-Guëmes, A. G., … Rohwer, F. (2016). Lytic to temperate switching of viral communities. *Nature*, *531*(7595), 466–470. https://doi.org/10.1038/nature17193

Knowles, B., Bailey, B., Boling, L., Breitbart, M., Cobián-Güemes, A., Del Campo, J., … Rohwer, F. (2017). Variability and host density independence in inductions-based estimates of environmental lysogeny. *Nat Microbiol*, *2*(April), 1–9. https://doi.org/10.1038/nmicrobiol.2017.64

Kukkaro, P., & Bamford, D. H. (2009). Virus-host interactions in environments with a wide range of ionic strengths. *Environ Microbiol Rep* 1(1), 71–77.

Kulpa, C. F., & Olsen, R. H. (1971). Properties of psychrophilic bacteriophage specific for *Micromonas cryophilus*. *Can J Microbiol* 17:157–160.

LaBelle, I. L., & Gerba, C. P. (1980). Influence of estuarine sediment on virus survival under field conditions. *Appl Environ Microbiol*, *39*(4), 749–755. https://doi.org/10.1128/aem.39.4.749-755.1980

Laganenka, L., Sander, T., Lagonenko, A., Chen, Y., Link, H., & Sourjik, V. (2019). Quorum sensing and metabolic state of the host control lysogeny-lysis switch of bacteriophage T1. *MBio*, *10*(5), 3–8. https://doi.org/10.1128/mBio.01884-19

Levin, B. R., Stewart, F. M., Chao, L. (1977). Resource-limited growth, competition, and predation: A model and experimental studies with bacteria and bacteriophage. *Amer Natur*, *111*(977), 3–24.

Luhtanen, A. M., Eronen-Rasimus, E., Kaartokallio, H., Rintala, J. M., Autio, R., Roine, E. (2014). Isolation and characterization of phage-host systems from the Baltic Sea ice. *Extremophiles*, *18*(1), 121–130. https://doi.org/10.1007/s00792-013-0604-y

Luhtanen, A. M., Eronen-Rasimus, E., Oksanen, H. M., Tison, J. L., Delille, B., Dieckmann, G. S., … Bamford, D. H. (2018). The first known virus isolates from Antarctic sea ice have complex infection patterns. *FEMS Microb Ecol*, *94*(4), 1–15. https://doi.org/10.1093/femsec/fiy028

Maat, D. S., Prins, M. A., Brussaard, C. P. D. (2019). Sediments from arctic tide-water glaciers remove coastal marine viruses and delay host infection. *Viruses*, *11*(2), 1–15. https://doi.org/10.3390/v11020123

Martin, A., Hall, J. A., O'Toole, R., Davy, S. K., Ryan, K. G. (2008). High single-cell metabolic activity in Antarctic sea ice bacteria. *Aquat Microb Ecol*, *52*(1), 25–31. https://doi.org/10.3354/ame01205

Martin, A., McMinn, A., Davy, S. K., Anderson, M. J., Miller, H. C., Hall, J. A., Ryan, K. G. (2012). Preliminary evidence for the microbial loop in Antarctic sea ice using microcosm simulations. *Antarctic Sci*, *24*(6), 547–553. https://doi.org/10.1017/S0954102012000491

Marx, J. G., Carpenter, S. D., Deming, J. W. (2009). Production of cryoprotectant extracellular polysaccharide substances (EPS) by the marine Colwellia psychrerythraea strain 34H under extreme conditions. *Can J Microbiol 55:*63–72.

Mateus, M. D. (2017). Bridging the gap between knowing and modeling viruses in marine systems-An upcoming frontier. *Front Mar Sci*, *3*(JAN), 1–16. https://doi.org/10.3389/FMARS.2016.00284

Meiners, K.M., & Michel, C. (2017) Dynamics of nutrients, dissolved organic matter, and exopolymers in sea ice. In Thomas, D.N. (Ed.), *Sea Ice* (3rd Ed.), Wiley and Sons, 415–432.

Meiners, K., Krembs, C., Gradinger, R. (2008). Exopolymer particles: Microbial hotspots of enhanced bacterial activity in Arctic fast ice (Chukchi Sea). *Aquat Microb Ecol*, *52*(2), 195–207. https://doi.org/10.3354/ame01214

Middelboe, M. (2000). Bacterial growth rate and marine virus-host dynamics. *Microb Ecol*, *40*(2), 114–124. https://doi.org/10.1007/s002480000050

Middelboe, M., Nielsen, T. G., Bjørnsen, P. K. (2002). Virus and bacterial production in the North Water: In situ measurements, batch-culture experiments and characterization and distribution of a virus-host system. *Deep-Sea Res II 49*, 5063–5079.

Middelboe, M., & Jørgensen, N. (2006). Viral lysis of bacteria: An important source of dissolved amino acids and cell wall compounds. *J Mar Biol Assoc UK, 86*(3), 605–612. doi:10.1017/S0025315406013518

Mikkelsen, D. M., Rysgaard, S., Glud, R. N. (2008). Microalgal composition and primary production in Arctic sea ice: A seasonal study from Kobbefjord (Kangerluarsunnguaq), West Greenland. *Mar Ecol Prog Series*, *368*, 65–74. https://doi.org/10.3354/meps07627

Moldovan, R., Chapman-McQuiston, E., Wu, X. L. (2007). On kinetics of phage adsorption. *Biophys J*, *93*(1), 303–315. https://doi.org/10.1529/biophysj.106.102962

Morris, R. M., Cain, K. R., Hvorecny, K. L., & Kollman, J. M. (2020). Lysogenic host–virus interactions in SAR11 marine bacteria. *Nat Microbiol 5*, 1011–1015. https://doi.org/10.1038/s41564-020-0725-x

Mykytczuk, N. C. S., Foote, S. J., Omelon, C. R., Southam, G., Greer, C. W., Whyte, L. G. (2013). Bacterial growth at -15 °C; molecular insights from the permafrost bacterium *Planococcus halocryophilus* Or1. *ISME J*, *7*(6). https://doi.org/10.1038/ismej.2013.8

Nedwell, D. B. (1999). Effect of low temperature on microbial growth: Lowered affinity for substrates limits growth at low temperature. *FEMS Microb Ecol*, *30*(2), 101–111. https://doi.org/10.1016/S0168-6496(99)00030-6

Nguyen, D., & Maranger, R. (2011). Respiration and bacterial carbon dynamics in Arctic sea ice. *Polar Biol*, *34*(12), 1843–1855. https://doi.org/10.1007/s00300-011-1040-z

Nichols, D. S., Greenhill, A. R., Shadbolt, C. T., Ross, T., McMeekin, T. A. (1999). Physicochemical parameters for growth of the sea ice bacteria *Glaciecola punicea* ACAM 611(T) and *Gelidibacter sp.* strain IC158. *Appl Environ Microbiol*, *65*(8), 3757–3760. https://doi.org/10.1128/aem.65.8.3757-3760.1999

Olsen, R. H. (1967). Isolation and growth of psychrophilic bacteriophage. *Appl Microbiol 15*, 198.

Olsen, R. H., Metcalf, E. S., Todd, J. K. (1968). Characteristics of bacteriophages attacking psychrophilic and mesophilic pseudomonads. *J Virol 2*, 357–364.

Owens, J. D., Legan, J. D. (1987). *Determination of the Monod substrate saturation constant for microbial growth*. *FEMS Microbiol Rev 46*, 419–432.

Parikka, K. J., Le Romancer, M., Wauters, N., Jacquet, S. (2017). Deciphering the virus-to-prokaryote ratio (VPR): Insights into virus–host relationships in a variety of ecosystems. *Bio Rev*, *92*(2), 1081–1100. https://doi.org/10.1111/brv.12271

Paterson, H., Laybourn-Parry, J. (2012). Antarctic sea ice viral dynamics over an annual cycle. *Polar Bio*, *35*(4), 491–497. https://doi.org/10.1007/s00300-011-1093-z

Payet, J. P., Suttle, C. A. (2013). To kill or not to kill: The balance between lytic and lysogenic viral infection is driven by trophic status. *Limnol Oceanogr*, *58*(2), 465–474. https://doi.org/10.4319/lo.2013.58.2.0465

Petrich, C., Langhorne, P. J., & Sun, Z. F. (2006). Modelling the interrelationships between permeability, effective porosity and total porosity in sea ice. *Cold Reg Sci Technol*, *44*(2), 131–144. https://doi.org/10.1016/j.coldregions.2005.10.001

Pringle, D. J., Miner, J. E., Eicken, H., Golden, K. M. (2009). Pore space percolation in sea ice single crystals. *J Geophys Res: Oceans*, *114*(12), 1–14. https://doi.org/10.1029/2008JC005145

Pomeroy, L. R., & Wiebe, W. J. (2001). Temperature and substrates as interactive limiting factors for marine heterotrophic bacteria. *Aquatic Microb Ecol*, *23*(2), 187–204. https://doi.org/10.3354/ame023187

Polashenski, C., Perovich, D., Courville, Z. (2012). The mechanisms of sea ice melt pond formation and evolution. *J Geophys Res: Oceans*, *117*(1), 1–23. https://doi.org/10.1029/2011JC007231

Polashenski, C., Golden, K. M., Perovich, D. K., Skyllingstad, E., Arnsten, A., Stwertka, C., Wright, N. (2017). Percolation blockage: A process that enables melt pond formation on

first year Arctic sea ice. *J Geophys Res: Oceans*, *122*, 413–440. https://doi.org/10.1038/175238c0

Priscu, J., Downes, M., Priscu, L., Palmisano, A., Sullivan, C. (1990). Dynamics of ammonium oxidizer activity and nitrous oxide (N_20) within and beneath Antarctic sea ice. *Mar Ecol Prog Ser*, *62*(1), 37–46. https://doi.org/10.3354/meps062037

Rapp, J. Z., Zhong, Z., Vik, D., Sullivan, M. B., Carpenter, S. D., Deming, J. W. (2019). Genomic signatures of virus-mediated gene transfer in subzero, hypersaline brine microbes. IGS Sea Ice Symposium, 19–23 August, Winnipeg, Canada.Record, N. R., Talmy, D., Våge, S. (2016). Quantifying tradeoffs for marine viruses. *Front Mar Sci*, *3*(Dec). https://doi.org/10.3389/fmars.2016.00251

Senčilo, A., Luhtanen, A. M., Saarijärvi, M., Bamford, D. H., Roine, E. (2015). Cold-active bacteriophages from the Baltic Sea ice have diverse genomes and virus-host interactions. *Environ Microbiol*, *17*(10), 3628–3641. https://doi.org/10.1111/1462-2920.12611

Sillankorva, S., Oliveira, R., Vieira, M.J., Sutherland, I., Azeredo, J. (2004). *Pseudomonas fluorescens* infection by bacteriophage φS1: the influence of temperature, host growth phase and media. *FEMS Microbiol Lett 241*, 13–20.

Smith, R. E., Clement, P., Cota, G. F. (1989). Population dynamics of bacteria in Arctic sea ice *Microb Ecol, 17*(1), 63–76.

Spencer, R. (1963). Bacterial viruses in the sea. In: Oppenheimer, C.H. (Ed.), *Symposium on marine microbiology*. Thomas, Springfield, IL, 350–365.

Suttle, C. A., & Chen, F. (1992). Mechanisms and rates of decay of marine viruses in seawater. *Appl Environ Microbiol*, *58*(11), 3721–3729. https://doi.org/10.1128/aem.58.11.3721-3729.1992

Thamatrakoln, K., Talmy, D., Haramaty, L., Maniscalco, C., Latham, J. R., Knowles, B., … Bidle, K. D. (2019). Light regulation of coccolithophore host–virus interactions. *New Phytol*, *221*(3), 1289–1302. https://doi.org/10.1111/nph.15459

Thomas, D. N., Lara, J. R., Eicken, H., Kattner, G., Skoog, A. (1995). Dissolved organic matter in Arctic multi-year sea ice during winter: major components and relationship to ice characteristics. *Polar Biol, 15*, 477–483.

Thomas, D. N., Kattner, G., Engbrodt, R., Giannelli, V., Kennedy, H., Haas, C., Dieckmann, G. S. (2001). Dissolved organic matter in Antarctic sea ice. *Ann Glaciol*, *33*, 297–303. https://doi.org/10.3189/172756401781818338

Troussellier, M., Bouvy, M., Courties, C., Dupuy, C. (1997). Variation of carbon content among bacterial species under starvation condition. *Aquat Microb Ecol*, *13*(2), 113–119. https://doi.org/10.3354/ame013113

Valentine, A. F., Chen, P. K., Colwell, R. R., Chapman, G. B. (1966). Structure of a marine bacteriophage as revealed by the negative staining technique. *J Bacteriol* 91:819–822.

Weitz, J. (2016). Quantitative Viral Ecology. Princeton: Princeton University Press. doi: https://doi-org.offcampus.lib.washington.edu/10.1515/9781400873968

Weitz, J. S., Beckett, S. J., Brum, J. R., Cael, B. B., Dushoff, J. (2016). Lysis, lysogeny, and virus-microbe ratios. *Nature, 549*, E1–E3.

Weitz, J. S., & Dushoff, J. (2008). Alternative stable states in host–phage dynamics. *Theor Ecol*, *1*(1), 13–19. https://doi.org/10.1007/s12080-007-0001-1

Weitz, J. S., Hartman, H., Levin, S. A. (2005). Coevolutionary arms races between bacteria and bacteriophage. *Proc Natl Acad Sci USA*, *102*(27), 9535–9540.

Weitz, J. S., Li, G., Gulbudak, H., Cortez, M. H., Whitaker, R. J. (2019). Viral invasion fitness across a continuum from lysis to latency†. *Virus Evol*, *5*(1), 1–9. https://doi.org/10.1093/ve/vez006

Weitz, J. S., Stock, C. A., Wilhelm, S. W., Bourouiba, L., Coleman, M. L., Buchan, A., … Eric Wommack, K. (2015). A multitrophic model to quantify the effects of marine viruses on microbial food webs and ecosystem processes. *ISME J*, *9*(6), 1352–1364. https://doi.org/10.1038/ismej.2014.220

Weitz, J. S., & Wilhelm, S. W. (2012). Ocean viruses and their effects on microbial communities and biogeochemical cycles. *F1000 Biol Rep*, *4*(1), 2–9. https://doi.org/10.3410/B4-17

Wells, L. E. (2006). Viral adaptations to life in the cold. *[Doctoral Dissertation, University of Washington]*, ProQuest Dissertations Publishing. https://doi.org/10.1109/wimesh.2006.288596

Wells, L. E., & Deming, J. W. (2006a). Modelled and measured dynamics of viruses in Arctic winter sea-ice brines. *Environ Microbiol*, *8*(6), 1115–1121. https://doi.org/10.1111/j.1462-2920.2005.00984.x

Wells, L. E., & Deming, J. W. (2006b). Characterization of a cold-active bacteriophage on two psychrophilic marine hosts. *Aquat Microb Ecol*, *45*(1), 15–29. https://doi.org/10.3354/ame045015

Wells, L. E., & Deming, J. W. (2006c). Effects of temperature, salinity and clay particles on inactivation and decay of cold-active marine Bacteriophage 9A. *Aquat Microb Ecol*, *45*(1), 31–39. https://doi.org/10.3354/ame045031

Weinbauer, M. G., Brettar, I., Höfle, M. G. (2003). Lysogeny and virus-induced mortality of bacterioplankton in surface, deep, and anoxic marine waters. *Limnol Oceanogr*, *48*(4), 1457–1465. https://doi.org/10.4319/lo.2003.48.4.1457

Whitman, P. A., & Marshall, R. T. (1971b). Characterization of two psychrophilic *Pseudomonas* bacteriophages isolated from ground beef. *Appl Microbiol, 22*, 463–468.

Wilhelm, S. W., & Suttle, C. A. (1999). Viruses and nutrient cycles in the sea. *BioScience*, *49*(Oct), 781–788. https://doi.org/10.2307/1313569

Wigington, C. H., Sonderegger, D., Brussaard, C. P. D., Buchan, A., Finke, J. F., Fuhrman, J. A., … Weitz, J. S. (2016). Re-examination of the relationship between marine virus and microbial cell abundances. *Nat Microbiol*, *1*(3). https://doi.org/10.1038/nmicrobiol.2015.24

Wommack, K. E., & Colwell, R. R. (2000). Virioplankton: Viruses in aquatic ecosystems. *Microbiol Molec Biol Rev*, *64*(1), 69–114. https://doi.org/10.1128/mmbr.64.1.69-114.2000

Yager, P. L., & Deming, J. W. (1999). Pelagic microbial activity in an arctic polynya: Testing for temperature and substrate interactions using a kinetic approach. *Limnol Oceanogr*, *44*(8), 1882–1893. https://doi.org/10.4319/lo.1999.44.8.1882

Yu, Z. C., Chen, X. L., Shen, Q. T., Zhao, D. L., Tang, B. L., Su, H. N., … Zhang, Y. Z. (2015). Filamentous phages prevalent in *Pseudoalteromonas* spp. confer properties advantageous to host survival in Arctic sea ice. *ISME J*, *9*, 871–881. https://doi.org/10.1038/ismej.2014.185

Zhong, Z.-P., Rapp, J. Z., Wainaina, J. M., Solonenko, N. E., Maughan, H., Carpenter, S. D., Cooper, Z. S., *et al*. (2020). Viral ecogenomics of Arctic cryopeg brine and sea ice. *MSystems*, *5*(3), 1–17. https://doi.org/10.1128/msystems.00246-20

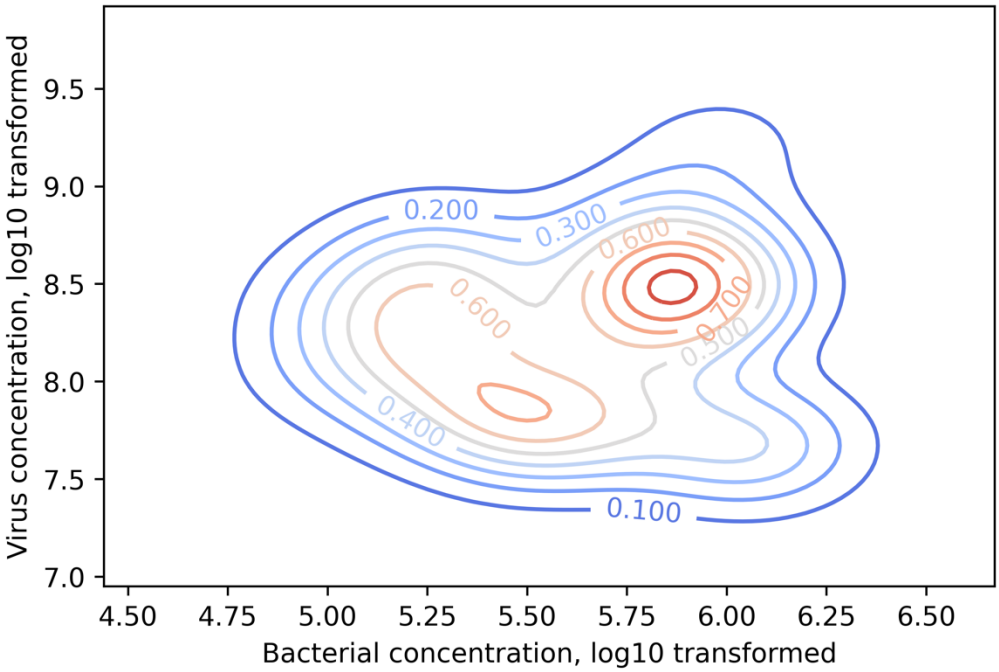

Figure 4.1 Observed concentrations of viruses and bacteria within sea-ice brines. Recreated from Collins and Deming (2011), this figure shows the kernel distribution estimate of virus and bacteria concentrations within sea-ice brines collated from literature. Values are log-normalized, and demonstrate high virus-to-bacteria ratios, approaching 10,000 to 1. Contours represent density of individual observations as a fraction between 0 and 1.

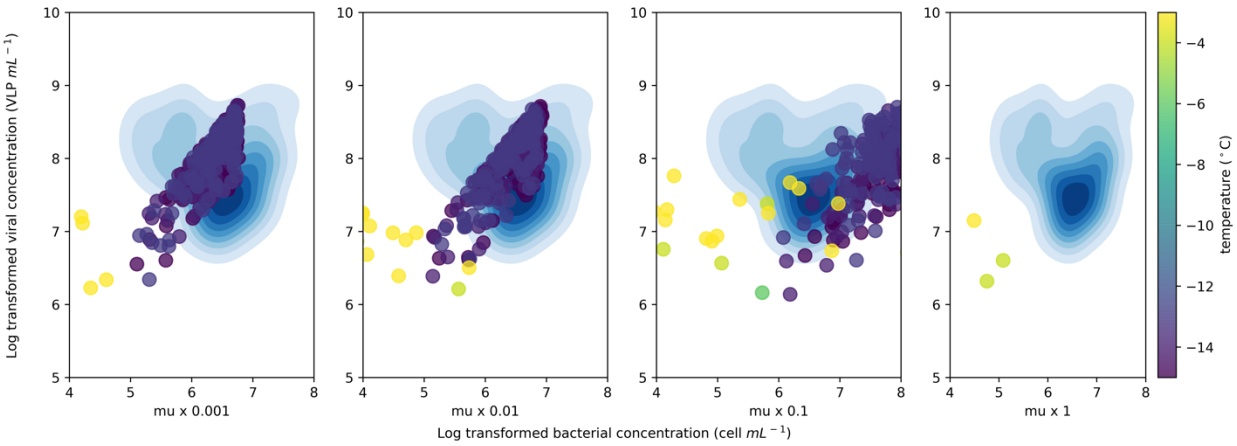

Figure 4.2 Parameter tuning of non-steady-state runs for bacterial growth rate μ. Four panels show the distribution of end-point VBR after 100 runs of 2500 hours (circles) in log-normalized space as a function of scaling factor, mu x, applied to a temperature-dependent distribution of bacterial growth rate, μ. From left to right, mu x is: 0.001, 0.01, 0.1, and 1. Values are laid over observed distributions as displayed in Figure 4.1 (here shown as filled, blue contours). Color of points indicates the temperature of the run in degrees Celsius, given in the color bar on the right.

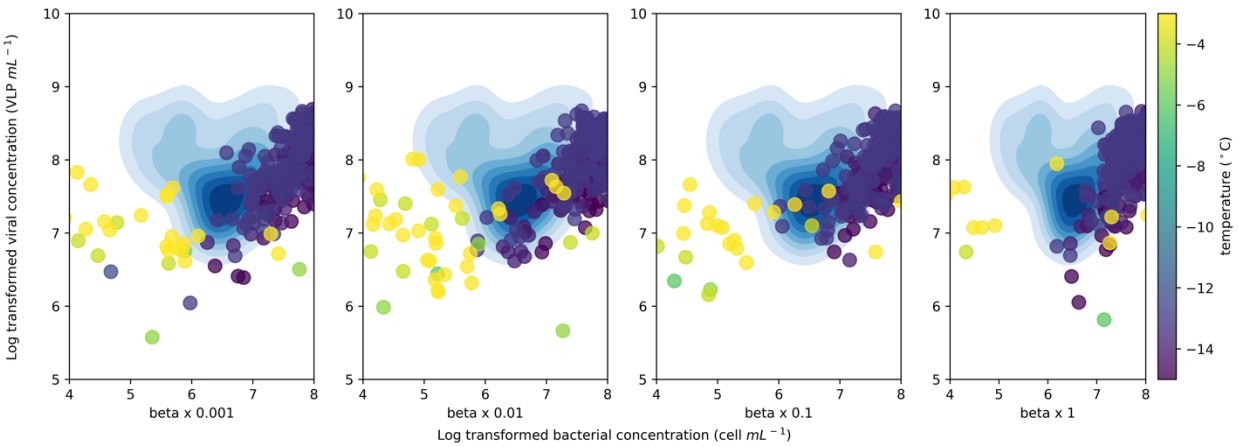

Figure 4.3 Parameter tuning of non-steady-state runs for virus burst size, β. Four panels show the distribution of end-point VBR after 100 runs of 2500 hours (circles) in log-normalized space as a function of scaling factor, beta x, applied to a temperature-dependent distribution of virus burst size, β. From left to right, beta x is: 0.001, 0.01, 0.1, and 1. Values are laid over observed distributions as displayed in Figure 4.1 (here shown as filled, blue contours). Color of points indicates the temperature of the run in degrees Celsius, given in the color bar on the right.

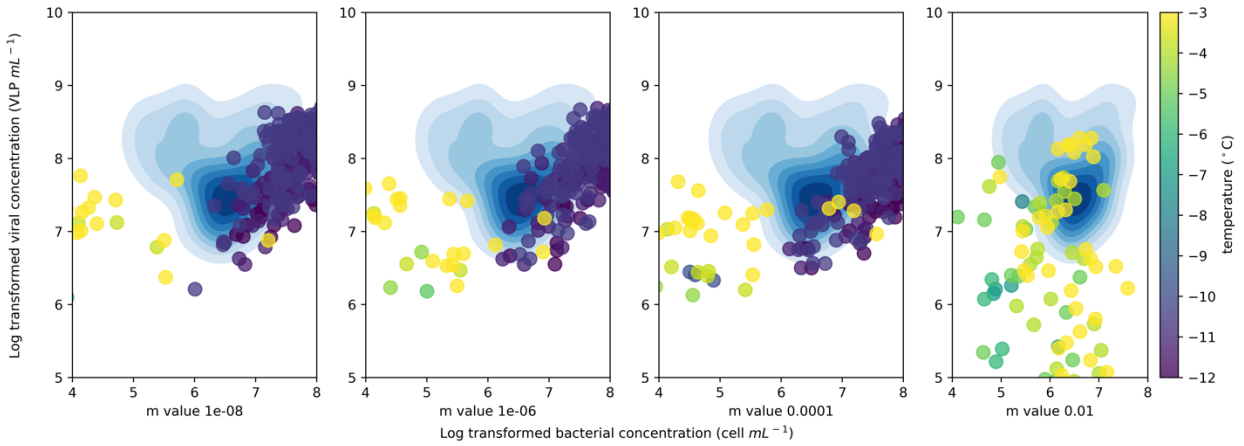

Figure 4.4 Parameter tuning of non-steady-state runs for viral decay rate, m. Four panels show the distribution of end-point VBR after 100 runs of 2500 hours (circles) in log-normalized space as a function of viral decay rate, m. From left to right, m is 1 x 10^{-8}, 1 x 10^{-6}, 1 x 10^{-4}, and 1 x 10^{-2} . Values are laid over observed distributions as displayed in Figure 4.1 (here shown as filled, blue contours). Color of points indicates the temperature of the run in degrees Celsius, given in the color bar on the right.

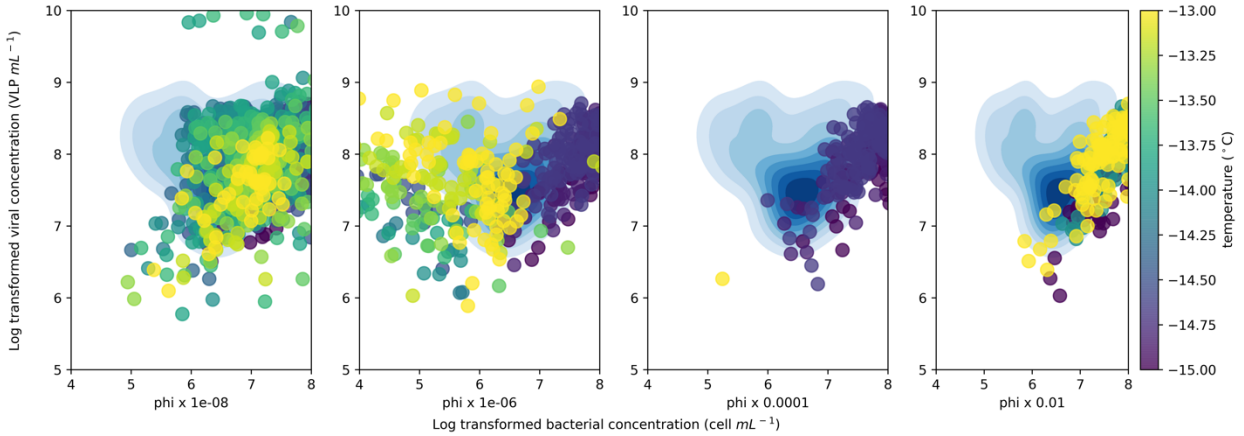

Figure 4.5 Parameter tuning of non-steady-state runs for viral adsorption rate, φ. Four panels show the distribution of end-point VBR after 100 runs of 2500 hours (circles) in log-normalized space as a function of scaling factor, phi x, applied to a temperature-dependent distribution of virus adsorption rate, φ . From left to right, phi x is: 1 x 10^{-8}, 1 x 10^{-6}, and 1 x 10^{-4}, 1 x 10^{-2}. Values are laid over observed distributions as displayed in Figure 4.1 (here shown as filled, blue contours). Color of points indicates the temperature of the run in degrees Celsius, given in the color bar on the right.

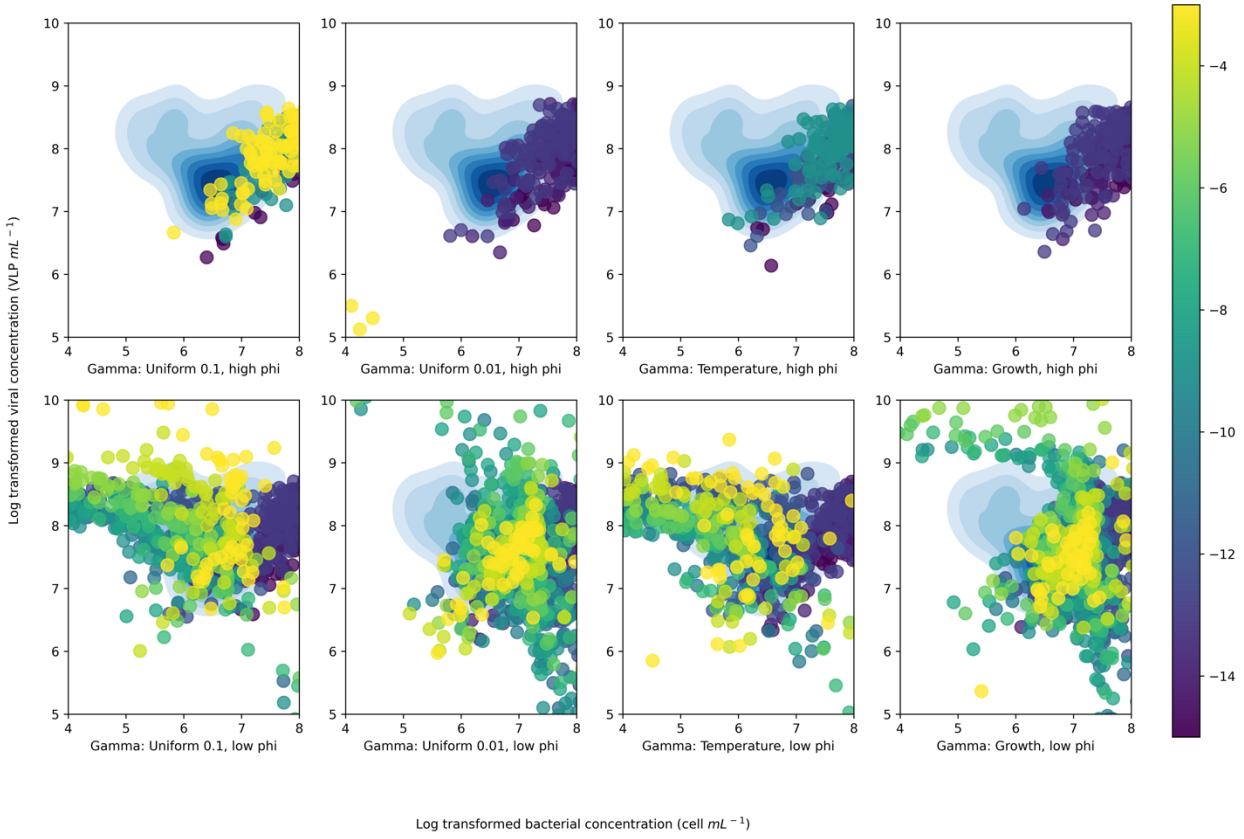

Figure 4.6 Parameter tuning of non-steady-state runs for lytic fraction, γ, covaried with viral adsorption rate, φ . Eight panels show the distribution of end-point VBR after 100 runs of 2500 hours (circles) in log-normalized space as a function of covaried lytic fraction and virus adsorption rate. The top row shows lytic fraction as a uniform value 0.1 (left), or 0.01 (center left), as a function of temperature (center right), or as a function of bacterial growth rate (far right) while phi x was held at a "high" scaling value of 1 x 10^{-2}. The bottom row follows the same pattern for lytic fraction treatments, with phi x was held at a "low" scaling value of 1 x 10^{-6}.

Values are laid over observed distributions as displayed in Figure 4.1 (here shown as filled, blue contours). Color of points indicates the temperature of the run in degrees Celsius, given in the color bar on the right.

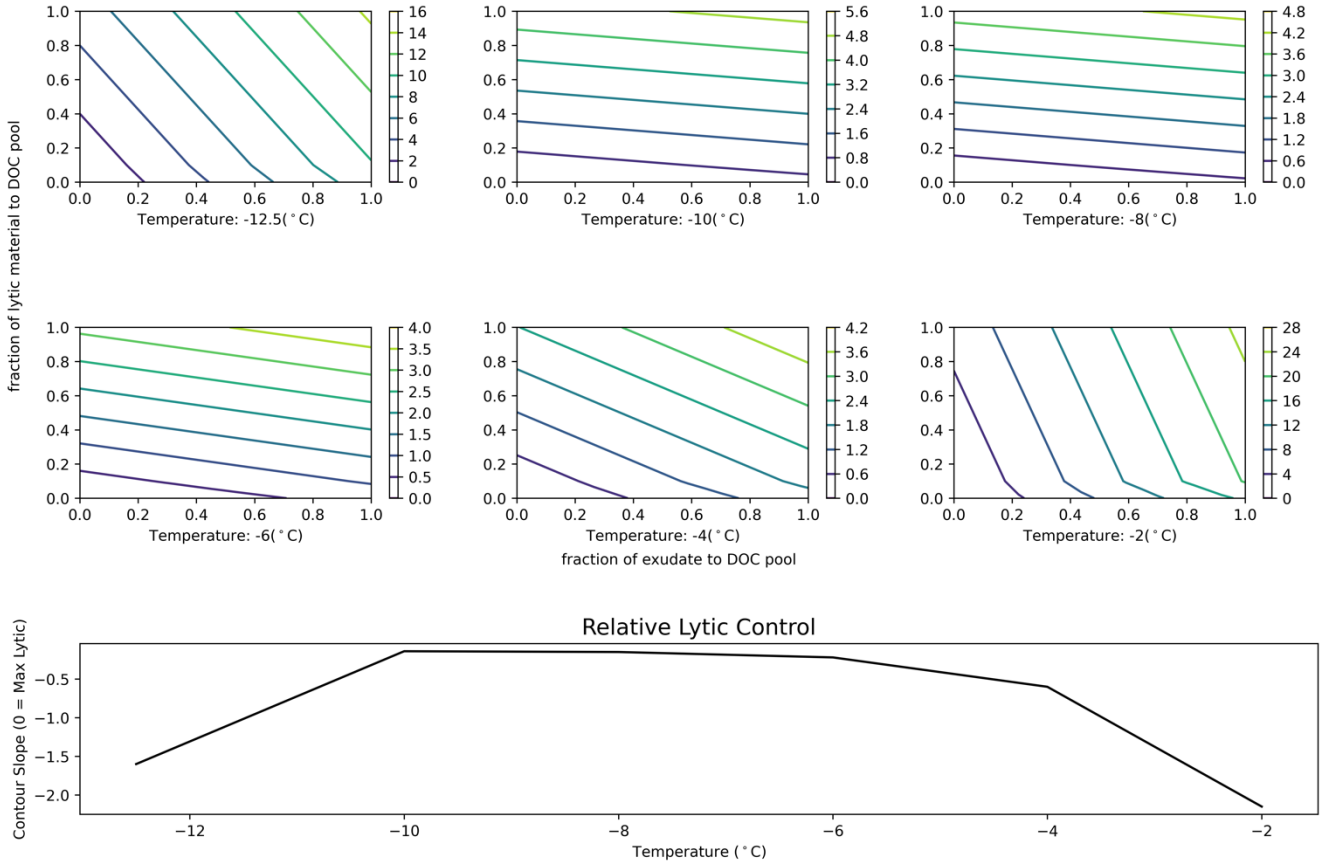

Figure 4.7 Recycled DOC content as a function of covaried recycled material from viral lysis and cellular exudate. The total content of recycled DOC was quantified after 2500 hours to determine relative contribution of viral lysis or cellular exudate, both of which are covaried between 0 and 1, where 0 represents zero input of lytic material or cell exudate to the DOC pool, and 1 represents either all lytic material or all cell exudate going into the DOC pool. Slope of the contours demonstrate relative control: vertical lines imply greater control from exudate, while

horizontal lines show greater viral control. Panels represent the experiment repeated at different temperatures from –15˚C to –2˚C. The bottom panel shows the average slope of the contours for each temperature; an average slope of zero suggests total viral control, while an infinite, negative slope suggests greater cellular control.

Table 4.1 Values and sources for model parameters and constants. Parameter name, symbol, and range of values are listed for constants (fixed values, determined from literature), dynamic parameters (those varied with each model run), tuned parameters (those determined from numerical experiments), or variables (those manipulated in model experiments).

Parameter	Symbol	Range	Mean (± SD[a])	Units	Sources	Type
Uptake rate	α	1.5 x 10^{-9}–5 x 10^{-6} [b]	–	μg cell^{-1} hr^{-1}	Levin *et al*., 1977; Kirchman *et al*., 2005; Connelly *et al*., 2014; Weitz, 2016	constant
Uptake saturation constant	ξ	–	0.022	μg	Owens & Legan, 1987; Brailsford *et al*., 2019; Weitz, 2016	constant
Carbon content per bacterial cell	σ	–	1 x10^{-7}	μg cell^{-1}	Bratkbak & Dundas, 1983; Troussellier *et al*., 1997; Fukuda *et al*., 1998. Braun *et al*., 2016	constant
Bacterial death rate	d	–	1 x10^{-7} c	hr^{-1}	Jörgensen & Kurland (1987)	dynamic
Bacterial genotype	h_i	0–1	–	–	–	dynamic
Viral genotype	v_i	0–1	–	–	–	constant
Bacterial growth rate	μ	6.2 x10^{-3}–0.99	0.15 ± 0.19	hr^{-1}	Guixa-Boixareu *et al*., 1996; Nichols *et al*., 1999; Huston, 2003; Smith *et al*., 2003; Kirchman *et al*., 2009; Collins & Deming, 2011; Mykytczuk *et al*., 2013; Chua *et al*., 2018	tuned parameter
Adsorption rate	φ	8.4 x10^{-10}–3.5 x10^{-6}	2.4 x10^{-7} ± 6 x10^{-7}	cells^2 mL^{-1} hr^{-1}	Wells & Deming 2006a; Moldovan, 2007; Wells, 2008; Collins & Deming, 2011; Weitz, 2016	tuned parameter
Burst size	β	5–529	75 ± 95	virions	Heldal & Bratbak, 1991; Guixa-Boixareu *et al*., 1996; Wommack and Colwell, 2000; Weinbauer *et al*., 2003; Wells & Deming 2006b; Anesio *et al*., 2007; Wells, 2008; Weitz, 2016	tuned parameter
Virus decay rate	m	8.3 x 10^{-4}–0.4	0.09	hr^{-1}	Heldal & Bratbak, 1991; Suttle and Chen, 1992; Wommack & Colwell, 2000; Danovaro *et al*., 2005; Middelboe & Jørgensen, 2006; Wells & Deming 2006c; Collins & Deming, 2011; Köstner, 2017	tuned parameter
Lysogenic fraction	γ	0–1	–	–	–	variable
Phage-host specificity constant	s	0–1000	–	–	–	variable
Exudate release fraction	ϱ	0–1	–	–	–	variable
Lytic release fraction	υ	0–1	–	–	–	variable

[a] Mean and standard deviation presented here was calculated from data from references the "sources" column, including data from which values were extracted using the Metropolitan-Hastings algorithm described in Chapter 4.2 . The n value of these data are thus equal to the number data points in the combined sources.

[b] This range was calculated according to an average uptake rate (1.2×10^{-7} μg C cell^{-1}) adjusted for temperature using a Q_{10} law of thermal dependence with a factor of 3, as suggested in Kirchman *et al*. (2005).

[c] Although a constant value is given here, very little data on bacterial death in the absence of grazing or viral mortality exists. An estimate for this value was taken from Jörgensen & Kurland (1987), but this study was performed with cultured *E. coli* under laboratory conditions rather than with natural assemblages at extremes of temperature or salinity. Thus, this parameter was tuned alongside the group of focal parameters, although it had negligible effect on the VBR when within ranges suggested in the above source. While bacteria within sea ice likely engage in some kind of 'warfare,' as is common in other marine environments, this process has not been well studied in sea ice (for a review of bacterial warfare, see Grenato *et al*., 2019). However, seasonal observations of bacterial abundances within sea-ice brines have suggested minimal loss due to factors other than viral lysis (Collins *et al*., 2010). Given the uncertainty and suggested insignificance of this constant, we ultimately chose to reduce this value to exhibit minimal death rates. Further investigations of this environment into the processes stated above would improve the accuracy of this value.

Appendix 1.

Equations of virus-bacteria population model

Nutrient-bacteria-virus (NBV) model of sea-ice brine population dynamics

The following equations were used to simulate simplified virus-host dynamics within sea-ice brine as described in Chapter 4. These equations were developing using a framework established by Weitz (2016) for a resource-explicit phage-host system model in which infected classes are not expressly considered.

Organic carbon (nutrients):

$$\dot{N} = \underbrace{-\alpha B \frac{N}{N+\xi}}_{\text{uptake}} + \underbrace{\varrho \alpha B \frac{N}{N+\xi}}_{\text{exudate}} + \underbrace{\upsilon \sigma B V}_{\text{lysis}}$$

Bacterial concentration:

$$\dot{B} = \underbrace{\mu \frac{N}{N+\xi}}_{\text{growth}} - \underbrace{\varphi B V}_{\text{infection}} - \underbrace{dB}_{\text{death}}$$

Viral concentration:

$$\dot{V} = \underbrace{\beta \varphi B V}_{\text{production}} - \underbrace{\varphi B V}_{\text{infection}} - \underbrace{mB}_{\text{decay}}$$

Following parameter tuning as described in Chapter 4, the equations were amended in the manner of Record *et al*. (2016) to add a lytic fraction parameter, γ, where lytic fraction is defined as the

proportion of viruses actively produced through lysis. This factor was applied to the virus production term, removing the fraction of lysogenic viruses (those that are not produced), as well as to the bacterial infection term, removing the fraction of cells infected by lysogenic viruses and thus not lysed by infection. This term is also included in the lytic fraction that contributes to organic carbon. Lytic fraction is indicated by the coefficient γ.

Organic carbon (nutrients): $$\dot{N} = \overbrace{-\alpha B \frac{N}{N+\xi}}^{\text{uptake}} + \overbrace{\varrho \alpha B \frac{N}{N+\xi}}^{\text{exudate}} + \overbrace{\gamma \upsilon \sigma B V}^{\text{lysis}}$$

Bacterial concentration: $$\dot{B} = \overbrace{\mu \frac{N}{N+\xi}}^{\text{growth}} - \overbrace{\gamma \varphi B V}^{\text{infection}} - \overbrace{dB}^{\text{death}}$$

Viral concentration: $$\dot{V} = \overbrace{\gamma \beta \varphi B V}^{\text{production}} - \overbrace{\varphi B V}^{\text{infection}} - \overbrace{mB}^{\text{decay}}$$

When considering the role of viral lysis and cellular exudate to DOC recycling, the concentration of recycled DOC was quantified by tracking the volume released from either lysis or cellular exudate, as given below.

Recycled DOC concentration: $$\dot{D} = \overbrace{\varrho \alpha B \frac{N}{N+\xi}}^{\substack{\text{DOC} \\ \text{from cell}}} + \overbrace{\gamma \upsilon \sigma B V}^{\substack{\text{DOC} \\ \text{from lysis}}}$$

Because no loss term is included in this equation, recycled DOC is a cumulative measure of recycled material.

Multispecies model of sea-ice brine populations dynamics

Modeled after Becket & Williams (2013), equations governing the multispecies model follow those presented in the NBV model, but with the added phage-host specificity coefficient θ, which was added to infection, production, and lysis terms as below. These equations are unique compared to the above equations by inclusion of the coefficient θ.

Organic carbon (nutrients): $$\dot{N} = \overbrace{-\alpha B \frac{N}{N+\xi}}^{\text{uptake}} + \overbrace{\varrho \alpha B \frac{N}{N+\xi}}^{\text{exudate}} + \overbrace{\theta \gamma \upsilon \sigma B V}^{\text{lysis}}$$

Bacterial concentration: $$\dot{B} = \overbrace{\mu \frac{N}{N+\xi}}^{\text{growth}} - \overbrace{\theta \gamma \varphi B V}^{\text{infection}} - \overbrace{dB}^{\text{death}}$$

Viral concentration: $$\dot{V} = \overbrace{\theta \gamma \beta \varphi B V}^{\text{production}} - \overbrace{\theta \varphi B V}^{\text{infection}} - \overbrace{mB}^{\text{decay}}$$

where θ is given as:

Specificity coefficient: $$\theta = e^{s(h_i - v_j)^2}$$

Appendix 2.

Cyropeg brines as a sub-zero, hypersaline environment comparison: Extracellular enzyme activity measurements

A2.1 Introduction

Cryopegs, discrete layers of unfrozen sediments, exist trapped within the permafrost matrix of Arctic coastal plains. Likely the byproduct of ancient seawater retreat during periods of glaciation, cryopegs are thought to originate from saturated marine sediments which experienced desiccation and concentration while being covered by permafrost (Gilichinsky *et al*., 2003; 2005). The resulting high salinity liquid remains unfrozen despite sub-zero temperatures within the permafrost matrix due to freezing-point depression by the concentrated salts. By virtue of this liquid brine, and similar to sea-ice brines, microbial communities are able to inhabit cryopegs despite the sub-zero temperatures. Cryopeg brines thus provide a sub-zero hypersaline microbial habitat for comparison to sea-ice brines, the focal habitat of this dissertation.

Dominated by bacteria, cryopeg brines host dense microbial assemblages reaching 10^7 cells mL^{-1}, with Gammaproteobacteria and Bacteroidetes representing the most abundant taxa (Cooper *et al*., 2019). Both taxa commonly thrive in the copiotrophic conditions that characterize the organic-rich brines of the Alaskan coastline, which were found to contain high concentrations of extracellular polysaccharides (EPS) (Colangelo-Lillis *et al*., 2016; Cooper *et al*., 2019). However, EPS and other dissolved organic material are often too large to pass through most cell membranes, and must therefore be broken down before uptake (Chróst, 1991). Bacteria commonly use extracellular enzymes (EE), hydrolytic enzymes expressed at the surface of the cell or beyond the

cell, to facilitate the breakdown of high molecular weight material. EE activity (EEA) is often considered the rate-limiting step of organic carbon cycling, and as such, demonstration of EEA within cryopeg brines may serve as a foundation for quantifying bacterial carbon uptake and population dynamics in the environment.

To investigate the activity of EE in cryopegs, we sampled brines from a cryopeg accessed from the Barrow Permafrost Tunnel near Utqiaġvik, Alaska. These brines, characterized by temperatures between –6˚C and –8˚C and salinities near 120 ppt, have been investigated previously with respect to viral and bacterial community diversity as well as geochemical properties (Colangelo-Lillis *et al*., 2016; Spirina *et al.*, 2017; Cooper *et al*., 2019; Iwahana *et al*., 2020; Zhong *et al*., 2020). Geochemical analysis suggests that the brines have been isolated for at least 14,000 years with minimal atmospheric exchange. Determining the rate of EEA within these cryopeg brines offers a measure of bacterial activity, and may further our understanding of how *in situ* communities actively cycle organic compounds under extreme conditions to sustain populations in an isolated frozen environment over a multi-millennial timescale.

A2.2 Methods

A2.2.1 *Sample collection*

Brine samples were collected from a cryopeg borehole previously drilled and re-entered in 2018 near Utqiaġvik, Alaska, as described in Cooper *et al*. (2019). Briefly, a hand pump was used to remove liquid from the cryopeg accessed through a borehole drilled in the floor of the Barrow Permafrost Tunnel (71.2944˚N, 156.7153˚W), and the sample was then stored in a sterile vacuum flask. A sample was collected again from the same borehole 4 days later after it yielded recharge fluid. Fluid was returned the Barrow Arctic Research Center (BARC) in a cooler to limit light

exposure and temperature changes, and was then immediately processed in a dark cold room set to near *in situ* temperature (–6˚C). The sampled fluid was later determined to be derived from a cryopeg brine within massive ice (or ice wedge), and thus labeled as either cryopeg brine ice-wedge (CBIW) or cryopeg brine ice-wedge following recharge (CBIW-R) according to the nomenclature of Cooper *et al*. (2019).

A2.2.2 *EEA measurements*

Extracellular enzyme activity was measured in the manner of Hoppe (1983) and as described in Chapter 2. Cryopeg fluid was filtered using a 0.2 μm syringe filter in the –6˚C into a sterile 50 mL Falcon tube to remove bacteria. Aliquots of the cell-free filtrate were distributed into clean glass tubes (1 mL) and then mixed with fluorescently-tagged substrate at 40, 100, 150, 200, 250, or 400 μM concentration for CBIW, and later at 250 μM concentration for CBIW-R. Fluorogenic substrates used were L-Leucine-7-amido-4-mtheylcoumarin hydrochloride (MCA-L), 4-methylumbelliferyl N-acetyl-β-D-glucosaminide (MUF-G), and 4-methylumbelliferyl N-acetyl-β-D-mannopyranoside (MUF-M) (Sigma).

Fluorescence was measured using a Trilogy Laboratory Fluorometer (Turner) at 4–6 time points over a 24 hour period. Change in fluorescence was converted to concentration of liberated tag in units of nM substrate mL^{-1} according to a standard curve made using known concentration of a free tag (MCA or MUF, with no attached substrate) as described in Chapter 2. Significant difference between rates was determined by a paired student's t-test.

A2.2.3 *Bacterial counts*

Cryopeg fluid was preserved for enumeration of bacteria as described in Cooper *et al*. (2019). Samples were preserved in 2% final concentration formaldehyde and kept at 4°C until returned to the University of Washington, where bacteria were stained using DAPI and acridine

orange, and counted using an epifluorescent microscope as described in Chapter 2. Final cell concentration was used to calculate cell-specific rates of EEA.

A2.3 Results and discussion

Measurements showed hydrolytic activity against all three substrates in CBIW, and of MCA-L and MUF-G in CBIW-R (Figure A2.1). These measurements serve as a demonstration not only of active enzyme hydrolysis but also of active microbial communities within the brine. MCA-L showed the highest rate of EEA in CBIW, approximately 1.5 x 10^{-8} nM MCA-L $cell^{-1}$ hr^{-1}, and significantly higher than EEA in response to MCA-L in CBIW-R ($p < 0.0001$). This result was on the same order of magnitude as cell-specific rates of free EEA measured at –4 and –8˚C in culture work with *Colwellia psychrerythraea* strain 34H as described in Chapter 2. Fluid from CBIW followed the expected pattern of enzyme activity based on prior work in Arctic waters (Huston *et al*., 2000; Kellogg *et al.,* 2014) with MCA-L demonstrating the highest EEA rate, and MUF-G and MUF-M showing lower rates. In contrast, fluid from CBIW-R showed the highest EEA rate against MUF-G, which was comparable to the rate in CBIW ($p = 0.39$), the lowest rate against MCA-L, and non-significant rates in response to MUF-M ($p < 0.05$).

Cryopeg brines are notable for high concentrations of organic material, especially in the form of EPS (Colangelo-Lillis *et al.*, 2016; Cooper *et al*., 2019). Quantification of both dissolved EPS and dissolved organic carbon in CBIW indicated levels 100 to 1,000 times higher than in sea-ice brines collected from nearby landfast ice, with values reaching millimolar concentrations (Cooper *et al*., 2019). High concentrations of organic material correspond to production of extracellular enzymes, as discussed in Chapter 2, which is especially relevant to complex EPS within the environment. In addition to amino sugars and uronic acids, bacterial EPS in marine and

extreme environments commonly contain monomeric components including glucose and mannose (Poli *et al*., 2010; Ewert & Deming, 2013); activity in response to MUF-G and MUF-M represents bacterial potential to degrade these components *in situ*. Activity of MUF-G and MUF-M may work to degrade and cycle EPS components within cryopeg brines, but the use of these relatively simple substrates invariably underestimates the true rate of degradation of complex polysaccharides (Arnosti, 2011). However, EPS can stabilize EE, such that they retain activity for long periods of time (Huston *et al*., 2004). Long lifetimes of EEA within low-temperature EPS-rich brines may lead to accumulation of enzymes (Steen & Arnosti, 2011). Lower activity in CBIW-R compared to CBIW may be the result of EPS-trapping as brine percolates into the borehole during recharge. Any EPS adsorbed to sediment may be left behind as brine percolates, along with any extracellular enzymes trapped within the EPS (Decho & Gutierrez, 2017).

The pattern of different hydrolytic activity in CBIW and CBIW-R may also be the result of perturbation due to fluid withdrawal from the borehole. The perturbation may have led to changes in the microbial community, either in composition or activity. Indeed, as indicated in Cooper *et al*. (2019), community composition changed slightly on genus-level between CBIW and CBIW-R, most apparently with an increase in relative abundance of *Marinobacter* and *Pseudomonas*, and decrease in *Flavimarina* and *Gillisia*. Whether the communities experienced significant changes in growth (and thus changes in EE production) owing to the perturbation is not clear, as abundance of dividing cells showed little change between these two samples (1.3% in CBIW; 1.1% in CBIW-R; Cooper *et al*., 2019). Instead, community composition may have changed as the result of the introduction of some oxygen to the likely anoxic cryopeg (Gilichinsky *et al*., 2003; 2005) or handling effects.

Another possible explanation for the different EEA patterns and community compositions between CBIW and CBIW-R is that the recharge brine was not sourced from the same fluid, instead representing a different community. Because auxiliary properties were measured only on CBIW and not CBIW-R, a comparison of chemical properties is not available to support this possibility. However, both samples contained closely similar abundances of cells as well as virus-like particles (Cooper *et al*., 2019), which, given overall similarities in community composition, suggest the recharge fluid was likely sourced from the same brine as the original sample. Geological evaluation of this portion of the cryopeg system beneath the permafrost tunnel also suggests a similar if not same source (Iwahana *et al.,* 2020).

The data shown here represent only the fraction of EE that was not attached to cell surfaces; measurements of total EEA, including those at the cell surface, may have shown different patterns. As described in Chapter 2, EE strategies are dependent on environmental and community parameters. For example, enzyme producers can be driven to extinction by "cheater" cells, those that do not produce extracellular enzymes but still reap the benefit, under conditions of well-mixed laboratory cultures (Alison, 2005; Alison *et al*., 2014). Microbes within cryopeg brines are likely to experience a heterogenous fluid despite long-residence times, as the low temperature, high salinity, and high organic content may contribute to a highly viscous system that mimics a structured biofilm, suggesting that free EE may be more beneficial.

At the same time, previous models of individual bacteria have suggested that non-motile bacteria should favor cell-attached enzymes, rather than free extracellular enzymes (Traving *et al*., 2015). Investigations of motility within cryopegs demonstrated that bacteria were likely non-motile *in situ*, although motility could be stimulated in response to a reduction in salinity (Bedrossian *et al*., 2020), and metagenomic evaluations have indicated the presence of motility

and chemotaxis genes in cryopeg brine communities (J. Rapp, personal communication). Future investigations of EEA in cryopeg brines may benefit from considering the relative contribution of free versus attached EE.

References

Allison, S. D. (2005). Cheaters, diffusion and nutrients constrain decomposition by microbial enzymes in spatially structured environments. *Ecol Lett*, *8*(6), 626–635. https://doi.org/10.1111/j.1461-0248.2005.00756.x

Allison, S. D., Lu, L., Kent, A. G., Martiny, A. C. (2014). Extracellular enzyme production and cheating in Pseudomonas fluorescens depend on diffusion rates. *Front Microbiol*, *5*(APR), 1–8. https://doi.org/10.3389/fmicb.2014.00169

Bedrossian, M., Snyder, C., Barr, C., Showalter, G. M., Deming, J. W., Nealson, K., *et al*. (2020) Prevalence and stimulation of motility in fresh field samples from diverse and extreme environments across North America. *Astrobiology*, *in prep*.

Chróst, R. J. (1991). Environmental control of the synthesis and activity of aquatic microbial ectoenzymes. In Chróst, R.J. (ed.). *Microbial Enzymes in Aquatic Environments*, (New York: Springer-Verlag), 84–95.

Colangelo-Lillis, J., Eicken, H., Carpenter, S. D., Deming, J. W. (2016). Evidence for marine origin and microbial-viral habitability of sub-zero hypersaline aqueous inclusions within permafrost near Barrow, Alaska. *FEMS Microbiol Ecol*, *92*(5), 1–15. https://doi.org/10.1093/femsec/fiw053

Cooper, Z. S., Rapp, J. Z., Carpenter, S. D., Iwahana, G., Eicken, H., Deming, J. W. (2019). Distinctive microbial communities in subzero hypersaline brines from Arctic coastal sea ice and rarely sampled cryopegs. *FEMS Microbiol Ecol*, *95*(12), 1–15. https://doi.org/10.1093/femsec/fiz166

Decho, A. W., & Gutierrez, T. (2017). Microbial extracellular polymeric substances (EPSs) in ocean systems. *Front Microbiol*, *8*(MAY), 1–28. https://doi.org/10.3389/fmicb.2017.00922

Ewert, M., & Deming, J. W. (2013). Sea ice microorganisms: Environmental constraints and extracellular responses. *Biology*, *2*(2), 603–628. https://doi.org/10.3390/biology2020603

Gilichinsky, D., Rivkina, E., Bakermans, C., Shcherbakova, V., Petrovskaya, L., Ozerskaya, S., *et al*. (2005). Biodiversity of cryopegs in permafrost. *FEMS Microbiol Ecol*, *53*(1), 117–128. https://doi.org/10.1016/j.femsec.2005.02.003

Gilichinsky, D., Rivkina, E., Shcherbakova, V., Laurinavichuis, K., Tiedje, J. (2003). Supercooled water brines within permafrost - An unknown ecological niche for microorganisms: A model for astrobiology. *Astrobiology*, *3*(2), 331–341. https://doi.org/10.1089/153110703769016424

Hoppe, H-G. (1983). Significance of exoenzymatic activities in the ecology of brackish water: measurements by means of methylumbelliferyl-substrates. *Mar Ecol Prog Ser, 11*, 299–308.

Huston, A. L., Krieger-Brockett, B. B., Deming, J. W. (2000). Remarkably low temperature optima for extracellular enzyme activity from Arctic bacteria and sea ice. *Environ Microbiol 2*(4): 383–388. DOI: 10.1046/j.1462-2920.2000.00118.x

Huston, A. L., Methe, B., Deming, J. W. (2004). Purification, characterization, and sequencing of an extracellular cold-active aminopeptidase produced by marine psychrophile *Colwellia psychrerythraea* strain 34H. *Appl Environ Microbiol*, *70*(6), 3321–3328. https://doi.org/10.1128/AEM.70.6.3321-3328.2004

Iwahana, G., Cooper, Z., Carpenter, S. D., Eicken, H., Deming, J. W. (2020) Intra-ice and intra-sediment brine occurrence in permafrost near Utqiaġvik (Barrow). *Permafrost Periglac* , *submitted.*

Kellogg, C. T. E., Deming, J. W. (2014). Particle-associated extracellular enzyme activity and bacterial community composition across the Canadian Arctic Ocean. *FEMS Microbiol Ecol*, 89(2), 360–375. https://doi-org.offcampus.lib.washington.edu/10.1111/1574-6941.12330

Poli, A., Anzelmo, G., & Nicolaus, B. (2010). Bacterial exopolysaccharides from extreme marine habitats: Production, characterization and biological activities. *Marine Drugs*, *8*(6), 1779–1802. https://doi.org/10.3390/md8061779

Spirina, E., Abramov, A., Romanovsky, V. E., Rivkina, E. (2017). Halophilic-psychrotrophic bacteria of an Alaskan cryopeg — a model for Astrobiology. *Paleonotolog J*, *51*(13), 1440-1452. *https*://doi.org/10.1134/S0031030117120036

Steen, A. D., & Arnosti, C. (2011). Long lifetimes of β-glucosidase, leucine aminopeptidase, and phosphatase in Arctic seawater. *Mar Chem*, *123*(1–4), 127–132. https://doi.org/10.1016/j.marchem.2010.10.006

Traving, S. J., Thygesen, U. H., Riemann, L., & Stedmon, C. A. (2015). A model of extracellular enzymes in free-living microbes: Which strategy pays off? *Appl Environ Microbiol*, *81*(21), 7385–7393. https://doi.org/10.1128/AEM.02070-15

Zhong, Z.-P., Rapp, J. Z., Wainaina, J. M., Solonenko, N. E., Maughan, H., Carpenter, S. D., Cooper, Z. S., Jang, H. Bin, Bolduc, B., Deming, J. W., & Sullivan, M. B. (2020). Viral ecogenomics of Arctic cryopeg brine and sea ice. *MSystems*, *5*(3), 1–17. https://doi.org/10.1128/msystems.00246-20

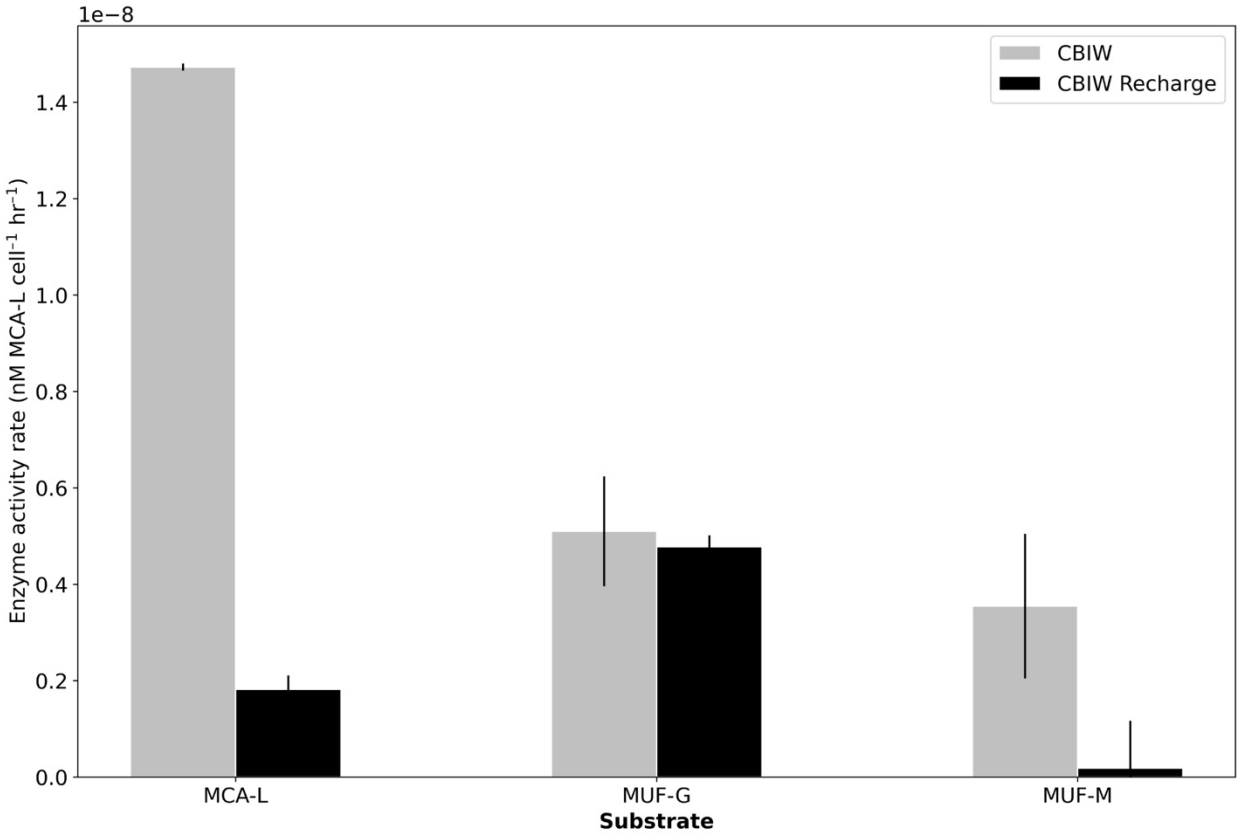

Figure A2.1. Extracellular enzyme activity of cryopeg brines in response to three fluorescently tagged substrates. Activity measurements in CBIW and CBIW-Recharge are shown in response to MCA-L (measure aminopeptidase activity), MUF-G (measure glucosidase activity), and MUF-M (measure mannosidase activity). Error bars represent one standard deviation from the mean rate (n = 3). Samples were measured at –6˚C, with salinity near 120 ppt as measured by handheld refractometer.

Appendix 3.

As with sea ice microbial communities, human communities living in the Arctic often rely on sea ice as a habitat (see Chapter 1.4). Here, I present a brief report of policies in Inuit Nunangat aimed to mitigate negative health effects of declining sea ice extent and other environmental changes due to climate change.

Climate change and public health:

A brief review of Canadian policies in Inuit Nunangat

The Canadian Northern and Arctic region is an area where both land and society are vulnerable to climate change. Though variably named and defined, the Northern and Arctic region is often considered to incorporate the territory above 60° latitude (Yukon, Northwest Territories, and Nunavut), as well land in Quebec north of 55° latitude and Nunatsiavut in Newfoundland and Labrador. Within this region, the land and water comprising the modern Inuit homeland is known as Inuit Nunangat (Inuit Tapiriit Kanatami, 2008). Inuit Nunangat is dominated demographically by Inuit, whose health is intimately associated with the environment. Health policies in these regions are crafted by federal and provincial governments as well as non-governmental organizations such as Inuit Tapiriit Kanatami (ITK), with territorial and provincial health care services administered by local boards. The need for specific health policies to unify the association

of health agencies has been identified in literature (Lavoie, 2013), and accordingly the Canadian federal government and Inuit communities have developed, both independently and in collaboration via the Inuit-Crown Partnership, a series of specific policies that identify leading health determinants associated with climate change, including food security, housing and sanitation, and mental health (Austin *et al.,* 2015; ITK, 2019a; Canadian Arctic and Northern Policy Framework [CANPF], 2019). The joint efforts of the federal government and Inuit organizations inspired, in part, by the Inuit-Crown Partnership represent a unique demonstration of policy co-development in the Arctic addressing the impact of climate change on health in Inuit Nunangat.

A3.1 Arctic food security is threatened by climate change.

Lack of food security is a leading issue facing Arctic and Northern communities. Identified as a key indicator of physical and holistic health (ITK, 2014a; 2017), food security is defined as "physical, social, and economic access to sufficient, safe, and nutritious food" at all times (Ferguson, 2011). Lack of access to food resources has been well documented in the Canadian Arctic (Nancarrow & Chan, 2010; Sharma *et al*, 2010; Huet *et al.,* 2012; ITK, 2014a; World Food Program, 2017), with 28% of households in Nunavut experiencing severe or moderate food insecurity (ITK, 2014a). This problem is especially prevalent among Inuit; a 2007 survey revealed 60% of respondents were worried about access to food, largely due to low income and high costs of market foods (Rosol *et al.,* 2011).

Climate change exacerbates food insecurity in Inuit Nunangat as warming temperatures, changes in precipitation, ice melt, and altered phenology threaten subsistence harvest and challenge traditional knowledge (Cannon, 1995; ACIA, 2005; Gregory *et al.,* 2005; IPCC, 2007),

while increased fuel prices inhibit access to hunting (Wesche & Chan, 2015). Research from the International Polar Year has suggested that climate change contributes to nutritional deficits, which in turn contribute to obesity, diabetes, and vitamin D deficiency (Owens *et al.,* 2012). The safety of country (traditional) food is also impacted by climate change: warmer temperatures have altered and enhanced uptake of toxic metals like mercury (MacDonald *et al.,* 2005) and increased the incidence of zoonosis (Owens *et al.,* 2012) in animals, including those traditionally hunted by Arctic Canadians. These connections have been recognized by both Inuit and the federal Government: the collaborative 2019 Canadian Arctic and Northern Policy Framework emphasizes the relationship between food insecurity and climate change, citing unpredictable ice conditions and melting ice as a source of continuing food insecurity in Inuit Nunangat (CANPF, 2019).

Inuit have also recognized food security within the broader context of "food sovereignty," a concept incorporating not only freedom from hunger, but also the political self-determination required to make legal decisions regarding food systems (Papatsie *et al*., 2013; ITK, 2017). This relationship is highlighted in the 2019 National Inuit Climate Change Strategy, in which food security is a common theme of multiple priority areas. Primarily, food security is connected to advancing capacity and knowledge in climate-related decision-making to enable "more effective use of Inuit knowledge," including knowledge of the land for travelling and hunting. Additionally, the Climate Change Strategy seeks to secure environmental health and document influences of land- and sea-based harvesting activities, while also aiming to reduce vulnerability of market-based foods (ITK, 2019a).

Examples of community commitment to improving food access in Inuit Nunangat are numerous. ITK's Food Security Working Group has documented over two dozen community-based food security initiatives in Inuit Nunangat as part of the Nuluaq Project, representing a strong

Inuit-led effort to maintain access to country foods, while provincial governments have also encouraged community-driven programs. In total, multiple local efforts, such as community freezers in Nain, Nunatsiavut (Organ *et al.,* 2014), and the successful community food program in Inuvik (Ford *et al.,* 2013), as well as collaborative strategic plans such as those developed by the Nunavut Food Security Coalition (ITK, 2014a), are evident in Inuit Nunangat, reflective of Inuit commitment to food security programs.

Federal commitments to food security have included environmental monitoring in the face of climate change. Health Canada has assisted in comprehensive reviews of environmental contaminants and human health in the Canadian Arctic in 1999, 2005, and 2010 (Oostman *et al.,* 1999; 2005; Donaldson *et al.,* 2010), and has established and staffed local laboratories to provide pathogen and biological contaminant diagnostics in food sources in Nain, Nunatsiavut and Yellowknife, Northwest Territories, as well as *Trichinella* diagnostics in Nunavik during walrus harvest (Owens *et al.,* 2012). Efforts to enhance public understanding of zoonotic and environmental contaminations among food sources, as well as increased material support for food and broader socio-economic programs, have been cited as potential future actions to improve food security in the Canadian Arctic (Owens *et al.,* 2012; Lawn & Harvey, 2003).

Federal and Inuit collaboration can be seen in recent policies developed to combat food insecurity in the Arctic compounded by climate change. In 2012, Canada initiated the Nutrition North Canada (NNC) program to encourage the consumption of traditional foods and ease access to commercialized country foods with subsidies (Nancarrow & Chan, 2010; Owens *et al.,* 2012; ITK, 2014a). NNC reopened engagement meetings with communities in 2016 and found communities were eager for the program to investigate efforts to build capacity for integration with other existing programs such as those documented in Nuluaq (Inuit Food Security Working Group,

2016). Likewise, many community members demonstrated concern regarding climate impacts on food availability as changing temperatures altered availability of country foods and affected transportation. In 2018, the Inuit-Crown Partnership established a Food Security Working group to "work towards a sustainable food system in Inuit Nunangat" as an expansion of the NNC program (CANPF, 2019). The NNC program is highlighted in the Canadian Arctic and Northern Policy Framework as a successful example of collaborative efforts (CANPF, 2019), with the Federal Government committing CAD $10.4 million to expanding the subsidy program. Thus, the Inuit-Crown Partnership has furthered collaborative efforts to establish food security and mitigate climate impacts on food availability in Inuit Nunangat.

A3.2 Climate change worsens infrastructure challenges.

Climate impacts on underdeveloped Arctic infrastructure, especially with respect to sanitation and housing, have been identified as another key public health priority by the Canadian government (CANPF, 2019). Freshwater resources in Arctic Canada, stressed by rapidly growing populations in towns like Iqaluit and Kangiqliniq (Rankin Inlet), are increasingly vulnerable to contamination due to climate change, which also accelerates uncertainty of freshwater availability (Warren *et al.,* 2005; Medeiros *et al*, 2007; Daley *et al.,* 2015). Similarly, high costs of construction and maintenance-repair contribute to housing shortages in Northern Canada, where 53% of Inuit homes are considered overcrowded (ITK, 2014a). Increase in extreme weather events, rising costs of fuel and material transport, and challenges of melting permafrost all link climate change to housing shortages in Inuit Nunangat (Owens *et al.,* 2012; ITK, 2014a). Housing shortages pose a very physical threat: crowded households increase incidences of domestic violence, especially against women, and poor mental health (Perreault *et al*., 2020), while poor ventilation propagates

infectious diseases such as tuberculosis and COVID-19 (ITK, 2014a), and has been shown to increase risk of respiratory infection in infants (Kovesi, 2012).

Need for improved housing and sanitation infrastructure has being noticed and acted upon by both national government and local jurisdictions in Canada, which has led to the development of housing plans by the Government of Nunavut and other regional organizations in the early 2000s. Likewise, in 2013, the Federal Budget established CAD $100 million for housing constructing in Nunavut (ITK, 2014a). However, Inuit organizations have highlighted that the budgetary process has traditionally excluded Inuit from Aboriginal housing development programs (ITK, 2014a). These voices were elevated in the 2017 Senate report *We Can Do Better: Housing in Inuit Nunangat,* which highlighted testimony from Inuit and other Arctic residents and clearly demonstrated the lack of sufficient housing in the region and consequential health impacts (Dyck & Patterson, 2017). A changing climate was listed among the factors contributing to the housing crisis, and adequate information on a changing climate to minimize such impacts was one of thirteen suggestions to alleviate the housing shortage (Dyck & Patterson, 2017).

Representative of the changing voice of Canadian governance, the Federal Budget for 2016 and 2018 included significant housing investments directly administered to Inuit communities. Following, the Inuit-Crown Partnership co-developed the Inuit Nunangat Housing Strategy in 2019, a landmark achievement highlighting further progress toward collaborative work across multiple levels of government. Key goals within this strategy included not only development of physical structures, but importantly also enhanced capacity for research and innovation, as highlighted in the 2017 Senate Report. Inclusion of this goal, brought forth by Indigenous voices in the 2017 Senate Report, illustrates ITK commitments to supporting Inuit-based research programs (ITK, 2018).

The Inuit-Crown Partnership has also participated in the co-development of elements of the 2019 Canada's Arctic and Northern Policy Framework, including a chapter authored by the ITK and a separate chapter authored by the Government of Nunavut. Here again, climate and infrastructure are intertwined with Inuit self-determination and health, with a focus on access to housing and transportation infrastructure, as well as clean water (Government of Nunavut, 2019).

Local commitments, especially at the territorial and provincial level, have focused on monitoring and standardization of infrastructure, such as the Nunavut Public Health Act of 2016 (Public Health Act, 2016). Nunavut Tunngavik Incorporated noted that definition of municipal, territorial, and government roles, as well as a timeline-driven strategic plan for improved infrastructure, is required to help redress housing and water needs in the North as climate change progresses (Nunavut Tunngavik Incorporated, 2006). Suggestions for development of public drinking water infrastructure and identification of alternative drinking water sources have come from academia, but remain difficult because of uncertainty in local impacts of climate change (Medeiros *et al.,* 2007). However, local monitoring for contaminants and pathogens or development of water resource vulnerability indices may identify and address certain infrastructure problems (Austin *et al.,* 2015; Bakaic & Medeiros, 2017). Clean water access was also a focus of the Government of Nunavut in the 2019 CANPF for future programming with acknowledgement that climate change will likely impact clean water within Inuit Nunangat (CANPF, 2019). As with food security, the co-development of housing and other infrastructure policies to mitigate climate impacts highlights the important role of the Inuit-Crown Partnership as a means of joining federal and Inuit voices.

A3.3 Psychological health is impacted by climate change.

Mental health has been increasingly recognized as a critical element of public health governance in the Canadian Arctic. Suicide rates in Inuit Nunangat are over three times the national average, and have risen dramatically among Inuit populations in recent decades, from 10 per 100,000 (1972) to 113 per 100,000 in 2014 (Alessa *et al.,* 2008). While many factors contribute to mental wellness, environmental and cultural changes as a result of climate change have been linked to poor mental health among Inuit. Loss of social structures, traditional knowledge, and a sense of self determination have been associated with climate change in Inuit communities (Codon *et al.,* 1995; Medeiros *et al.,* 2007). Inuit focus groups have made direct links between the ability to hunt and travel on sea ice and their mental health (Durkalec *et al.,* 2015).

The Canadian federal government has demonstrated a commitment to solving the mental health crisis in Inuit Nunangat. During Canada's chairmanship of the Arctic Council, the government sponsored two research groups to address the factors contributing to high Arctic suicide rates, identifying community-focused approaches to redressing mental health problems (SDWG, 2015). The 2017 Canadian federal budget offered CAD $118.2 million to specifically address mental health in First Nation and Inuit communities (Minister of Finance, 2017). Projects funded by the federal government to address mental health in Northern communities included those administered by Health Canada's Climate Change and Health Adaptations for Northern First Nations and Inuit Communities program that supported 95 local projects between 2008 and 2016 including those with key themes on mental health. Local governments have also presented suicide prevention strategies to help mitigate the mental health crisis in the North including a focus on intergenerational access to the traditional lifestyle (ITK, 2014a; 2016).

Both the federal Government and Inuit organizations represented in the Inuit-Crown partnership have made efforts toward redressing climate change impacts on mental health in Inuit

Nunangat. Suicide prevention, as described in the National Inuit Suicide Prevention Strategy (ITK, 2016), as well as broader mental health, is listed as a top priority for Inuit within the National Inuit Climate Change Strategy (2019). Notably, goals from this strategy are echoed in the 2019 Canadian Arctic and Northern Policy Framework in the ITK Chapter, in which similar commitments to suicide reduction and mental well-being specifically address climate change (CANPF, 2019). The Inuit-Crown Partnership demonstrates improved commitment to co-development of holistic psychological health policies for Inuit Nunangat which recognizing the deep connections of culture, environment, and mental health for Inuit.

A3.4 Canada is creating resilient Northern communities.

The development of the Inuit-Crown Partnership in 2017 and continuing outcomes in the form of strategy commitments demonstrate a recognition of the interconnected levels of governance influencing responses to climate change impacts on Inuit health. From municipal to federal levels, Canada has recognized that individual determinants of health in Northern communities – food security, housing and sanitation access, and mental health – are part of a larger, holistic health vulnerable to climate change (Minister of Health, 2012; ITK 2014b). Notably, the 2019 Canadian Arctic and Northern Policy Framework has stated this connection explicitly and made holistic health of Indigenous communities in the Arctic a primary goal and, more importantly, begun to recognize the importance of Inuit voices being involved in the co-development of policies. Climate change plans have been developed for Arctic communities to address individual determinants of health while simultaneously enacting strategies for cultural adaptation, economic development, and improved access to medical infrastructure (Minister of Health, 2012). In 2013, Canada's Arctic Council chairmanship focused on creating sustainable

circumpolar communities (Canada's Arctic Council Chairmanship, 2013). This commitment is echoed in Canada's modern Arctic strategy, with over CAD $700 million committed to support Arctic and northern regions through 2030 (CANPF, 2019). With a nod to its future in a changing Arctic landscape, the Inuit-Crown Partnership has begun to co-develop climate change plans for Arctic and Northern communities to address individual determinants of health while ensuring Inuit voices are present and heard in the future.

References

ACIA. (2005). Arctic Climate Impact Assessment, Cambridge, UK: Cambridge University Press.

Alessa, L., Kliskey, A., Lammers, R., Arp, C., White, D., Hinzman, L., Busey, R. (2008). The Arctic Water Resource Vulnerability Index: An integrated assessment tool for community resilience and vulnerability with respect to freshwater. *Environ Mgt 42,* 523–541.

Austin, S. E., Ford, J. D., Berrang-Ford, L., Araos, M., Parker, S., Fleury, M. D. (2015). Public health adaptation to climate change in Canadian jurisdictions. *Int J Environ Res Public Health 2015*(12), 623–651.

Bakaic, M., & Medeiros, A.S. (2017). Vulnerability of northern water supply lakes to changing climate and demand. *Arctic Sci*, *3*, 1–16.

Canada's Arctic Council Chairmanship. (2013). Ottawa: Government of Canada.

Canadian Arctic and Northern Policy Framework (CANPF). (2019). Ottawa: Government of Canada. https://www.rcaanc-cirnac.gc.ca/eng/1562782976772/1562783551358

Cannon, T. (1995). Indigenous peoples and food entitlement losses under the impact of externally influenced change. *GeoJournal 35*, 137–150.

Daley, K. (2017) Meeting the northern housing challenge. Polar Knowledge Canada. https://www.canada.ca/en/polar-knowledge/publications/polarleads/vol1-no1-2016.html

Daley, K., Castelden, H., Jamieson, R., Furgal, C., Ell, L. (2015). Water systems, sanitation, and public health risks in remote communities: Inuit resident perspectives from the Canadian Arctic. *Soc Sci, Med, 135*(2015), 124–132.

Donaldson, S. G., Oostdam, J. V., Tikhonov, C., Feeley, M., Armstrong, B., Ayotte, P., *et al.* (2010). Environmental contaminants and human health in the Canadian Arctic. *Sci Total Environ, 408*, 5165–5234.

Durkalec, A., Furgal, C., Skinner, M. W., Sheldon, T. (2015). Climate change influences on environment as a determinant of Indigenous health: Relationships to place, sea ice, and health in an Inuit community. *Soc Sci Med*, *136–137*(2015), 17–26.

Dyck, L. E., & Patterson, D. G. (2017). We Can Do Better: Housing in Inuit Nunangat. *Report for Standing Senate Committee on Aboriginal Peoples*, *Senate of Canada.* https://www.nunivaat.org/doc/document/2019-12-19-02.pdf

Ferguson, H. (2011) Inuit food (in)security in Canada: Assessing the implications and effectiveness of policy. *Queen's Pol Rev*, *2*(2), 54-79.

Ford, J. D., Lardeau, M., Blackett, H., Chatwood, S., Kurzewski, D. (2013). Community food program use in Inuvik, Northwest Territories. *BMC Public Health, 13,* 970.

Government of Nunavut. (2019). Nunavut's vision. https://www.gov.nu.ca/sites/default/files/arctic_and_northern_policy_framework_-_nunavut_vision_-eng.pdf

Gregory, P. J., Ingram, J. S. I., Brklacich, M. (2005). Climate change and food security. *Philos T R Soc B,* 360, 2139–2148.

Huet, C., Rosol, R., Egeland, G. M. (2012). The prevalence of food insecurity is high and the diet quality poor in Inuit communities. *J Nutr 142*, 541–547.

Inuit Food Security Working Group. (2016) .Nutrition North Canada Program Engagement. https://www.nutritionnorthcanada.gc.ca/eng/1491505202346/1491505247821

Inuit Tapiriit Kanatami (ITK). (2008). An Integrated Arctic Strategy. https://www.itk.ca/wp-content/uploads/2016/07/Integrated-Arctic-Stratgey.pdf

Inuit Tapiriit Kanatami (ITK). (2014a). Social Determinants of Inuit Health in Canada. https://www.itk.ca/wp-content/uploads/2016/07/ITK_Social_Determinants_Report.pdf

Inuit Tapiriit Kanatami (ITK). (2014b). Inuit Priorities for Canada's Climate Strategy: A Canadian Inuit vision for our common future in our homelands. https://www.itk.ca/wp-content/uploads/2016/09/ITK_Climate-Change-Report_English.pdf

Inuit Tapiriit Kanatami (ITK). (2016). National Inuit Suicide Prevention Strategy. https://www.itk.ca/wp-content/uploads/2016/07/ITK-National-Inuit-Suicide-Prevention-Strategy-2016.pdf

Inuit Tapiriit Kanatami (ITK). (2017). An Inuit-Specific Approach for the Canadian Food Policy. https://www.itk.ca/inuit-specific-approach-for-canadian-food-policy/

Inuit Tapiriit Kanatami (ITK). (2018). National Inuit Strategy on Research. https://www.itk.ca/wp-content/uploads/2018/03/National-Inuit-Strategy-on-Research.pdf

Inuit Tapiriit Kanatami (ITK). (2019a). National Inuit Climate Change Strategy. https://www.itk.ca/wp-content/uploads/2019/06/ITK_Climate-Change-Strategy_English.pdf

Inuit Tapiriit Kanatami (ITK). (2019b). Arctic and Northern Policy Framework: Inuit Nunangat. https://www.itk.ca/wp-content/uploads/2019/09/20190925-arctic-and-northern-policy-framework-inuit-nunangat-final-en.pdf

Kovesi, T. (2012). Respiratory disease in Canadian First Nations and Inuit children. *Paediatr Child Health 17*(7), 376–380.

Lavoie, J. G. (2013). Policy silences: why Canada needs a National First Nations, Inuit, and Métis health policy. *Int J Circumpolar Health 72,* 2269.

Lawn, J. & Harvey, D. (2003). Nutrition and food security in Kugaaruk, NU: Baseline survey for the Food Mail Pilot Project. Ottawa: Ministry of Indian Affairs and Northern Development.

MacDonald, R. W., Harner, T., Fyfe, J. (2005). Recent climate change in the Arctic and its impact on contaminant pathways and interpretation of temporal trend data. *Sci Total Environ*, *342*, 5–86.

Medeiros, A. S., Wood, P., Wesche, S. D., Bakaic, M., Peters, J.F. (2007). Water security for northern peoples: Review of threats to Arctic freshwater systems in Nunavut, Canada. *Reg Environ Change 17*, 635–647.

Minister of Finance. (2017). Budget 2017. Ottawa: House of Commons. https://www.budget.gc.ca/2017/docs/plan/budget-2017-en.pdf

Minister of Health. (2012). First Nations and Inuit health strategic plan: A shared path to improved health. Ottawa: Health Canada. https://www.canada.ca/content/dam/hc-sc/migration/hc-sc/fniah-spnia/alt_formats/pdf/pubs/strat-plan-2012/strat-plan-2012-eng.pdf

Nancarrow, T. L. and Chan, H. M. (2010). Observations of environmental changes and potential dietary impacts in two communities in Nunavut, Canada. *Rural Remote Health*, 10, 1370.

Nunavut Tunngavik Incorporated. (2006). Annual Report. Iqaluit, NU: Nunavut Tunngavik Incorporated. https://www.tunngavik.com/documents/publications/2006-Nunavut-Tunngavik-Annual-Report.pdf

Oostman J. V., Gilman, A., Dewailly, E., Usher, P., Wheatley, B., Kuhnlein, H., *et al*. (1999). Human health implications of environmental contaminants in Arctic Canada: a review. *Sci Total Environ*, *230*, 1–82.

Oostman, J. V., Donaldson, S. G., Feeley, M., Arnold, D., Ayotte, P., Bondy, G., *et al*. (2005). Human health implications of environmental contaminants in Arctic Canada: a review. *Sci Total Environ, 351–352*, 165–246.

Organ, J., Castleden, H., Furgal, C., Sheldon, T., Hart, C. (2014) Contemporary programs in support of traditional ways: Inuit perspectives on community freezers and a mechanism to alleviate pressures of wild food access in Nain, Nunatsiavut. *Health & Place 30*, 251–259.

Owens, S., De Wals, P., Egeland, G., Furgal, C., Mao, Y., Minuk, G. Y. *et al.* (2012) Public health in the Canadian Arctic: contributions from International Polar Year research. Climate Change. DOI 10.1007/s10584-012-0569-3

Papatsie, L., Ellswroth, L., Meakin, S., Kurvits, T. (2013). The right to food security in a changing Arctic: the Nunavut Food Security Coalition and Feeding My Family campaign. Report: Hunger- Nutrition-Climate Justice, 4.

Perreault, K., Rive, M., Dufresne, P., Fletcher, C. (2020). Overcrowding and sense of home in the Canadian Arctic. *Housing Studies, 35*(2), 353–375.

Public Health Act. (2016). Iqaluit, NU: Nunavut Legislative Assembly. https://www.canlii.org/en/nu/laws/stat/snu-2016-c-13/latest/snu-2016-c-13.html

Rosol, R., Huet, C., Wood, M. Lennie, C., Osborne, G., Egeland G. M. (2011). Prevalence of affirmative responses to questions of food security: International Polar Year Inuit Health Survey, 2007–2008. *Int J Circumpolar Health 70*(5), 488–497.

Sharma, S., Gittelsohn, J., Rosol, R., Beck, L. (2010). Addressing the public health burden caused by nutrition transition through the healthy foods north nutrition and lifestyle intervention programme. *J Hum Ntr Diet 23*, 120–128.

Sustainable Development Working Group (SDWG). (2015). Sharing hope: Circumpolar perspectives on promising practices for promoting mental wellness and resilience. Arctic Council, Iqaluit NU: Ministerial Meeting. https://oaarchive.arctic-council.org/handle/11374/411?show=full

Warren, J. A., Berner, J. E., Curtis, T. (2005). Climate change and human health: Infrastructure impacts to small remote communities in the North. *Int J Circumpolar Health 64*(5), 487–497.

Wesche, S. D. & Chan, H. M. (2010). Adapting to the impacts of climate change on food security among Inuit in the Western Canadian Arctic. *EcoHealth*, *7,* 361–373.

Vita.

Max (Gordon) Showalter

gmshowalter@gmail.com

gmshowalter.com

Experience

Feb. 2021	**NOAA Sea Grant Knauss Marine Policy Fellow** Feb 2021 – Feb 2022 Executive Branch
Sept. 2020	**Interim Postdoctoral Researcher, University of Washington** Sept 2020 – Feb 2021 School of Oceanography Supervisor, Prof. Jody Deming

Education

August 2020	**PhD in Oceanography and Astrobiology, University of Washington** School of Oceanography Dissertation: Acquisition, exploitation, and recycling of organic matter within sea ice brines by bacteria and their viruses. Advised by Prof. Jody Deming
February 2017	**MS in Oceanography, University of Washington** Thesis: Bacterial chemotaxis in cold and sub-zero brines Advised by Prof. Jody Deming
May 2014	**BS in Biological Engineering, Purdue University** Minor in Russian Language

Publications

Submitted	Torstensson, A., Margolin, A.R., **Showalter, G.M**., Smith, W.O., Shadwick, E.H., Carpenter, S.D., *et al.* (*submitted)* Sea-ice microbial communities in the central Arctic Ocean: Limited responses to short-term pCO_2 perturbations. *Limnology and Oceanography.*
Published	**Showalter, G.M.** and Deming, J.W. (2018) Low-temperature chemotaxis, halotaxis, and chemo-halotaxis in a model marine psychrophile *Colwellia psychrerythraea* strain 34H. *Environmental Microbiology Reports.*
	Lindensmith, C.A., Rider, S., Bedrossian, M., Wallace, J.K., Serabyn, E., **Showalter, G.M.**, *et al.* (2016) A submersible, off-axis microscope for

detection of microbial motility and morphology in aqueous and icy environments. *PLOS one*.

Wallace, J.K., Rider, S., Serabyn, E., Kühn, J., Liewer, K., Deming, J., **Showalter, G.M.**, *et al.* (2015) Robust, compact implementation of an off-axis digital holographic microscope. *Optics Express* 23(13).

Ha, S.J., **Showalter, G.M.**, Cai, S., Wang, H., Liu, W.M., Cohen-Gadol, A., *et al*. (2014) Lipidomic analysis of glioblastoma multiforme using mass spectrometry. *Current Metabolomics* 2:132-143.

Other writing

Showalter, G.M. (2019) Revisiting the Titanic. *Ocean Memory Newsletter*, National Academies/Keck Foundation.

Showalter, G.M. (2019) Defining Ocean Memory. *Ocean Memory Newsletter*, National Academies/Keck Foundation.

Showalter, G.M. (2018) A small oyster poised for a big comeback. *Sea Star*. Washington Sea Grant.

Showalter, G.M. (2018) Researchers document salmon diversity using ancient DNA. *Sea Star*. Washington Sea Grant.

Showalter, G.M. (2018) The faces of Washington Sea Grant workshops. *Sea Star*. Washington Sea Grant.

Showalter, G.M. (2016) *HiveBio*: Access Granted. *BioCoder Magazine.*

Presentations

2020

McKinley, C., **Showalter, G.M.**, Crofoot, T. (*submitted*) Systematic evaluation of Geoscience education programs that are designed for American Indian Alaska Native students, use Indigenous epistemologies or Traditional Ecological Knowledge. American Geophysical Union Annual Meeting, 1-17 Dec., virtual.

Gomez-Buckley, A., **Showalter, G.M.**, Wong, M. (*submitted*) The viral elevator: Modeling virus and bacteria populations in Europa's icy ocean. American Geophysical Union Annual Meeting, 1-17 Dec., virtual.

2019

McKinley, C., **Showalter, G.M.**, Crofoot, T. (2019) Centering Indigenous communities in geoscience education. American Geophysical Union Annual Meeting, 9-13 Dec, San Francisco, CA.

Showalter, G.M., Young, J.C., Koutnik, M., Fabbi, N.F. (2019) Analyzing the Inuit role in Arctic environmental security. Paper, 25th Biennial Meeting of the Assoc. for Canadian Studies in the US, 13-16 Nov, Montreal, QC.

Showalter, G.M., Deming, J.W. (2019) Who controls organic matter recycling in sea ice? Talk, Biological Oceanography Seminar, University of Washington, 5 Nov, Seattle, WA.

Showalter, G.M., Talmy, D., Deming, J.W. (2019) Modeling virus-host dynamics in sea ice brines. Talk, Astrobiology Colloquium, University of Washington, 29 Oct, Seattle, WA.

Showalter, G.M., Talmy, D., Deming, J.W. (2019) Modeling virus-host dynamics in sea ice brines. Talk, International Symposium on Sea Ice, 17-21 Aug, Winnipeg, MB.

Showalter, G.M. and Deming, J.W. (2019) Extreme enzymes: Activity of extracellular enzymes in analog subzero brines. Poster, Astrobiology Science Conference, 23-28 June, Bellevue, WA.

Showalter, G.M. (2019) Extracellular enzymes: From sea ice to biotech. Graduate student and Postdoc Symposium, University of Washington, 31 May, Seattle, WA.

Showalter, G.M., Deming, J.W. (2019) Foraging strategies in sea ice: Exploring the potential role of bacterial extracellular enzymes. Talk, Biological Oceanography Seminar, University of Washington, 28 May, Seattle, WA.

2018 **Showalter, G.M.**, Deming, J.W. (2018) Conflict, competition, and cooperation: Sea ice ecosystems from microbes to humans. Talk, Biological Oceanography Seminar, University of Washington, 27 Feb, Seattle, WA.

Showalter, G.M., Bedrossian, M., Nadeau, J., Deming, J.W. (2018) Microbial motility in subzero brines. Poster, Ocean Sciences Meeting, 12-17 Feb, Portland, OR.

Showalter, G.M. (2018) Looking for life in the coldest places. Invited speaker, Astronomy on Tap, 24 Jan, Seattle, WA.

2017 **Showalter, G.M.**, and Deming, J.W. (2017) Modeled virus-host dynamics in sea ice brines. Poster, Polar Alpine Microbiology Meeting, 8-12 Sept, Nuuk, Greenland.

2016 **Showalter, G.M.** (2016) Home is where the bacteria are. Invited speaker, Museum of Flight, 22 Oct, Seattle, WA.

Showalter, G.M. (2016) Finding life when the trail goes cold: From the poles to icy moons. Seattle Town Hall Speaker Series, 21 Mar, Seattle, WA.

2015 **Showalter, G.M**., and J.W. Deming. (2015) Swimming in the cold: Motility and taxis of the model marine psychrophile *Colwellia psychrerythraea* 34H. Poster, ASM 2015, 115th General Meeting, 30 May–2 June, New Orleans, LA.

Showalter, G.M., and J.W. Deming. (2015) Swimming to the limits: Microbial motility in extreme polar environments. Poster, GRC on Polar Marine Sciences, 15–20 Mar, Lucca (Barga), Italy.

Showalter, G.M., Nadeau, J., Deming J.W. (2015) Swimming in the cold: Motility and taxis of the model marine psychrophile *Colwellia*

psychrerythraea 34H. Poster, Moore Imaging Meeting, Dec, Sausalito, CA.

Field experience

2019 ***Norseman II*, Bering Strait**
(September 1st – 15th)
Sailed with Dr. Rebecca Woodgate to recover and deploy moorings to measure long-term changes in hydrography of the Bering Strait. Served as science head of night watch, including repeat CTD deployments.

2018 **Ice Breaker *Oden*, High Arctic**
(July 22th – September 23rd)
Performed extensive ice-coring operations of first and multi-year ice facilitated by helicopter deployment. Helped complete experiments on natural ice cores investigating response of sea ice algae to ocean acidification. 60-day deployment aboard Swedish icebreaker with multi-national crew and science team.

Utqiaġvik (Barrow), Alaska
(May 7th – 15th)
Collected samples of sea ice brines and cryopeg fluid for study of microbiological interactions with viruses and phytoplankton in extreme cold, and measured bacterial enzyme activity on brines.

2017 **Utqiaġvik (Barrow), Alaska**
(May 4th – 17th)
Collected samples of sea ice brines and cryopeg fluid for study of microbiological interactions with viruses and phytoplankton in extreme cold. Included extensive laboratory component in addition to field collection.

2016 **Palmer Station, Antarctica**
(July 22nd – August 5th)
Learned principals of multi-trophic marine ecology during six-week deployment as part of the NSF's 10th Antarctic Biology Training Program. Included 15 days aboard the icebreaker *Laurence M Gould*.

2015 ***Norseman II*, Bering Strait**
(June 27th – July 9th)
Analyzed biofouling patterns on recovered moorings during eight-day deployment aboard the *Norseman II* with Dr. Rebecca Woodgate to deploy three moorings between Nome, AK and Point Hope, AK.
Nuuk, Greenland
(March 23rd – 30th)
Deployed and validated a digital holographic microscope for bacterial detection in sea ice brines as an eight-day field excursion in Greenland, in collaboration with engineers from Caltech and NASA JPL.

Writing and communication experience

2020 **Newsletter Editor, Ocean Memory Project**
(March 2019 - March 2020)
Conceptualize, develop, and publish quarterly newsletter campaigns for the Keck Foundation-funded Ocean Memory project, writing long-form articles and group updates. Includes experience using MailChimp and WordPress.

Polar Science Weekend, Pacific Science Center
(March 2015 – 2020, annually)
Co-led table-top activity introducing kids to the biology of and methods for studying life in sea ice, engaging over 1000 museum visitors of all ages. Included development of new activity and visuals for children.

2018 **Communications Fellow, Washington Sea Grant**
(October 2017 – March 2018)
Developed and wrote full-length articles for Washington Sea Grant newsletter *Sea Star* including in-person interviews with researchers funded by WSG (see *Publications*). Created and published social media posts and press releases with the WSG communications team. Paid fellowship for 10 hrs/week.

2017 **Science Writer,** HiveBio Community Lab
(2014-2017)
Wrote postings, articles, and developed public discussions as volunteer science writer for community bioscience laboratory. Responsibilities included weekly postings on website *HiveBio.org* (WordPress) and occasional articles to promote classes and events. Led monthly discussion topics managing crowds of 15-20 people to discuss topics in modern biotechnology, as well as created and distributed promotional materials. Work included a publication in online biotech magazine *BioCoder* (see *Publications*).

Engage Science Communication Directors Board
(September 2016 – May 2017)
Curated *Engage Science* twitter account (@EngageScience), adding over 200 followers and increased monthly engagements from ~200 to ~1600 during tenure. Helped advised direction of Engage Science class, an all-graduate student led course teaching graduate students public speaking skills for science communication.

2016 **Science Communications Fellow, Pacific Science Center**
(February – March 2016)

Developed and implemented a youth-targeted public engagement activity at the Pacific Science Center after completion of a six-week course covering principles of public science engagement.

Engage Science Communication Course
(January - March 2016)
Completed graduate student led science communication course, culminating in a public talk at Seattle Town Hall. Learned principles of distilling complex topics, effective visual design, and narrative-based scientific speaking for maximum public engagement.

Teaching experience

Winter 2020 **Guest Lecture, Task Force: Arctic Sea Ice and International Policy (JSIS 495H)**
Canadian Arctic and Northern Strategy
Life in Sea Ice

Spring 2017 **Guest Lecture, NASA research Seminar (ESS 495) "**Life in Extreme Environments"

Spring 2016 **Teaching Assistant, Arctic Change (OCN 235)**
Independently designed and delivered weekly lectures to 15-25 students on a variety of Arctic topics including atmospheric science, oceanography, microbiology, politics and governance, and history. Graded weekly homework and exams of 50+ students and held weekly office hours.

Spring 2015 **Teaching Assistant, Marine Bacteria Archaea and Viruses (OCN 431)**
Coordinated homework assignments and graded student presentations in class of 30 students. Held weekly office hours.

Relevant workshops and training

2019 **Cold Water Safety Training, Seattle, WA**
(August)
Completed two day Coast Guard-certified training course on techniques for survival in cold water including immersion suit donning and raft survival, administered by North Pacific Fishing Vessel Owners' Association.

2017 **Science and Diplomacy in the Arctic, Dartmouth, NH**
(June 25 – 30th)
Learned principals of diplomacy, negotiation, and Arctic policy at weeklong workshop, including participation in Model Arctic Council.

Received Outstanding Paper award for policy paper on climate change and health in the Canadian North.

2016 **Astrobiology Workshop, Mt. Rainier National Park**
(Sept 11th – 14th)
Worked with scientists from Georgia Tech and astrobiology graduate students to develop a plan for sample collection on Mt. Rainier's snow fields as an analogue for sample collection strategies on Mars.

2015 **Astrobiology Workshop, Yellowstone National Park**
(Sept 8th – 11th)
Worked with scientists from NASA Ames to investigate the distribution of photosynthetic organisms under extreme temperature and pH regimes of Yellowstone's geysers and hot springs as an analogue for understanding extreme life and life detection in space.

Cold Water Safety Training, Seattle, WA
(June)
Completed two day Coast Guard-certified training course on techniques for survival in cold water including immersion suit donning and raft survival, administered by North Pacific Fishing Vessel Owners' Association.

2014 **Astrobiology Workshop Washington Coast**
(October 24th – 27th)
Helped lead demonstrations of microbial ecology techniques aboard the *RV Thompson* during a four-day research cruise along the Washington Coast.

Awards

2020 Graduate Dean's Medalist, College of the Environment, University of Washington
2019 College of the Environment Travel Award, University of Washington ($500)
Graduate School Travel Award, University of Washington ($500)
International Sea Ice Symposium student travel award ($750 CAD)
Best Talk, School of Oceanography Graduate and Post Doc Symposium
UW Astrobiology external rotation additional travel stipend ($1500)
2017 Best Poster Presentation, Polar Alpine Microbiology Conference ($250)
Congressional Antarctic Service Medal
Best Policy Paper Award, Dartmouth Arctic Science and Diplomacy Program
2016 ASLO Student Travel Grant ($500)
2014 Egvedt Scholarship, University of Washington
2010-2014 Purdue University President's Scholarship ($40,000)

Greiner Scholarship ($1000)
Reynolds Scholarship ($2000)
Purdue University Agricultural & Biological Engineering Student Travel Award ($250)

Volunteer and professional service

2020 **SeaTalk,** University of Washington
(2018 – present)
Helped develop quarterly workshops for anti-harassment training aimed at preventing and dealing with harassment, difficult situations, and aspects of life in the field.

2019 **Session Chair**, Assoc. for Canadian Studies in the US 25th Biennial Meeting (November 13 - 16)
Served as session chair for session *Inuit Governance and Diplomacy* at 25th Biennial ACSUS conference in Montreal, QC.

Lead Session Chair, Astrobiology Science Convention
(June 24 - 28)
Proposed and led the session *Pushing the Envelope: Genomic and physiological adaptations among microbes in extreme Earth analogues* at the Astrobiology Science Convention in Bellevue, WA.

Oceanography Graduate Student Club, University of Washington
(March – September)
Officer in the Academic and Recreational Graduate Oceanographers (ARGO) Club, which included work coordinating relations between the department and graduate student body.

Science Fair Mentor, John Stanford International School
(January – March 2019)
Worked with two pairs of 4th grade students weekly to develop and execute a science fair project in the field of sustainability.

Professional associations

Association for the Sciences of Limnology and Oceanography (ASLO), American Society of Microbiology (ASM), Tau Beta Pi Honors Engineering Society (TBP), Association of Polar Early Career Scientists (APECS)

Language Skills

Native **English**
Intermediate **Russian**
Minor in Russian Language, Purdue University, Indiana (2010-2014)

	US State Dept. funded study, Kazan State Technical University, Kazan Russia (2010) US State Dept. funded study, Afina Center, Gatchina, Russia (2009) **German** Secondary education (2006-2010) Immersive study, Gymnasium Melanchthon, Nürnberg, Germany (2008)
Elementary	**Norwegian** Skogfjorden Summer Language Camp, Bemidji, Minnesota (2006-2008) **Inuktitut** Distance learning course, University of Washington, Seattle, WA (2018 – current)